Title
Induction of lignocellulose degrading enzymes in Neurospora crassa by cellodextrins

Author
Znameroski, Elizabeth A.

Publication Date
2012

Peer reviewed|Thesis/dissertation

Induction of lignocellulose degrading enzymes in *Neurospora crassa* by cellodextrins

by

Elizabeth Anne Znameroski

A thesis submitted in partial satisfaction of the requirements for the degree of

Doctor of Philosophy

in

Molecular and Cell Biology

in the

Graduate Division
of the
University of California, Berkeley

Committee in charge:
Professor Jamie H.D. Cate, Co-Chair
Professor N. Louise Glass, Co-Chair
Professor Richard Calendar
Professor Michelle Chang
Professor Markus Pauly

Spring 2012

Induction of lignocellulose degrading enzymes in *Neurospora crassa* by cellodextrins

Abstract

Induction of lignocellulose degrading enzymes in *Neurospora crassa* by cellodextrins

by

Elizabeth Anne Znameroski

Doctor of Philosophy in Molecular and Cell Biology

University of California, Berkeley

Professor Jamie H.D. Cate, Co-Chair

Professor N. Louise Glass, Co-Chair

Neurospora crassa colonizes burnt grasslands in the wild and metabolizes both cellulose and hemicellulose from plant cell walls. When switched from a favored carbon source such as sucrose to cellulose, *N. crassa* dramatically upregulates expression and secretion of a wide variety of genes encoding lignocellulolytic enzymes. However, the means by which *N. crassa* and other filamentous fungi sense the presence of cellulose in the environment remains unclear. Here, I show that a *N. crassa* mutant carrying deletions of two genes encoding predicted extracellular β-glucosidase enzymes and one intracellular β-glucosidase enzyme (Δ3βG) lacks β-glucosidase activity, but efficiently induces cellulase gene expression and cellulolytic activity in the presence of cellobiose as the sole carbon source. These data indicate that cellobiose, or a modified version of cellobiose, functions as an inducer of lignocellulolytic gene expression and activity in *N. crassa*. In addition, I have identified two cellodextrin transporters involved in sensing cellulose. A *N. crassa* mutant carrying deletions for both transporters is unable to induce cellulase gene expression in response to crystalline cellulose. Furthermore, a mutant lacking β-glucosidase enzymes and transporters (Δ3βGΔT) does not induce cellulase gene expression in response to cellobiose.

Acknowledgements

There are many people who have directly or indirectly provided me support over the past several years and deserve thanks and recognition for their contributions. There are too many to list here and therefore the following is an abbreviated list.

First, I would like to recognize my advisors. Jamie Cate, thanks for sticking with me through all of my crazy ideas. With your gentle pushing, it appears I finally found the right path. Louise Glass, thank you for adopting me as one of your own in the middle of my studies. The time I have spent with you (and the rest of the lab) has been invaluable in my development as a scientist. Your willingness to support, challenge and direct me in this project was truly a blessing.

My fellow scientists at the EBI who provided me with both academic and emotional support. The teachers, advisors and mentors who helped introduce me to the wonders of late nights in the lab alone moving small volumes of liquids between tubes (aka research), especially, geg and mdw.

Those who I consider my family: ego and sg, thank you for the many hours I spent napping on your couch, the many loads of laundry you allowed me to do and the many empty calories in dr. pepper you allowed me to drink. dz and nc, I've enjoyed getting to know you as adults and look forward to raising the next generation of znameroski's together. nm, thank you for becoming my mom, I am looking forward to making up all of the years we missed. mz and to, I miss you both and wish you were here. hs, I'm not sure if it's kosher to put you in this list, but I'm going to; thank you for both the hours we spent actively conversing as well as the times you just sat with me.

Last, but not least, flo, thank you for sticking with me along this entire journey. At times, your love and encouragement were the only things that kept me going. I'm looking forward to the well-deserved vacation we will take before setting out on our next adventure.

Contents

Figures

List of Tables

Chapter 2

Chapter 3

1 Introduction

Partially taken from: Znameroski, EA and Glass, NL. *Neurospora crassa* as a model system to study lignocellulose degradation. *Microbial Engineering: Recent developments*. Manuscript in preparation.

1.1 Context and Motivation

Our current energy consumption patterns are both physically and socially unsustainable. In 2007, the International Panel on Climate Change (IPCC) presented several estimates for global temperature change based on various greenhouse gas emission scenarios. Between the years 2000 and 2010, CO_2 emissions increased from 23.5 gigatons per year to 30.6 gigatons per year (1); if CO_2 emissions continue to increase at this rate, the IPCC predicted that by the year 2099 we should expect an increase in global average temperature between 2.0 and 5.4 degrees Celsius. According to the IPCC, such an increase would have numerous negative consequences to human society and natural ecosytems (2).

The UN estimates that 1.6 billion people lack any access to electricity and up to half of the world already faces severe energy shortages (3). While current estimates on the amount of non-renewable energy reserves may or may not be a limiting factor, the environmental consequences of increasing demands on such sources has led many countries to begin the transition to renewable sources of energy. The 2007 Energy Independence and Security Act (EISA) mandates the production of 36 billion gallons of biofuels per year by 2022, of which 21 billion gallons must be non-cornstarch based. Evidence suggests that lignocellulosic biomass represents the most scalable alternative fuel source. The production of lignocellulosic biofuels is composed of three steps (1) production and pretreatment of biomass, (2) enzymatic degradation/saccharification and (3) fermentation of sugars to ethanol or longer chain alcohol.

1.2 Lignocellulosic biofuels

1.2.1 Production and pretreatment of biomass

In general, plant biomass consists of 40-50% cellulose, 25-30% hemicellulose and 15-20% lignin, however the exact composition of plant cell walls varies between plant species and in different tissues and developmental stages within a single plant species (4). Cellulose is a linear polymer of glucose linked together by β-(1,4)-glycosidic bonds. The linear and flat nature of cellulose chains allows for extensive hydrogen bonding both within and between chains as well as van der Waals stacking interactions between the chains (5). Hemicellulose is a branched heteropolymer of D-xylose, L-arabinose, D-mannose, D-glucose, D-galactose and D-glucuronic acid, which bonds to the surface of the cellulose microfibrils and forms a matrix between fibers (5, 6). The third component, lignin, is a complex hydrophobic, cross-linked aromatic polymer composed of three major phenolic components (p-coumaryl alcohol, coniferyl alcohol and sinapyl alcohol). Plant cell walls are composed of cellulose chains that are packed into microfibrils. These fibrils are attached to each other by hemicellulose and covered by lignin, an assemblage referred to as lignocellulose. The cell wall gives cells rigidity and strength, offering protection against mechanical stress (5, 6). Because the cell wall provides such physical

strength, breaking it down to easily metabolized sugars first requires a pretreatment step that includes physical, chemical and/or thermal processes [reviewed in (5, 6)]. This step does not fully degrade the plant cell wall, but instead helps to relax the structure thereby allowing enzymes greater accessibility to their substrates.

1.2.2 Enzymatic degradation/saccharification

The degradation of cellulose into its monomeric sugars requires the action of three types of enzymes: (1) exoglucanases (cellobiohydrolase), which release cellobiose from either the reducing or non-reducing end of cellulose, (2) endoglucanases, which hydrolyze accessible intramolecular β-1,4-glucosidic bonds of cellulose chains to produce new free ends for the exoglucanases to act on, and (3) β-glucosidases which hydrolyze cellobiose and other soluble cellodextrins to produce glucose. While initial cocktails of enzymes for cellulose degradation contained only these three types of enzymes, more recently the inclusion of other enzyme classes, such as the GH61s, has resulted in a greater amount of soluble sugar production without an increase in total enzyme loading. Hemicellulases facilitate cellulose hydrolysis by exposing the cellulose fibers, thus making them more accessible to the cellulases. Unlike cellulose, hemicellulose is chemically complex and therefore requires more classes of enzymes for its breakdown. The most relevant classes include (1) endoxylanase, which attacks the main chains of xylan, (2) β-xylosidase, which hydrolyzes xylooligosaccharides to xylose, (3) α-arabinofuranosidase and α-glucuronidase, which remove the arabinose and 4-0-methyl glucuronic acid substituents, respectively, from the xylan backbone, (4) acetyl esterases, which hydrolyze the acetyl substitutions on xylose moieties, (5) feruloyl esterases, which hydrolyze the ester bond between the arabinose substitutions and ferulic acid (which aids the release of hemicellulose from lignin and renders the free polysaccharide product more amenable to degradation) (5-7).

1.2.3 Fermentation

Following enzymatic degradation, the soluble hexose and pentose sugars derived from lignocellulose are fed to microorganisms, which ferment the sugars to produce ethanol or other higher chain alcohols. Microbial fermentation can be performed by a number of organisms including both yeasts (such as *Saccharomyces cerevisiae* or *Pichia stipitis*) and bacteria (such as *Zymomonas mobilis* and *Clostridia acetobutylicum*) (5-7).

1.3 Production of cellulases and hemicellulases in filamentous fungi

The costs associated with the conversion of insoluble polysaccharides in plant biomass to easily fermentable sugars represents a significant barrier to the production of cost-competitive biofuels (8). Filamentous fungi have the capacity to secrete large amounts of lignocellulosic degrading enzymes, and this ability has been exploited by industry to produce cellulases in quantities exceeding 100 g/L of culture (4). The most commonly used organism for the production of cellulases in an industrial setting is *Trichoderma reesei* (*Hypocrea jecorina*). While this organism was selected for its innate ability to secrete large quantities of plant cell wall degrading enzymes, it has since undergone several rounds of random mutagenesis producing a strain that secretes cellulases several times higher than the original wild isolate. With the availability of low cost and high-throughput sequencing methods, studies have recently begun to shed light on some of the mutations that may be relevant for the cellulase hyperproduction

phenotype (9). While these mutations were easy to identify, the genetic, molecular and biochemical techniques to easily work with and study *T. reesei* are still in their infancy. The difficulty to perform even basic recombinant gene expression is a major drawback to the use of *T. reesei* as an academic model.

The related filamentous fungus, *Neurospora crassa* also has an innate ability to secrete lignocellulose-degrading enzymes. While Bruce Eberhart first examined this characteristic in the late 1970s, almost nothing further was reported until our group published a systems analysis of *N. crassa* grown on *Miscanthus* in 2009 (10). While *N. crassa* might not be known as an industrial workhorse like *H. jecorina*, it has the unique advantage of being a NIH model organism, most commonly known for its role proving the "one gene, one enzyme" hypothesis by Edward Beadle and George Tatum (11). Because of its status as a model organism there is a significant community of researchers who have spent many years perfecting a library of molecular, genetic and biochemical techniques. Given the high conservation of the lignocellulose degrading machinery in filamentous fungi, we have begun to develop *N. crassa* as a model to understand the global change such an organism requires to go from energy generation using a simple sugar to a much more complex and recalcitrant molecule such as cellulose.

1.2 Cellulose signaling from the outside in

1.2.1 Signals

The ability of any filamentous fungus, including *N. crassa*, to grow on an insoluble substrate requires that organism to first recognize its presence in the environment (Fig. 1-1). The recognition step is crucial for the transcription, translation and secretion of the proper suite of enzymes to degrade the substrate into smaller, more easily transported components.

The best inducers of plant cell wall degrading enzyme expression by filamentous fungi are insoluble substrates that include cellulose, hemicellulose or mixtures of plant polymers. However, the use of insoluble substrates to induce enzyme secretion is not ideal for industrial processes. Since these naturally inducing substances cannot enter fungal cells, it is generally believed that basal levels of cellulolytic enzymes are required to generate small amounts of soluble breakdown products from the insoluble substrate. It is these soluble oligosaccharides released from the polymers and their derivatives that function as the actual molecules that trigger enzyme induction (12). In support of this hypothesis, it was reported in *T. reesei* that cellulase induction can be blocked by the addition of antibodies against the main cellulases immediately before the addition of cellulose (13). In addition, the expression of antisense RNA against *gh51*, *gh71*, and *gh62* inhibits the induction of *cbh1* by cellulose, but not by a soluble inducer (14).

Several small molecules have been identified that induce the expression of cellulases in individual species of filamentous fungi. However, the molecular mechanisms by which they act have yet to be established. Some of these inducing molecules include: lactose, sophorose, cellobiose, laminaribiose, gentiobiose and sorbose. The two most commonly studied inducers in *T. reesei* are sophorose and lactose, although neither can exactly reproduce the response to insoluble cellulose (15, 16). The most potent inducer in *T. reesei* is the disaccharide sophorose (two β-1,2-linked glucose units) and has been considered the "natural" inducer of cellulases in *T. reesei* as it is

predicted to be generated by the transglycosylation of cellobiose by an extracellular β-glucosidase (17, 18). In support of this hypothesis, sophorose was produced when 10% w/v cellulose was incubated with purified *T. reesei* enzymes for one day at 50˚C (17). However, the production of sophorose has never been reported from a purified β-glucosidase (19). The first soluble inducer of cellulases identified for *T. reesei* was the disaccharide lactose. The mechanism of this induction has been fairly well characterized, but the relevance of lactose is questionable given that lactose is not a component of plant cell walls. Nevertheless, it has been shown that an extracellular β-galactosidase in *T. reesei* can hydrolyze lactose to D-glucose and D-galactose, which can then be taken up by their respective permeases. More recently, studies looking at the Leloir pathway in *T. reesei* showed that deletion of *gal1* (galactokinase; responsible for the first step in galactose catabolism) does not prevent growth on lactose, but does inhibit the transcription of *cbh1* and *cbh2* (20). Interestingly, this study also found that deletion of *gal1* does not inhibit the induction of cellulases by sophorose, indicating that the induction mechanisms for these two molecules are different (20).

While sophorose and lactose both induce cellulases in *H. jecorina*, these results are not reproducible in other species of filamentous fungi. For example, sophorose does not induce cellulase gene expression or activity in either *Aspergillus niger* (21) or *Phanerochaete chrysosporium* (22) and lactose has been found to repress cellulase transcription when added to cellulose induced cultures in several basidiomycete species (19).

Because cellobiose is the major soluble end product of cellulases, it has been predicted that cello-oligosaccharides, including cellobiose, are the most likely natural inducers. Cellobiose moderately induces cellulase gene expression and activity in *T. reesei* (17, 23) and *Aspergillus* species (24), which are commonly used for high-level enzyme production (25). However, cellobiose is unable to induce cellulase gene expression in the more distantly related fungus *P. chrysosporium*, which instead responds to cellotriose or cellotetraose (26). In support of the hypothesis that cellobiose acts as an inducer of cellulases, studies using *T. reesei* have shown that Nojirimycin inhibition of β-glucosidase, the enzyme that converts cellobiose into glucose in the final step of cellulose hydrolysis, allows a moderate induction of cellulases by cellobiose (27, 28), implying that the transglycosylation activity of a β-glucosidase is not required for cellulase induction.

1.2.2 Signal transport

Uptake of cellobiose has been demonstrated in yeasts (29) as well as in *Escherichia coli* (30), however only one study has been performed examining cellobiose uptake in filamentous fungi. This study confirmed the presence of an uptake system specific for β-linked diglucosides, including cellobiose, laminaribiose and sophorose, in *T. reesei* (31). The uptake system was inhibited by the presence of glucose and uptake was increased following sophorose treatment (induction). It has a high affinity for cellobiose, but low activity (K_m 0.3 μM; 2.5 milliunits/mg dry cell weight). Despite characterization of this “β-linked diglucoside permease”, no specific gene or genes have been identified.

More recently, our group characterized the activities of two *N. crassa* cellodextrin transporters in *Saccharomyces cerevisiae* (32). These transporters were initially identified

in the systems analysis of *N. crassa*, as members of the major facilitator superfamily of sugar transporters which showed increased transcription when *N. crassa* is grown on cellulose (10). While this study identified three cellodextrin transporters, only two transport cellodextrins in *S. cerevisiae* (NCU00801, *cdt-1*; NCU08114, *cdt-2*) while the third (NCU05853) is still uncharacterized. In *S. cerevisiae*, CDT-1 and CDT-2 are both high-affinity cellobiose transporters with Michaelis constant (K_m) values of 4.0 ± 0.3 μM and 3.2 ± 0.2 μM respectively (32) and V_{max} values equal to 0.7 pmol/sec and 0.35 pmol/sec, respectively. Cellobiose transport by CDT-1 and CDT-2 is inhibited by excess cellotriose, and CDT-1 activity is also inhibited by cellotetraose. (32). In addition, by showing growth on cellotriose and cellotetraose, it is implied that these transporters can transport longer oligosaccharides, as the only mechanism to metabolize cellodextrins requires the intracellularly expressed β-glucosidases (32).

1.2.3 Carbon catabolite repression

In an environment where resources are scarce and competition is plentiful, the ability of microbes to rapidly adapt to a changing environment is key to survival. To achieve survival, mechanisms evolved that allow a rapid adaptation to changing nutrient conditions. One such mechanism, Carbon Catabolite Repression (CCR), allows for the preferred assimilation of carbon sources with high nutritional value by actively repressing the expression of genes involved in the catabolism of those less energetically valuable, such as lignocellulose. CCR is conserved in most fungal species and therefore our knowledge is shaped not only by work performed in filamentous fungi, but also in the yeast, *S. cerevisiae.*

One of the main players in CCR is the zinc finger transcription factor Mig1/CreA/CRE1, which has been extensively examined in *S. cerevisiae* where it is involved in repressing transcription of genes encoding enzymes for the utilization of maltose, sucrose and galactose (33, 34) with approximately 90 genes as direct targets (35-37). Upon glucose depletion, Mig1p is phosphorylated by the kinase Snf1p, resulting in the exit of Mig1p from the nucleus (38). In addition, Mig1p recruits the global repressor complex, Cyc8p-Tup1p, to repress transcription (39). In *H. jecorina*, phosphorylation of CRE1 is required for DNA binding (40), although the Snf1p homolog in *T. reesei* appears not to regulate CRE1 (41), suggesting a divergence of the regulatory pathways in yeasts and filamentous fungi.

In *Aspergilli*, *T. reesei* and *N. crassa*, research has shown that CreA/CRE1 binds to the promoters of the respective target genes via the consensus motif 5'-SYGGRG-3'. Typically genes under direct control of CreA/CRE1 have two closely linked consensus motifs and it has been suggested that direct repression would only occur through such double-binding sites (42, 43). Historically, research in *Aspergilli* and *T. reesei* has suggested that CreA/CRE1 was directly involved in the regulation of certain cellulase and hemicellulase genes as many specific gene promoters contain the consensus motif. For example, ten CRE1 binding sites are present in the promoter of *T. reesei xyr1* (44) and CRE1 was shown to bind to adjacent motifs in the promoter of *cbh1* (45).

More recently, work in both *T. reesei* (46) and *N. crassa* (47) suggests that CRE1 mediates the expression of cellulase and hemicellulase genes via repression, thus acting as a negative regulator in conditions of high glucose. Under conditions of low glucose, de-repression occurs and expression levels of cellulase and hemicellulase genes are

elevated, but are substantially lower than under inducing conditions (46-48). This implies that the induction of cellulase and hemicellulase genes requires two steps, de-repression (via CRE1) and induction (via activation by a different transcription factor). In 2011, reports on in both *T. reesei* and *N. crassa* were published comparing gene expression under conditions of repression and de-repression in the wild-type versus Δ*cre-1* strains. Significant differences in culture conditions resulted in gene sets that show only limited overlap. Genes identified in *T. reesei* are focused more on genes expressed under conditions of low glucose, as these cultures were grown under conditions of high or low glucose availability. This study identified 207 genes that were differentially regulated, with 118 predicted to be repressed by CRE1 and 72 predicted to be induced. On the other hand, because the study in *N. crassa* used culture conditions with either the presence of high glucose or crystalline cellulose, this gene set focuses more on genes directly involved in catabolism of crystalline cellulose. This study identified 102 genes that show greater than 2-fold increase above wild-type in the *Δcre-1* mutant when grown on Avicel. These genes are primarily enriched for those related to C-compound and carbohydrate metabolism, protein synthesis and proteins with binding function or co-factor requirement. In addition, by comparing the wild-type and Δ*cre-1* mutant when grown under conditions of high glucose, 75 genes were identified that show an increase in relative expression. These genes are predicted to be direct targets of CRE-1. By comparing these two studies, Sun and Glass found that of the 190 genes reported to be directly controlled by CRE1 in *H. jecorina*, the orthologs of only 103 of those genes could be identified in *N. crassa*. Of those 103 genes, only 6 genes showed increased expression levels and 10 genes showed decreased expression levels in both studies (46, 47).

The main conclusion from both of these papers is that while the deletion of *cre1/cre-1* allows for greater production of cellulases when grown on Avicel, the primary defect is the inability to repress cellulase/hemicellulase gene expression once growth on Avicel has been established (47). However, in the absence of a cellulase-inducing substrate, the *cre-1* deletion strain does not produce cellulases (46, 47) even when allowed to grow into starvation, indicating that relief from CCR is not sufficient for the expression of cellulase genes and that active induction is also required.

1.2.4 Cellulase and hemicellulase specific transcription factors

As described above, cellulase and hemicellulase genes are only expressed and produced under conditions of low glucose (de-repression) and in the presence of a specific inducer (induction) (Fig 1-2). Because catabolism of lignocellulose is less energetically valuable when compared to a simple sugar, cellulase and/or hemicellulase genes are never highly expressed in the presence of simple sugars, even with the presence of an inducer. Several transcription factors have been described in filamentous fungi that regulate the expression of cellulase and/or hemicellulase genes including XlnR, Ace2, and the newly characterized CLR-1 and CLR-2.

The most highly studied transcriptional regulator for lignocellulose degradation is XlnR/XYR1/XLR-1, which has a zinc binuclear cluster DNA-binding domain that has been proposed to bind to regions of DNA containing the sequence 5'-GGCTAA-3', 5'-GGCTGA-3', or 5'-GGCTAG-3' (49-54). In *T. reesei* and several species of *Aspergilli*, XYR1/XlnR co-regulates both hemicellulase and cellulase gene expression (21, 55-57).

In *A. niger* the xylanolytic and cellulolytic systems are co-regulated via the inducer D-xylose (21, 55, 57) while in *T. reesei* several inducers are used, though none of them triggers expression of all major cellulase and hemicellulase genes (58). In *Fusarium* species and *N. crassa*, only xylose and xylan utilization is affected by XlnR homologs (59, 60).

The *T. reesei* specific ACE2 transcription factor was isolated in a yeast expression screen designed to identify factors binding to the promoter of *cbh1* (61). While an *ace2* deletion strain resulted in a reduction in expression of the main cellulase genes, induction by sophorose was not affected in the *ace2* deletion strain (62). These observations imply that sophorose and cellulose use somewhat different induction mechanisms.

Most recently, work in *N. crassa* led to the identification of two conserved transcription factors (CLR-1 and CLR-2) that are required for growth on crystalline cellulose, but are not required for growth on xylan (63). While a specific mechanism of action has yet to be determined, based on sequencing it is predicted that CLR-1 regulates *clr-2* as well as the genes required for efficient import and utilization of cellobiose (NCU08755, the β-glucosidase *gh3-3*; NCU08114, the cellodextrin transporter *cdt-2*). Following this initial response, CLR-2 regulates the genes required for more complex lignocellulose degradation (including 16 cellulases and 6 hemicellulases).

1.3 Research objectives

While historically the ability of *T. reesei* to mass-produce plant cell wall degrading enzymes was enhanced by random mutagenesis (9), we expect that a better understanding the underlying mechanisms will provide us with the knowledge to begin rationally engineering organisms, including but not limited to *H. jecorina*. The work performed here has helped support several hypotheses in the field. Chapter 2 examines the role of β-glucosidase enzymes while Chapter 3 examines the transport of cellobiose into the cell and how this transport relates to cellulase induction.

Specifically, in Chapter 2 we show that a strain lacking the major β-glucosidase enzymes induces cellulases in response to cellobiose. This induction recapitulates, on both a transcriptional and protein level, the wild-type response to crystalline cellulose. In Chapter 3,we examine three specific cellodextrin transporters and show that deletion of two results in a strain completely unable to induce the transcription and secretion of cellulases in response to crystalline cellulose. This work indicates that these two transporters are required for *N. crassa* to sense cellulose in its environment; while this process is not yet fully understood, it implies that cellobiose is recognized intracellularly as the signal for the presences of insoluble cellulose in its environment.

2 Induction of lignocellulose degrading enzymes in *Neurospora crassa* by cellodextrins

Partially taken from: Znameroski EA, Coradetti ST, Roche CM, Tsai JC, Iavarone AT, Cate JH, Glass NL (2012). Induction of lignocellulose-degrading enzymes in *Neurospora crassa* by cellodextrins. *Proceedings of the National Acadamy of Sciences of the United States of America*. 109(16):6012-7.

Author contributions: EAZ, STC, CMR, JCT, ATI, JHDC and NLG designed research; EAZ, STC, CMR, JCT and ATI performed research; EAZ, STC, CMR, JCT, ATI, JHDC and NLG analyzed data; and EAZ, JHDC and NLG wrote the paper.

2.1 Introduction

Liquid biofuels produced from lignocellulosic biomass are an environmentally clean and renewable source of energy that could displace a significant fraction of the current demand for petroleum (64, 65). However, the costs associated with conversion of insoluble polysaccharides in plant cell walls to easily fermentable sugars represent significant barriers to the production of cost-competitive biofuels (8). Filamentous fungi have the capacity to secrete large amounts of lignocellulosic enzymes that release fermentable sugars from plant cell walls, and this ability has been exploited by industry to produce cellulases in quantities exceeding 100 g/L of culture (66).

The ability to control the induction of enzyme production is crucial for the economics of biofuel production from lignocellulose. The best inducers of plant cell wall degrading enzyme expression by filamentous fungi are insoluble substrates that include cellulose, hemicellulose or mixtures of plant polymers. However, the use of insoluble substrates to induce enzyme secretion is not ideal for industrial processes. Since these naturally inducing substances cannot enter fungal cells, it is generally believed that oligosaccharides released from the polymers and their derivatives function as the actual molecules that trigger enzyme induction (12). Cellobiose, the major soluble end product of cellulases, moderately induces cellulase gene expression and activity in *Hypocrea jecorina (Trichoderma reesei)* (23) and *Aspergillus* species (24), which are commonly used fungi for high-level enzyme production (25). However, cellobiose is unable to induce cellulase gene expression in the more distantly related fungus *Phanerochaete chrysosporium*, which instead responds to cellotriose or cellotetraose (26). Notably, the oligosaccharide sophorose, which can be generated by transglycosylation of cellobiose by an extracellular β-glucosidase, acts as a potent inducer of cellulases in *T. reesei* (17, 18), although differences in both gene expression and protein production are apparent in cellulose versus sophorose-induced cultures (67, 68). Sophorose does not induce cellulase gene expression or activity in *A. niger* (21) or *P. chrysosporium* (22). A complicating factor in understanding the regulation of cellulase gene expression is the potent inhibition of cellulase production due to carbon catabolite repression (CCR) (12) by the end product of cellulose hydrolysis, glucose. Previous studies in *T. reesei* have shown that Nojirimycin inhibition of β-glucosidase, the enzyme that converts cellobiose into glucose in the final step of cellulose hydrolysis, allows a moderate induction of cellulases by cellobiose (27, 28).

In this study, we use the model cellulolytic fungus *Neurospora crassa* (10) to show that deletion of key genes encoding predicted extracellular and intracellular β-glucosidase enzymes allow cellobiose to induce cellulase gene expression to the same level as insoluble cellulose. Further deletion of *cre-1*, which encodes a carbon catabolite repressor transcription factor (47), enables *N. crassa* to produce a higher level of secreted active cellulases when induced with cellobiose, as compared to enzyme levels observed on growth on crystalline cellulose (Avicel). An analysis of the transcriptome and secretome of these deletion strains lays the foundation for understanding the molecular mechanism underlying the induction of lignocellulose degrading enzymes in filamentous fungi. These results also provide insights that can be applied to industrial fungi that produce high levels of cellulases.

2.2 Production and characterization of deletion strains

2.2.1 Introduction to Mating

The first historical report of *N. crassa* dates back to 1843 (69), when it was reported as a contaminant of French bakeries and since has been well developed as a model organism for genetic studies. Because of its long history, both sexual and asexual reproduction are well understood (Fig. 2-1). The majority of the time, *N. crassa* grows as haploid mycelia. Nutrient depletion and light results in the formation of macroconida on aerial hyphae that rely on wind for dispersal. To undergo reproduction via the sexual cycle, the parents must be of opposite mating types (*a* and *A*), however either mating type can act as a female/male. The female forms multicellular protoperithecia, which are fertilized by single conidia from the male strain of the opposite mating type. When the female recognizes the pheromone released by the male conidia, the trichogyne grows towards it with eventual contact and cell fusion. Following nuclear fusion, these diploid nuclei undergo meiosis followed by mitosis resulting in the formation of eight haploid ascospores, each of which will develop into a haploid colony (69).

2.2.2 Characterization of the single β-glucosidase deletion strains

Lignocellulolytic genes are not induced nor is cellulolytic enzyme activity detected when wild-type *N. crassa* (WT) is grown on either sucrose or cellobiose as the sole carbon source (Fig. 2-2), even when allowed to grow into conditions of starvation. We hypothesized that when *N. crassa* is grown on cellobiose, the glucose produced by β-glucosidase enzymes masks the inducing capacity of cellobiose (Fig. 2-3). While the genome of *N. crassa* encodes at least 7 genes encoding predicted β-glucosidase enzymes, a previous systems-level study indicated that only three (NCU00130, NCU04952 and NCU08755) showed a significant increase in transcription during growth on Avicel or *Miscanthus* (Fig. 2-4) (10). NCU00130 encodes an intracellular member of the glycosyl hydrolase family one (GH1-1) (32). Glycosyl hydrolase family three member NCU04952 (GH3-4) was identified by mass spectrometry in the supernatant of a *N. crassa* culture grown on Avicel and *Miscanthus* while NCU08755 (GH3-3) was identified in the cell wall fraction of conidia (70) and its enzymatic activity was recently verified (71). All three β-glucosidase proteins show significant homology to both predicted and experimentally verified β-glucosidase enzymes in other filamentous fungi (Fig. 2-5). Based on the expression data, we predicted that GH1-1, GH3-3 and GH3-4 would be

most relevant to converting cellobiose to glucose when *N. crassa* was grown on either Avicel or cellobiose as sole carbon sources.

To examine the hypothesis that cellobiose induces cellulase gene expression in *N. crassa*, we tested whether the expression of three major cellulase genes (*cbh-1*, NCU07340, *cbh-1*; NCU09680, *gh6-2*; and NCU00762, *gh5-1*) were induced in strains carrying deletions in the β-glucosidase genes *gh1-1, gh3-3* or *gh3-4* via a transfer experiment (see Methods 2.6.8). Following a 4 hour induction with 0.2% cellobiose (Fig. 2-6), the individual β-glucosidase deletion strains (Δ*gh1-1,* Δ*gh3-3* or Δ*gh3-4*) did not show a significant induction of *cbh-1, gh6-2* or *gh5-1* expression. In addition, the single β-glucosidase deletion strains did not show a significant growth phenotype on sucrose, cellobiose or Avicel (Fig. 2-7), implying that there is redundancy between the β-glucosidase enzymes. To eliminate this redundancy, double and triple mutant strains carrying different combinations of β-glucosidase gene deletion sets were also constructed (Methods 2.6.2).

2.2.3 Production and characterization of multiple β-glucosidase deletion strains

Each of the multiple deletion strains was genotyped using two different sets of PCR primers. The first used a hygromycin-specific forward primer and a gene-specific reverse primer (outside of the deletion cassette); a product for this reaction indicates that the knockout cassette was inserted properly. The second set used a forward primer specifically designed to be within the gene and a gene-specific reverse primer (outside of the deletion cassette); a product for this reaction indicates the presence of an intact gene (Fig 2-8). Again, we examined if the expression of three major cellulase genes (*cbh-1*, NCU07340, *cbh-1*; NCU09680, *gh6-2*; and NCU00762, *gh5-1*) were induced with 0.2% cellobiose via a transfer experiment (Fig. 2-9). While cellobiose was not able to significantly increase the expression of our three representative cellulases in a strain lacking both *gh1-1* and *gh3-4* (Δ*gh1-1*; Δ*gh3-4*), the strain lacking *gh3-4* and *gh3-3* (Δ*gh3-3;* Δ*gh3-4*) had a ten-fold increase in induction over the WT strain and the strain lacking both *gh3-3* and *gh1-1* (Δ*gh1-1* Δ*gh3-3*) was equivalent to about 90% the WT induction by Avicel. Finally, the expression of our three representative cellulases in strain lacking all three β-glucosidase genes (Δ3βG: Δ*gh1-1* Δ*gh3-3*; Δ*gh3-4*) was able to show full induction when transferred to cellobiose as compared to the WT transferred to Avicel. In addition, while all of the double deletion strains only showed a mild growth phenotype on cellobiose and Avicel (Fig. 2-10), the Δ3βG strain had a significant reduction in growth on cellobiose and Avicel while its growth on sucrose was unaffected (Fig. 2-11).

The transcriptional response in the Δ3βG mutant was specific for cellobiose and was not due to starvation as the expression of *cbh-1* and *gh5-1* in WT and the Δ3βG strain when transferred to media lacking any carbon source showed only a small increase in transcription levels (less than 50-fold induction). These values are negligible when compared to the ~20,000-fold (minimum) induction of *cbh-1* and *gh5-1* by Avicel in WT *N. crassa* and in the Δ3βG strain shifted to cellobiose (Fig. 2-12). This data supports the hypothesis that cellobiose can act as an inducer of cellulases and prompted us to do a more thorough characterization of the Δ3βG strain using both transcriptomics and proteomics.

2.2.4 Alternative inducers

While the above indicates that cellobiose acts as an inducer of cellulases in *N. crassa*, it is unable to induce cellulase gene expression in the more distantly related fungus *P. chrysosporium*, which instead responds to cellotriose or cellotetraose (26). We therefore examined if longer cellodextrins could induce cellulases in *N. crassa*. Following a transfer experiment similar to those described above, we found that cellotriose and cellotetraose were unable to induce the expression of three major cellulase genes (*cbh-1*, NCU07340, *cbh-1*; NCU09680, *gh6-2*; and NCU00762, *gh5-1*) in the WT strain following a 4 hour induction (Fig. 2-13). In contrast to these results, the Δ3βG strain showed similar relative expression levels of *cbh-1, gh5-1* and *gh6-2* when shifted to cellobiose, cellotriose or cellotetraose. Interestingly, while the induction of cellobiose and cellotetraose are equivalent, when the Δ3βG strain is transferred to cellotriose the induction is slightly less. Given that cellobiohydrolase enzymes (72, 73) show activity on cellotriose we expect that the cellotriose is cleaved to cellobiose and glucose (74), which would therefore result the decreased induction. Based on these data, we expect that the results seen in *P. chrysosporium* are as a result of the presence of both extracellular and intracellular β-glucosidase enzymes and expect that if researchers were able to make a similar knockout strain that *P. chrysosporium* would respond to cellobiose as strongly as cellotriose or cellotetraose.

The most widely used soluble inducer of cellulases in the industrial species *T. reesei* is sophorose. It has been suggested that sophorose can be generated by the transglycosylation of cellobiose by an extracellular β-glucosidase (17, 18) and because the reaction is irreversible, sophorose is persistent in the environment and can therefore act as a nonmetabolizable signal. While data indicate that sophorose can be metabolized extremely slowly (75), and sophorose can be detected in trace quantities when *T. reesei* is grown on cellulose (17, 18), studies have also shown that sophorose does not replicate the induction seen by cellulose, but instead only induces a subset of the genes required for cellulose metabolism (76). Differences in both gene expression and protein production are apparent in cellulose versus sophorose-induced cultures (67, 68). In addition, sophorose does not induce cellulase gene expression or activity in *A. niger* (21) or *P. chrysosporium* (22).

The other widely used soluble inducer of cellulases in *T. reesei* is lactose (77), however the mechanism of induction is also unknown. Unlike sophorose, lactose, a disaccharide of glucose and galactose, is not expected to be found in the natural environment of plant cell wall degrading fungi. Recently, the mechanism of lactose induction was shown to be the result of β-D-galactose, a breakdown product of lactose and more likely to be encountered by filamentous fungi (78). *T. reesei*, lacks the gene encoding the mutarotase to convert β-D-galactose to α-D-galactose. As conversion to α-D-galactose is required for entrance to the Leloir pathway indicating that the metabolism of β-D-galactose requires the use of a reductive pathway (78). However, the mechanism of cellulase induction by β-D-galactose is unknown.

Because of the history using both sophorose and lactose as cellulase inducers, we examined if either sophorose or lactose could induce cellulase gene expression in *N. crassa*. As observed in other filamentous fungal species (21), transfer of either WT *N. crassa* or the Δ3βG mutant to media containing sophorose, lactose or by β-D-galactose did not significantly induce cellulase gene expression (Fig. 2-14). These results help

support the hypothesis that these molecules are not inducing cellulases through the traditional induction pathway and instead may be inducing an incomplete set of cellulases through an alternative mechanism.

2.3 Global transcriptional response to cellobiose in Δ3βG.

2.3.1 Introduction to transcriptomics.

Over the past decade researchers have made significant progress in high-throughput sequencing technologies, which has allowed for the examination of how the transcriptome changes in response to an individual signal. Before the development of high-throughput sequencing, researchers were required to either follow the expression of individual RNAs (using quantitative RT-PCR) or spend a significant amount of money developing microarrays to infer transcript abundance (relative transcript levels) from hybridization intensity. The development of next-generation sequencers has allowed researchers to inexpensively and accurately quantify the abundance of every transcript in an organism's transcriptome (79).

Sequencing a transcriptome requires very little method development as the protocols for isolating high quality RNA were developed for either RT-PCR or microarrays and once equipped with RNA the methods are standardized across samples and species. This study used the method developed by Illumina, which requires that mRNA be purified using poly(A) beads. The isolated mRNA is then sheared and reverse transcribed into cDNA. After adapters are ligated to the ends, the product is amplified before being sequenced. The recovered data go through several programs, including Tophat (80), Cufflinks and Cuffdiff (81), which maps transcripts to the *N. crassa* genome and normalizes for transcript length with the resulting data in FPKMs (fragments per kilobase of exon per million fragments mapped) (Fig 2-15). With upwards of 4 million reads and genes that go from 10 FPKMs to 127,000 FPKMs under conditions of induction, this makes analyzing changes in the transcriptome of *N. crassa* when grown under non-cellulolytic vs. cellulolytic conditions very easy to analyze.

2.3.2 Recapitulation of wild-type *N. crassa* cellulolytic response in the triple β-glucosidase mutant on cellobiose.

High-throughput sequencing (RNA-Seq) was used to assess whether the full genomic response in the Δ3βG strains to cellobiose was similar to or different from a WT strain exposed to Avicel. Scatter plots comparing full genomic patterns of gene expression changes showed that the response of the Δ3βG mutant to cellobiose closely matched that of WT *N. crassa* induced with Avicel, but was significantly different from the response of WT cultures on cellobiose or subjected to starvation (Fig. 2-16). To identify which genes were significantly and specifically induced in WT *N. crassa* in response to Avicel, a pairwise analysis was performed between expression profiles of WT *N. crassa* transferred to Avicel versus WT *N. crassa* transferred to no added carbon source. These analyses identified 321 genes (including the three deleted β-glucosidase genes) that were significantly and specifically induced in WT cultures in response to Avicel (cellulose regulon) (see Methods 2.6.12). This gene set included 16 predicted cellulase and 12 predicted hemicellulase genes. Additional genes in the cellulose regulon included 41 genes encoding proteins predicted to be active on carbohydrates by CAZy (82) and 111

genes encoding secreted proteins (signalP) (83). Of the 321 genes in the cellulose regulon, 156 encode proteins that are characterized as unclassified proteins (MIPS FunCat database) (84).

Hierarchical clustering of genes within the cellulose regulon from expression data of WT transferred to media containing no carbon source, cellobiose or Avicel and the Δ3βG strain transferred to media containing cellobiose or Avicel resulted in the identification of four distinct expression clusters (Fig. 2-17). The largest cluster (cluster 2) contained 210 genes that showed high expression in the WT strain on Avicel, as well as in the Δ3βG strain on either cellobiose or Avicel-induced conditions. This group of 210 genes contained all 16 predicted cellulases (NCU00762, *gh5-1*; NCU00836, *gh61-7*; NCU01050, *gh61-4*; NCU02240, *gh61-1*; NCU02344, *gh61-12*; NCU02916, *gh61-3*; NCU03328, *gh61-6*; NCU04854, *gh7-2*; NCU05057, *gh7-1*; NCU05121, *gh45-1*; NCU07190, *gh6-3*; NCU07340, *cbh-1*; NCU07760, *gh61-2*; NCU07898, *gh61-13*; NCU08760, *gh61-5*; and NCU09680, *gh6-2*) as well as three genes identified in previous analyses (10, 85) to be accessory proteins for cellulose degradation (NCU00206, *cdh-1*; NCU07143, *lac-2*; and NCU09764, a CBM1-containing protein). This cluster also contained 9 hemicellulase genes (NCU02343, *gh51-1*; NCU02855, *gh11-1*; NCU04997, *gh10-3*; NCU05924, *gh10-1*; NCU05955, *gh74-1*; NCU07225, *gh11-2*; NCU07326, *gh43-6*; NCU08189, *gh10-2*; and NCU09775, *gh54-1*). Of the 182 proteins remaining in this cluster, 29 are predicted to be active on carbohydrates by CAZy and 76 are predicted to be secreted by signalP, with 25 genes falling into both categories. The remaining 102 genes were grouped into their predicted functional category (84) resulting in 10 genes expected to be involved in C-compound and carbohydrate metabolism, 8 genes involved in protein folding, modification or transport, and 62 genes encoding unclassified proteins.

A small cluster of 36 genes (cluster 1) showed high expression levels in either the WT or Δ3βG deletion strain exposed to Avicel (Fig. 2-17), but had lower expression levels in the Δ3βG deletion strain on cellobiose. This group contained a predicted β-xylosidase gene (NCU09652, *gh43-5*) and several other genes encoding proteins active on hemicellulose (NCU00710, acetyl xylan esterase; NCU01900, xylosidase/arabinosidase; NCU00891, xylitol dehydrogenase; and NCU08384, xylose reductase). These results suggest that these genes were induced by the 0.5-1.0% hemicellulose found in Avicel (10) and are not part of the regulon induced by cellobiose.

When comparing the induction of the Δ3βG strain on cellobiose versus WT on Avicel, a striking pattern appears (Fig. 2-18). Genes induced in the WT by Avicel are very close to the value seen in the Δ3βG mutant. For example, the FPKM for *cbh-1* in the WT on Avicel is 126,816 ± 53,016 while the FPKM in Δ3βG on cellobiose is 130,865. This pattern extends even to the lesser-induced cellulases like NCU07760 (*gh61-2*), which has a FPKM of 239±62 for WT on Avicel and 538 for Δ3βG mutant on cellobiose. In contrast, some hemicellulase genes in the Δ3βG mutant were induced in response to cellobiose (Fig. 2-19), but to a lesser degree than in WT and the Δ3βG cultures induced by Avicel. For example, while NCU05924 (endoxylanase, *gh10-1*) has 20,023 ± 9,888 FPKMs in WT induced with Avicel, an expression level of 10,000 FPKMs was observed in the Δ3βG mutant induced with cellobiose. These results indicate that while all of the cellulase genes are in the same regulon, the hemicellulase genes are divided into those that are coordinately regulated with cellulases and those that require an additional signal for full induction.

The third cluster contained 67 genes that showed no response to conditions of starvation, but were most highly induced by cellobiose in WT (Fig. 2-17). This cluster can be further subdivided into two groups: 31 genes that were most highly induced in the WT strain by cellobiose, but were not induced by the Δ3βG strain, and 36 genes that are moderately induced by cellobiose in the WT and Δ3βG strains, but were most highly induced in the Δ3βG strain in response to Avicel. The majority of these genes fall into one of two categories: unclassified proteins or proteins involved in the metabolism of amino acids, nitrogen, phosphate or carbohydrates, with only 3 that are predicted to have activity towards carbohydrates by CAZy. The final cluster contains 4 genes that are induced by cellobiose or Avicel in WT cultures, but are not induced by the Δ3βG mutant when challenged with either cellobiose or Avicel. Three of the four were predicted to be active on carbohydrates by CAZy, and one, NCU08087 (*gh26-1*) is predicted to be a hemicellulase (10).

2.3.4 Addition of Cre1 to Δ3βG – RT-PCR.

Carbon catabolite repression (CCR) acts in filamentous fungi to repress cellulase and hemicellulase gene expression in the presence of preferred carbon sources, such as glucose or sucrose, even when lignocellulose is present in the culture (12). The C2H2 zinc finger transcription factor CreA/CRE1/CRE-1 (46) plays a key role in CCR as strains lacking CreA/CRE1/CRE-1 in *Aspergillus sp., T. reesei* and *N. crassa*, respectively, produce increased amounts of both cellulases and hemicellulases when grown on cellulose or hemicellulose (47, 86, 87). Consistent with previous data (47), quantitative RT-PCR analysis of RNA isolated from an *N. crassa cre-1* deletion strain (ΔNCU08807 or Δ*cre-1*) showed that the basal expression of *cbh-1* and *gh5-1* increased about ten-fold relative to a WT strain (Fig. 2-12). When shifted from sucrose to 0.2% cellobiose for 4 hours, the Δ*cre-1* strain showed increased induction of *cbh-1*, *gh5-1* and *gh6-2* (3,000-, 500-, and 85-fold, respectively). However, the level of induction in the Δ*cre-1* mutant was significantly lower than induction levels obtained for WT *N. crassa* exposed to Avicel or the Δ3βG mutant exposed to cellobiose (Fig. 2-6 and Fig. 2-12). Notably, a Δ3βG strain that also carried the Δ*cre-1* deletion (Δ3βGΔcre) exhibited stronger induction of *cbh-1, gh5-1* and *gh6-2* than either the WT strain shifted to Avicel or the Δ3βG strain shifted to cellobiose (Fig. 2-20). These data indicate that the induction of cellulase gene expression in the Δ3βG mutant when exposed to cellobiose is comparable to induction by cellulose and is not a consequence of relief from CCR.

2.4 Protein production by the Δ3βG strain in a bioreactor

2.4.1 Transcription of plant cell wall degrading enzymes in the Δ3βG mutant correlates with cellulase secretion and activity.

Historically, studies examining cellulases in filamentous fungi have used transcription as a readout for enzyme induction (26, 88). To determine whether the transcriptional response of the Δ3βG and Δ3βGΔ*cre* strains in response to cellobiose corresponds to an increase in functional protein, we assessed secreted proteins and cellulase activity of the Δ3βG and Δ3βGΔ*cre* strains in response to induction with either cellobiose or Avicel, as compared to WT cultures. As expected, supernatants from all sucrose-grown cultures (Δ3βG, Δ3βGΔ*cre* and WT) were unable to produce glucose or cellobiose from

crystalline cellulose in an Avicel hydrolysis assay, while supernatants from all three Avicel–induced cultures (Δ3βG, Δ3βGΔ*cre* and WT) were able to degrade crystalline cellulose to cellobiose and glucose (Fig. 2-21). When grown on cellobiose, the Δ3βG and Δ3βGΔ*cre* strains displayed a secreted protein pattern similar to WT Avicel-grown cultures (Fig. 2-21) (10). Importantly, supernatants from both the Δ3βG and Δ3βGΔ*cre* deletion strains induced by cellobiose hydrolyzed crystalline cellulose, while supernatants from WT cellobiose-grown cultures did not. The Δ3βG and Δ3βGΔ*cre* strains, which lack three β-glucosidases, produced mostly cellobiose. These data are consistent with the hypothesis that the three β-glucosidase enzymes provide the bulk of the glucose-generating activity in WT cultures (74).

2.4.2 Expression of plant cell wall degrading enzymes in the Δ3βG mutant using a bioreactor.

Filamentous fungi used extensively by industry are grown in submerged cultures for high-level production of a variety of products including antibiotics, metabolites such as citric acid, and enzymes such as glucoamylase and cellulases (89). We therefore examined the induction of cellulases in the Δ3βG and Δ3βGΔ*cre* deletion strains in a controlled bioreactor process (Fig. 2-22). After 24 hours growth on sucrose, WT, Δ3βG and Δ3βGΔ*cre* produce a similar amount of biomass (~3.5 g/L) (Fig. 2-17A-C). After induction with 0.2% cellobiose, WT *N. crassa* did not secrete a significant amount of protein (0.05 mg/mL; Fig. 2-22C). In contrast, the Δ3βG and Δ3βGΔ*cre* cultures produced 0.12 mg/mL and 0.24 mg/mL, respectively, total protein concentration in the supernatant (Fig. 2-22A-B). In addition, the cellobiose-induced Δ3βG and Δ3βGΔ*cre* cultures showed a significant increase in endoglucanase activity over this same period of induction (Fig2-23D). Examining the aggregate Avicelase activity from the 24 hour time point indicated that the Δ3βGΔ*cre* strain produced 60% more glucose equivalents (0.424 mg/mL) as compared to the Δ3βG strain (0.296 mg/mL) (Fig. 2-23A). However, when the total concentration of protein was normalized, the Δ3βGΔ*cre* strain had less specific activity than either the WT or Δ3βG culture supernatants (Fig. 2-23B-C). These data indicate that while the addition of the *cre-1* deletion to Δ3βG strain allowed for greater protein secretion, this secretion was not specific for cellulases.

2.4.6 Proteomic analysis of secreted proteins.

In order to compare the identity of proteins secreted by WT *N. crassa* grown on Avicel versus the Δ3βG strains when induced with cellobiose, we analyzed the secretome using a shotgun proteomics approach (Table 2-2). There were 39 proteins identified in the WT *N. crassa* Avicel-grown culture supernatant. In cellobiose-grown cultures, 38 proteins were identified in the Δ3βG broth and 24 were identified in the Δ3βGΔ*cre* broth (Table 2-3). Using quantitative mass spectrometry Phillips, *et al*. concluded that 76% of the WT *N. crassa* secretome on Avicel is composed of six individual proteins (85). All of these proteins were identified in the WT, Δ3βG and Δ3βGΔ*cre* culture broths (except for the deleted β-glucosidase, *gh3-4*) (Table 2-2). In addition to the cellulases, we identified a number of lower abundance accessory proteins which make up a total of 6.5% of the secretome (85): a cellobiose dehydrogenase (CDH-1), a type 2 lactonase (LAC-2) and two hypothetical proteins: NCU09764, a CBM1-containing protein of unknown function, and NCU05137, a gene that when deleted leads to an increase in cellulase activity (10).

These data indicate that, similar to the transcriptional response of the Δ3βG mutant to cellobiose, the identity of proteins secreted and the amount of protein secreted in the Δ3βG strain on cellobiose mimicked the WT *N. crassa* response to Avicel.

2.5 Discussion

In this study, we examined the hypothesis that cellobiose functions as an inducer of cellulase gene expression and secretion when filamentous fungi, such as *N. crassa*, are exposed to cellulose, but that the action of extracellular and intracellular β-glucosidases and CCR mask this inducing activity. Our results revealed that a strain of *N. crassa* carrying deletions for the three major β-glucosidases induces cellulases when exposed to cellobiose and this induction recapitulates, on both a transcriptional and protein level, the WT response to Avicel.

While many industrially focused studies have attempted to determine the best inducers of lignocellulose degrading enzymes, little is known about the molecular mechanism of this induction. Early studies used the β-glucosidase inhibitor Nojirimycin to show that cellobiose induces cellulases in the lignocellulose-degrading filamentous fungus, *T. reesei* (27, 28). However, this induction was not as robust as with other soluble inducers including lactose (77) and sophorose (18). While both molecules have been used extensively to induce cellulases in *T. reesei*, neither can induce the complete set of cellulases generated in response to cellulose (68, 76). In contrast to these results, exposure of the Δ3βG mutant to cellobiose recapitulated the response of WT strain to Avicel.

Our results indicate that deletion of the predicted major β-glucosidase genes enabled *N. crassa* to induce both transcription and secretion of the complete repertoire of cellulases upon exposure to cellobiose. In *P. chrysosporium*, cellobiose does not induce cellulase gene expression (26), although cellotriose or cellotetraose were able to do so. We hypothesize that in *P. chrysosporium*, as in *N. crassa*, any inducing affect of cellobiose is masked by its degradation to glucose by endogenous β-glucosidases, leading to catabolite repression. In addition, our results indicate that sophorose does not act as an inducer in *N. crassa*. In *T. reesei* sophorose is likely produced by a transglycosylation of cellobiose by an extracellular β-glucosidase (17) and readily transported into the mycelium by a β-linked disaccharide permease (31). However, in the *N. crassa* Δ3βG mutant all of the predicted extracellular β-glucosidase enzymes were deleted suggesting that transglycosylation of cellobiose to sophorose is not relevant to cellulase induction. Given the high conservation of the lignocellulose degrading machinery in filamentous fungi, we predict that deletion of the bulk of β-glucosidase activity in other fungi would enable the use of cellobiose for full induction of the cellulose regulon in these species.

An advantage for the industrial production of cellulolytic enzymes in *T. reesei* is the ability to use a soluble inducer, although different genes are induced by lactose/sophorose when compared to cellulose induction (68, 76). Since the action of sophorose is not generally applicable to other filamentous fungi, we predict that the production of cellulases in filamentous fungi will be possible upon exposure to cellobiose, providing that either mutational inactivation or chemical inhibition of their major β-glucosidases associated with plant cell wall utilization can be achieved. Since the number of predicted cellulases and hemicellulases in the genomes of filamentous fungi varies considerably, this approach may provide a tool for analysis of such proteins

in a soluble environment, avoiding the complication of separating enzymes from insoluble plant cell wall material. Furthermore, a considerable number of unclassified and hypothetical proteins are induced as part of the *N. crassa* cellulose regulon, many of which are secreted or are predicted to be secreted. A comparative analysis of the cellulose regulon in a variety of filamentous fungi should reveal which of these genes/proteins are conserved and thus worthy of further characterization. By understanding the mechanism of cellulase induction and utilization in a model organism using reverse genetics, we expect that this knowledge can be translated into currently used industrial filamentous fungi, to further improve their ability to produce lignocellulose degrading enzymes and allow for the production of a renewable source of cost-competitive biofuels.

2.6 Methods

2.6.1 Strains

All strains were obtained from the Fungal Genetics Stock Center (FGSC) (90, 91). The homokaryon *cre-1* deletion strain (Δ*ncu08807*) was created by Jianping Sun (47). Multiple deletion strains were made by performing sequential crosses as described on the FGSC website (92). The mating type was determined using the mating type tester strains fl(OR) A (FGSC 4317) and fl(OR) a (FGSC 4347) (92).

2.6.2 Mating

Conidia from the parent strain of one mating type were plated on a Westergaard's plate and the conidia from the other parent of the opposite mating type were inoculated onto a minimal media slant. Both the plate and the slant were incubated in the dark at 30°C for 2-3 days to allow for sufficient hyphal growth. They were then placed at room temperature in the light for an additional 5-7 days to allow for the development of protoperithecia (on the plate) and conidia (on the slant). After visual confirmation of protoperithecia, the conidia were resuspended in 2 mL of sterile water and diluted 1:100. Approximately 100 µL of this dilution was added to the plate and gently spread using a pipette tip. The plates were then allowed to undergo mating for approximately 2 weeks, with the result being the production of ascospores which are ejected from the perithecium and adhere to the lid of the petri plate. The ascospores were collected by pipetting 1 mL of water onto the lid and then collecting in a 1.5-mL microfuge tube. The ascospores were stored at 4°C.

2.6.3 Germination and selection of ascospores

The ascospores were counted using a hemocytometer and diluted to approximately 500 ascospores per 100 µL water. This dilution underwent a 60°C heat shock for 30 minutes and the entire volume was plated on a minimal media plate supplemented with 200 µg/mL hygromycin as a selection for the knockout genotype. The ascospores were allowed to germinate for 16 hours, right side up at room temperature. Using a dissecting microscope the germinated ascospores were carefully cut out of the plate and transferred to a minimal media slant. This slant was grown for 2 days in the dark at 30°C and then transferred to room temperature for an additional 3 days. Each slant was subcultured, and the genomic DNA was extracted for genotyping.

2.6.4 Genomic DNA extraction

Conidia were isolated by adding 2 mL water to each slant and vortexing for 5-10 seconds. The resulting slurry was transferred to a 2-mL screw cap tube and conidia were pelleted at 4000 rpm for 4 minutes. The supernatant and floating mycelia were removed and ~0.3 g of 0.5 mm silica beads and 400 µL of lysis solution (0.05 M NaOH, 1 mM EDTA, 1% Triton-X 100) was added to the pelleted conidia. The sample was shaken in a bead beater for 2 minutes and placed in a 65°C water bath for 30 minutes, vortexing 2-3 times during the incubation to mix. After the addition of 80 µL of 1 M Tris pH 7.5, samples were centrifuged at max speed in a bench top centrifuge (5 minutes) and the supernatant was removed. An equal volume of phenol-chloroform was added; samples were again vortexed briefly to mix and then centrifuged again for 10 minutes at max speed. The aqueous phase was transferred to a new tube with 600 µL ice-cold ethanol and placed at -20°C for at least one hour, but typically overnight to precipitate the genomic DNA. After precipitation, the sample was centrifuged for 15 minutes at 4°C and the pellet was washed with 75% ethanol. The resulting pellet was dried in a speedvac for 10 minutes at 30°C and resuspended in 100 µL water. The concentration was examined using a Nanodrop and volume adjusted to produce 300 ng/µL final concentration.

2.6.5 Genotyping multiple deletion strains

The genotype of each deletion strain was confirmed by performing two different PCR reactions. The first used a gene-specific primer and a common primer for the hygromycin (hph) cassette to confirm the presence of the cassette. The primer for hph was 5'-CGA CAG ACG TCG CGG TGA GTT CAG-3'. Reverse primers were:
NCU00130: 5'-TAG TGT ACA AAC CCC AAG C-3'
NCU004952: 5'-AAC ACA CAC ACA CAC ACT GG-3'
NCU08755: 5'-ACA GTG GAG GTG AGA AAG G-3'
NCU08807: 5'-GTA CTT ACG CAG TAG CGT GG-3'
NCU00801: 5'-TTA GGG TTG TAG ACA CCT GC-3'
NCU08114: 5'-GAC GAC CAG AAC TAG GTA GG-3'
NCU05853: 5'-GAG CAA GGT TAT AGG ACT GC-3'

The second reaction used both a gene specific forward primer and a gene specific reverse primer. The presence of a product in this reaction indicates a wild-type copy of the specific gene. The forward primers were:
NCU00130: 5'-ACA TCA AGC ACA AGA AGG GCG TC-3'
NCU04952: 5'-CCT CAA AAT ATG CAG CCT ACA CGA-3'
NCU08755: 5'-ACG ACA TCA TGT ACA CTG TTA CGG-3'
NCU08807 5'-CAC TCA AAG GAA ACT TCC TGT GCC-3'
NCU00801: 5'-GGC CGC TTA CTT CCT CTT CAA CG-3'
NCU08114: 5'-GCT CAA TAC TTA TGC GAA CCC TGT-3'
NCU05853: 5'-ATA ACA TGG GTT ATA ACG CCC TGA-3'
and the reverse primers were the same as above. In each reaction the presence of a 1500 bp product indicated proper amplification for the reaction.

2.6.6 Phenotyping multiple deletion strains

Conidia from strains were inoculated at a concentration equal to $2x10^6$ conidia per milliliter into 100 mL Vogel's salts (93) with 2% w/v sucrose, cellobiose or Avicel in a 250-mL Erlenmeyer flask and grown under constant light at 200 rpm for 2 days (sucrose), 5 days (cellobiose) and 7 days (Avicel). Photos were taken daily.

2.6.6 4-Methylumbelliferyl β-D-cellobioside (MuLac) assay

Cellobiohydrolase I activity was measured using 4-Methylumbelliferyl β-D-cellobioside (MuLac). Each assay was run in triplicate by mixing 20 µL filtered culture supernatant combined with 80 µL MuLac reagent (1.0 mM MuLac and 50 mM NaAc pH5) in a black 96 well, clear bottom plate and read in a plate reader using an assay to measure the MuLac kinetics. Time points were read every 15 seconds for 10 minutes using 360 nm excitation and 465 nm emission. The slope of the resulting line represents the relative amount of cellobiohydrolase I activity as a function of time.

2.6.5 Phylogenetic analysis

GenBank accession numbers (PID), Joint Genome Institute protein ID (JGI), or Broad Institute Fusarium Comparative Database Genes (FGSG) numbers for β-glucosidases used in phylogenetic analysis are as follows. For NCU08755: *Myceliophthora thermophila*, JGI 80304; *A. niger*, PID 254674400; *P. chrysosporium*, PID 19352194; *T. reesei*, JGI 121735; *Fusarium graminearum*, FGSG_06605; *Sclerotinia sclerotiorum*, PID 156051478; *Botryotinia fuckeliana*, PID 154301968; *Penicillium chrysogenum*, PID 255942539; *Schizophyllum commune*, JGI 256304; and *Postia placenta*, JGI 107557. For NCU00130: *M. thermophila*, JGI 115968; *A. niger*, PID 213437; *P. chrysosporium*, PID 127920; *T. reesei*, JGI 120749; *F. graminearum*, FGSG_07274; *S. sclerotiorum*, PID 156037816; *B. fuckeliana*, PID 156037816; *P. chrysogenum*, PID 255941826; *S. commune*, JGI 57050; and *P. placenta*, JGI 45922. For NCU04952: *M. thermophila*, JGI 66804; *A. terreus*, PID 115401928; *P. chrysosporium*, PID 3320413; *T. reesei*, JGI 76672; *S. sclerotiorum*, PID 156050519; *B. fuckeliana*, PID 154293970; *P. chrysogenum*, PID 255945487; *S. commune*, PID 302694815.

All proteins used in the alignments were identified using BLASTp. Homologous proteins sequences were aligned in MEGA5 using ClustalW. Maximum Likelihood phylogeny was determined using the Poission model to estimate distances and the Nearest-Neighborhood-Interchange (NNI) tree searching strategy with 500 bootstrap replications (94, 95).

2.6.6 Starvation studies

Conidia from strains were inoculated at a concentration equal to $2x10^6$ conidia per milliliter into 100 mL Vogel's salts (93) with 1% w/v sucrose in a 250-mL Erlenmeyer flask and grown under constant light at 200 rpm for 4 days. Two milliliters supernatant was removed at 1, 2, 3.5, 3 and 3.5 days. Samples were spun at 4000 rpm for 5 minutes to pellet biomass and the supernatant was filtered through a 0.2 µM PES filter before being stored at -20˚C until all samples were collected. When all time points were collected, 15 uL of unconcentrated supernatant was run on a Criterion 4-14% Tris-HCl polyacrylamide gel and stained with Thermo Scientific GelCode Blue Stain Reagent. In addition, the total Avicelase activity was measured as described below.

2.6.7 Examination of *T. reesei* inducers

Conidia from strains were inoculated at a concentration equal to $2x10^6$ conidia per milliliter into 50 mL Vogel's salts (93) with 2% w/v sucrose in a 250-mL Erlenmeyer flask and grown under constant light at 200 rpm for 16 hours. Biomass was then spun at 4000 rpm for 10 minutes and washed in Vogel's salts (without carbon) twice to remove any excess sucrose. The biomass was divided in thirds and added to a new flask (25 mL) containing 10 mL Vogel's salts supplemented with 1% w/v sucrose, 1 mM Sophorose (Serva), 1 mM Lactose (Sigma), 1mM D-(+)-Galactose (Sigma) or 1% w/v Avicel PH 101 (Sigma). Cultures were induced for 4 hours under constant light at 200 rpm. The culture biomass was then harvested by filtration over a Whatman glass microfiber filter (GF/F) on a Buchner funnel and washed with 50 mL Vogel's salts. The biomass was flash frozen in liquid nitrogen and stored at -80°C. The RNA was isolated and Quantitative RT-PCR were performed as described below.

2.6.8 Transcriptional studies

Conidia from strains were inoculated at a concentration equal to $2x10^6$ conidia per milliliter into 50 ml Vogel's salts (93) with 2% w/v sucrose in a 250-mL Erlenmeyer flask and grown under constant light at 200 rpm for 16 hours. Biomass was then spun at 4000 rpm for 10 minutes and washed in Vogel's salts (without carbon) twice to remove any excess sucrose. The biomass was then added to a new flask containing 50 mL Vogel's salts supplemented with 1% w/v sucrose, 0.2% w/v cellobiose (Sigma) or 1% w/v Avicel PH 101 (Sigma). Cultures were induced for 4 hours under constant light at 200 rpm. The culture biomass was then harvested by filtration over a Whatman glass microfiber filter (GF/F) on a Buchner funnel and washed with 50 mL Vogel's salts. The biomass was flash frozen in liquid nitrogen and stored at -80°C. Three independent biological duplicates (flasks) were evaluated for each time point.

2.6.9 RNA isolation

RNA was prepared as previously described (10). Total RNA from frozen samples was isolated using Zirconia/Silica beads (0.5-mm diameter; Biospec) and a Mini-Beadbeater-96 (Biospec) with 1 mL TRIzol reagent (Invitrogen) according to the manufacturer's instructions. The total RNA was further purified by digestion with TURBO DNA-free (Ambion) and an RNeasy kit (Qiagen). RNA concentration and integrity was checked by Nanodrop and agarose gel electrophoresis.

2.6.10 Quantitative RT-PCR

Quantitative RT-PCR was performed using the EXPRESS One-Step SYBR GreenER Kit (Invitrogen) and the StepOnePlus Real-Time PCR System (Applied Biosystems). Reactions were performed in triplicate with a total reaction volume of 10 µL including 300nM each forward and reverse primers and 75 ng template RNA. Data analysis was performed by the StepOne Software (Applied Biosystems) using the Relative Quantitation/Comparative CT ($\Delta\Delta$CT) setting. Data was normalized to the endogenous control actin with expression on sucrose as the reference sample.

2.6.11 RT-PCR primers

The primers for actin (NCU4173) were: forward 5'-TGA TCT TAC CGA CTA CCT-3' and reverse 5'-CAG AGC TTC TCC TTG ATG-3'. The primers for *cbh-1* (NCU07340) were: forward 5'-ATC TGG GAA GCG AAC AAA G-3' and reverse 5'-TAG CGG TCG TCG GAA TAG-3'. The primers for *gh6-2* (NCU09680) were: forward 5'-CCC ATC ACC ACT ACT ACC-3' and reverse 5'-CCA GCC CTG AAC ACC AAG-3'. The primers for *gh5-1* (NCU00762) were: forward 5'- GAG TTC ACA TTC CCT GAC A-3' and reverse 5'-CGA AGC CAA CAC GGA AGA-3'. RT-PCR primers were previously identified and optimized in Tian, *et al*. (10) and Dementhon, *et al*. (96).

2.6.12 mRNA sequencing

mRNA sequencing was performed using an Illumina kit (RS-100-0801) with RNA isolated as described above. The final cDNA library was quantified by an Agilent bioanalyzer 2000 (Functional Genomics Laboratory, UC Berkeley) and sequenced using an Illumina Genome Analyzer-II (Vincent J. Coates Genomic Sequencing Laboratory, UC Berkeley) using standard Illumina operating procedures. Sequenced libraries were mapped against predicted transcripts from the *N. crassa* OR74A genome (version 10) with Bowtie (80) and transcript abundance was estimated with Cufflinks in FPKMs (fragments per kilobase of exon per million fragments mapped) (81) using upper quartile normalization and mapping against reference isoforms from the Broad Institute. To establish biological variation, triplicate cultures were sampled and analyzed for the WT strain on cellulose and sucrose at 4 hours after the media shift. For all other strains and conditions, a single RNAseq library was analyzed.

2.6.13 Hierarchical clustering analysis

Genes exhibiting statistically significant expression changes between strains or growth conditions were identified with Cuffdiff, using upper quartile normalization and a minimum of mapped reads per locus. These genes were then filtered to select only those exhibiting a 2-fold change in estimated abundance between all biological replicates of each strain/condition tested and only those genes with an FPKM consistently above 10 in at least one strain/condition.

The hierarchical clustering analysis was performed using Cluster 3.0 (97) according to the FPKMs in the WT strain on cellulose, WT on cellobiose, mutant strains on cellobiose and mutant strains on cellulose. Prior to clustering, FPKMs were log transformed, normalized across strains/conditions on a per-gene basis and centered on the mean value across strains/conditions. The Pearson correlation coefficient (uncentered) was used as the similarity metric and average linkage as the clustering method.

2.6.14 Shake flask studies

Sucrose and cellobiose cultures were grown in 1% sucrose for 24 hours followed by the addition of 2% sucrose or 0.2% cellobiose. Culture supernatant was harvested after an additional 24 hours induction (WT, Δ3βG and Δ3βGΔ*cre*) or 72 hours (Δ3βG). The WT Avicel culture was grown for 5 days on 2% Avicel, Δ3βG was grown in 1% sucrose for 24 hours followed by 48 hours in 1% Avicel and Δ3βGΔ*cre* was grown in 1% sucrose for 24 hours followed by 24 hours in 1% Avicel.

2.6.15 Bioreactor studies

Cellulase production was carried out in a 3.7 L bioreactor (BioEngineering AG) at an operating volume of 1 L. The bioreactor was equipped with one 48 mm Rushton impeller and four equally spaced baffles to provide adequate mixing. Impeller speed was controlled at 200 rpm for 8 hours to allow spore germination followed by 500 rpm for the remainder of the experiment. The temperature was maintained at 25°C, and medium pH was controlled at 5.5 using 40% phosphoric acid and 1:5 diluted ammonium hydroxide. The dissolved oxygen was maintained at a level greater than 20% of the saturation value of the medium by varying the aeration rate between 0.5 and 3 VVM in response to the dissolved oxygen tension. Minimal growth medium with 1% w/v sucrose as the sole carbon source (unless otherwise noted) was inoculated with 10^9 conidia. After 24 hours initial growth, cellulase production was induced with cellobiose added to a final concentration of 0.2% w/v. Supernatant samples were collected at timepoint 0, 12 hours before induction, at induction, as well as 4, 8, 12, 24 and 36 hours post induction. Samples were spun at 4000 rpm for 5 minutes to pellet biomass and the supernatant was filtered through a 0.2 µm PES filter before being stored at -20˚C until all samples were collected.

2.6.16 Enzyme activity measurements

Total secreted proteins were measured using the Bio-Rad Protein Assay kit (Bio-Rad) and visualized by running 15 µL of unconcentrated supernatant on a Criterion 4-14% Tris-HCl polyacrylamide gel and stained with Thermo Scientific GelCode Blue Stain Reagent.

2.6.17 Enzymatic hydrolysis

Total Avicelase activity was conducted in 250-mL media bottles incubated at 50°C on a orbital shaker at 200 rpm. Each bottle contained 1% cellulose (Avicel) and 50 mM (pH 5.0) sodium acetate in a working volume of 50 mL. Tetracycline (10 µg/mL) was added to prevent microbial contamination. Bioreactor culture broth samples were buffer exchanged using a 10 kDa MWCO centrifugal filter to remove any soluble sugars prior to initiating hydrolysis experiments. After pre-incubating the hydrolysis mixture to 50°C, enzyme was added (1 mL filtered culture broth). Samples were taken every 4 hours for the first 12 hours and then every 12 hours thereafter for a total of 48 hours. Hydrolysis experiments were performed in triplicate.

2.6.18 Sugar analysis

Sucrose, fructose, glucose and cellobiose were measured on a DIONEX ICS-3000 HPLC (Dionex Corp., Sunnyvale, CA) using a CarboPac PA20 Analytical Column (3x150 mm) and a CarboPac PA20 guard column (3x30 mm) at 30°C. Following injection of 25 µL of diluted samples, elution was performed with 100 mM KOH (isocratic) at 0.4 mL/minute. Sugars were detected using PAD, Four-Potential Carbohydrate Waveform and Peaks were analyzed using the Chromeleon software package.

2.6.19 Mass spectrometry

Trypsin-digested proteins were prepared as previously described (10, 85). The culture supernatants were concentrated with 10 kDa MWCO PES spin concentrators (Sartorious

Stedim) until the protein concentration was 2-3 mg/ml. Cellulose binding proteins were isolated from the culture supernatant by addition of phosphoric acid swollen cellulose (PASC). 500 µL of a suspension of 10 mg/mL PASC was added to 1 mL culture supernatant. After incubation at 4°C for 5 minutes, the mixture was centrifuged and the pelleted PASC was then washed three times with 1 mL 100 mM sodium acetate pH 5.0. The supernatant after treatment with PASC was saved as the unbound fraction. Thirty-six milligrams urea, 5 µL of 1 M Tris, pH 8.5, and 5 µL of 100 mM DTT were then added to culture supernatant or protein-bound PASC and the mixture was heated at 60°C for 1 hour. After heating 700 µL of 25 mM ammonium bicarbonate and 140 µL methanol were added to the solution followed by treatment with 50 µL of 100 g/mL trypsin in 50 mM sodium acetate, pH 5.0. For the PASC bound proteins, the PASC was removed by centrifugation after heating, and the supernatant was then treated with trypsin. The trypsin was left to react overnight at 37°C. After digestion the volume was reduced by speedvac and washed with MilliQ water three times. Residual salts in the sample were removed by using OMIX microextraction pipette tips according to the manufacturer's instructions.

Acetonitrile (Fisher Optima grade, 99.9%) and formic acid (Pierce, 1 mL ampules, 99+%) purchased from Fisher Scientific (Pittsburgh, PA), and water purified to a resistivity of 18.2 MΩ·cm (at 25°C) using a Milli-Q Gradient ultrapure water purification system (Millipore, Billerica, MA), were used to prepare mobile phase solvents for liquid chromatography-mass spectrometry.

Trypsin-digested proteins were analyzed using an orthogonal acceleration quadrupole time-of-flight (Q-tof) mass spectrometer that was connected in-line with an ultraperformance liquid chromatograph (UPLC). Peptides were separated using a nanoAcquity UPLC (Waters, Milford, MA) equipped with C_{18} trapping (180 µm × 20 mm) and analytical (100 µm × 100 mm) columns and a 10 µL sample loop. Solvent A was 99.9% water/0.1% formic acid and solvent B was 99.9% acetonitrile/0.1% formic acid (v/v). Sample solutions contained in 0.3 mL polypropylene snap-top vials sealed with septa caps (Wheaton Science, Millville, NJ) were loaded into the nanoAcquity autosampler compartment prior to analysis. Following sample injection (10 µL), trapping was performed for 3 minutes with 100% A at a flow rate of 15 µL/minute. The injection needle was washed with 500 µL each of solvents A and B after injection to avoid cross-contamination between samples. The elution program consisted of a linear gradient from 8% to 35% B over 30 minutes, a linear gradient to 95% B over 0.33 minutes, isocratic conditions at 95% B for 3.67 minutes, a linear gradient to 1% B over 0.33 minutes, and isocratic conditions at 1% B for 11.67 minutes, at a flow rate of 500 nL/minute. The analytical column and sample compartment were maintained at 35ºC and 8ºC, respectively.

The UPLC column exit was connected to a Universal NanoFlow Sprayer nanoelectrospray ionization (nanoESI) emitter that was mounted in the nanoflow ion source of the mass spectrometer (Q-tof Premier, Waters, Milford, MA). The nanoESI emitter tip was positioned approximately 3 mm from the sampling cone aperture. The nanoESI source parameters were as follows: nanoESI voltage 2.4 kV, nebulizing gas (nitrogen) pressure 0.15 mbar, sample cone voltage 35 V, extraction cone and ion guide voltages 4 V, and source block temperature 80ºC. No cone gas was used. The collision cell contained argon gas at a pressure of $8x10^{-3}$ mbar. The Tof analyzer was operated in

"V" mode. Under these conditions, a mass resolving power (94) of $1x10^4$ (measured at *m*/*z* = 771) was routinely achieved, which was sufficient to resolve the isotopic distributions of the singly and multiply charged precursor and fragment ions measured in this study. Thus, an ion's mass and charge were determined independently, *i.e.* the ion charge was determined from the reciprocal of the spacing between adjacent isotope peaks in the *m*/*z* spectrum. External mass calibration was performed immediately prior to analysis using a solution of sodium formate. Survey scans were acquired in the positive ion mode over the range *m*/*z* = 400-1500 using a 0.45 second scan integration and a 0.05 second interscan delay. In the data-dependent mode, up to five precursor ions exceeding an intensity threshold of 20 counts/second (cps) were selected from each survey scan for tandem mass spectrometry (MS/MS) analysis. Real-time deisotoping and charge state recognition were used to select 2+, 3+, and 4+ charge state precursor ions for MS/MS. Collision energies for collisionally activated dissociation (CAD) were automatically selected based on the mass and charge state of a given precursor ion. MS/MS spectra were acquired over the range *m*/*z* = 100-2000 using a 0.20 second scan integration and a 0.05 second interscan delay. Ions were fragmented to achieve a minimum total ion current (TIC) of 30,000 cps in the cumulative MS/MS spectrum for a maximum of 2 seconds. To avoid the occurrence of redundant MS/MS measurements, real-time dynamic exclusion was used to preclude re-selection of previously analyzed precursor ions over an exclusion width of ±0.2 *m*/*z* unit for a period of 300 seconds.

Data resulting from LC-MS/MS analysis of trypsin-digested proteins were processed using ProteinLynx Global Server software (version 2.3, Waters), which performed background subtraction (threshold 35% and fifth order polynomial), smoothing (Savitzky-Golay, 10 times, over three channels), and centroiding (top 80% of each peak and minimum peak width at half height four channels) of mass spectra and MS/MS spectra. Processed data were searched against the *N. crassa* protein database (Broad Institute, Cambridge, MA). The following criteria were used for the database search: precursor ion mass tolerance 100 ppm, fragment ion mass tolerance 0.15 Da, digest reagent trypsin, allowing for up to three missed cleavages, and methionine oxidation as a variable modification. The identification of at least three consecutive fragment ions from the same series, *i.e.* β- or γ-type fragment ions (98), was required for assignment of a peptide to an MS/MS spectrum. MS/MS spectra were inspected to verify the presence of fragment ions that identify the peptides. A protein was determined to be present if at least one peptide was detected in two out of three biological replicates (whole supernatant, PASC bound or PASC unbound).

3 Transport of cellodextrins in *Neurospora crassa*

3.1 Introduction

The ability of filamentous fungi to efficiently degrade lignocellulosic biomass to its component sugars has been examined since 1950 (99). More recently, industrial biotechnology has developed these organisms to secrete cellulases in quantities greater than 100 g/L for use in the production of lignocellulosic biofuels (66).

Many studies have been performed examining the induction of cellulases and have used various inducing molecules including sophorose and lactose in *Trichoderma reesei* (18, 77). Previously, I showed that in the absence of any β-glucosidase activity, cellobiose is the shortest cellodextrin necessary and sufficient to induce the transcription, translation, and secretion of the enzymes required to degrade lignocellulose (100). While most researchers assume that the extracellular inducer is transported into the cell where it interacts with one or more proteins to result in the up-regulation in transcription of genes associated with plant cell wall deconstruction, only two studies have been published which directly examine the ability of cells to import these inducers.

The first study, published in 1993, confirmed the presence of an uptake system specific for β-linked diglucosides in *T. reesei* (31). The uptake system was inhibited by the presence of glucose and uptake was increased following sophorose treatment (induction). Despite characterization of this "β-linked diglucoside permease", no specific gene or genes were identified and therefore the authors were unable to show that such uptake was required for enzyme induction. With the recent advancements in sequencing and computational genomics one can easily able to identify genes predicted to encode such transporters. In 2009, a systematic analysis of plant cell wall degradation by the model cellulolytic fungus *N. crassa*, revealed that it increases transcription of 10 major facilitator superfamily (MFS) transporters when grown on pure cellulose (10). Transcriptional profiling of *N. crassa* after a 4 hour transfer to crystalline cellulose (Avicel), hemicellulose (xylan), cellobiose, sucrose and no carbon (starvation) revealed that only three transporter genes (NCU08114, *cdt-2*; NCU00801, *cdt-1*; and NCU05853) of the 10 showed their highest relative expression level on cellulose (Fig 3-1) (10). More recently, Galazka, *et al.* showed that *Saccharomyces cerevisiae* expressing either of two transporters (*cdt-1* or *cdt-2*, but not NCU05853), along with a gene encoding an intracellular β-glucosidase, could grow using cellobiose as the sole source of carbon – a carbon source that wild-type *S. cerevisiae* is unable to metabolize (32). Mechanistic studies indicate that both transporters act as high affinity cellobiose transporters (3-4 μM), with CDT-1 using the plasma membrane proton gradient to act as a symporter to efficiently transport cellobiose, cellotriose or cellotetraose while CDT-2 functions as a permease to equilibrate cellobiose or cellotriose (101).

In this study, I use the model cellulolytic fungus *N. crassa* to examine the role of CDT-1 and CDT-2 transporters in both the induction of plant cell wall degrading enzymes and their involvement in growth on crystalline cellulose. Using transporter deletion strains I show that CDT-1 and CDT-2 are equally involved in cellulose sensing, but that CDT-2 is most important for growth on crystalline cellulose. Furthermore, using a strain lacking β-glucosidase activity, I showed that CDT-1 and/or CDT-2 can transport cellobiose and their presence is required for the induction of plant cell wall degrading enzymes by the inducer cellobiose.

3.2 Production and characterization of deletion strains

3.2.1 Characterization of single cellodextrin transporter deletion strains

Initially, to examine the involvement of the transporters CDT-1, CDT-2 and NCU05853 in cellulose sensing and/or utilization in *N. crassa*, I confirmed and expanded the previously reported growth phenotype for the individual deletion strains (10, 32). After 36 hours, while all of the strains grew similarly to wild-type *N. crassa* on sucrose, a strain lacking *cdt-2* did not produce as much biomass on Avicel when compared to either the wild-type or the *cdt-1* deletion strain (Fig 3-2).

In order to directly examine if these CDT-1 and/or CDT-2 transporters are involved in the ability of *N. crassa* to recognize cellulose, I examined the expression of three major cellulase genes (NCU07340, *cbh-1*; NCU09680, *gh6-2*; and NCU00762, *gh5-1*) following induction with crystalline cellulose via a transfer experiment (see Methods 3.6.6). Following a 4 hour induction with 1% Avicel, the individual transporter deletion strains (Δ*cdt-1*, Δ*cdt-2* or Δ*ncu05853*) did not show a significant difference in induction levels of *cbh-1*, *gh6-2* or *gh5-1* as compared to the wild-type (Fig. 3-8). These observations suggest redundancy among the cellodextrin transporters. To eliminate this redundancy, double and triple mutant strains carrying different combinations of transporter gene deletions were constructed (see Methods 3.6.2).

3.2.2 Production and characterization of multiple cellodextrin transporter deletion strains

The single deletion strains were made by replacing the gene of interest with a cassette encoding a gene to provide resistance to hygromycin B, as described in Colot *et al*. (90), an antibiotic to which wild-type *N. crassa* is sensitive. Following crossing and selection of individual ascospores, each of the potential multiple deletion strains were genotyped using two different sets of PCR primers (Methods 3.6.5). The first used a primer specific for the hygromycin cassette and a primer that was designed to a region downstream of the deletion cassette; a product for this reaction indicates the presence of the knockout cassette at the gene of interest. The second set used a primer specifically designed to fall within the coding region of the gene and a primer that pairs with a region downstream of the deletion cassette; a product for the second reaction indicates the presence of the wild-type gene (Fig 3-3). Because the first PCR reaction is specific for the correct insertion of the deletion cassette and the second PCR reaction is specific for the wild-type copy of the gene, I confirmed that the gene of interest was deleted by a positive result for the first PCR reaction and a negative result for the second reaction. By performing PCR reactions with primers designed for each gene individually I determined if the correct recombination events occurred to result in a strain with multiple gene deletions.

Similar to our studies with the single *cdt* transporter deletion strains (above), I examined if the multiple *cdt* transporter deletion strains showed a phenotype with regards to either cellulose sensing or utilization of cellulose using both growth assays and transcriptional response assays, as described above. The growth assay indicated that the strain lacking all three transporters (Δ3T: Δ*cdt-2* Δ*cdt-1*; Δ*ncu05853*) as well as the strain lacking *cdt-1* and *cdt-2* (Δ2T; Δ*cdt-2* Δ*cdt-1*) were almost completely unable to grow on crystalline cellulose, while their growth on sucrose appeared equivalent to wild-type.

Strains lacking NCU05853 and either *cdt-1* or *cdt-2* were identical in growth to the single deletion strains (Fig 3-4).

To examine the initial response to cellulose in these mutants, I compared the change in expression levels of three major cellulase genes (*cbh-1*, *gh6-2*, and *gh5-1*) following 4 hours induction with 1% Avicel (Fig. 3-8). Similar to the results seen in the growth assay, the strain lacking all three transporters as well as the strain lacking *cdt-1* and *cdt-2* were almost completely unable to respond to crystalline cellulose on a transcriptional level. While the wild-type shows approximately a 25,000-, 1,600- and 500-fold induction of *cbh-1*, *gh5-1,* and *gh6-2*, respectively, when transferred to media containing Avicel, the Δ2T and Δ3T transporter deletion strains showed a significant decrease in induction when transferred to media containing Avicel (Fig 3-8). While these values do not match those seen when transferred to sucrose, the approximate 20-, 10- and 3-fold induction of *cbh-1*, *gh5-1*, and *gh6-2*, respectively, match the values expected for conditions of starvation (de-repression) (63, 100). In summary, only the strains that contained at least one of the transporters CDT-1 or CDT-2 were able to sense cellulose and induce cellulase gene expression.

Taken together, the results from the single, double and triple deletion strains indicate that while *cdt-1* or *cdt-2* is required for the recognition of crystalline cellulose, the predicted transporter NCU05853, is not. In addition, because the transcriptional expression of *cbh-1*, *gh5-1*, and *gh6-2* in the Δ2T and Δ3T transporter deletion strains showed only a slight increase in expression on Avicel, it implies that these strains are capable of cellulase de-repression, but are unable to sense the presence of cellulose as a source of carbon.

3.3 Cellulase induction in the Δ3βGΔTransporter strains

Our previous work indicated that cellobiose is the shortest cellodextrin sufficient to induce the complete set of cellulose degrading enzymes (100). Because the above transporters were shown to transport cellobiose in *S. cerevisiae* (32), I hypothesized that cellobiose induction of *N. crassa* would require the presence of *cdt-1* and/or *cdt-2*. In order to examine this hypothesis directly, I used the Δ3βG strain described in Chapter 2 and made quadruple, quintuple and sextuple mutants lacking the genes encoding the three β-glucosidase enzymes and one or more of the genes encoding the cellodextrin transporters. As before, these deletion strains were genotyped using two different sets of PCR primers to ensure that the genes were properly deleted (Fig 3-5). The resulting strains and their genotypes are listed in Table 3-1.

Similar to the transporter deletion strains above, I examined the quadruple, quintuple and sextuple mutant strains using both the growth assay as well as the expression induction assay. All of these multiple deletion strains had wild-type growth on sucrose (data not shown), but had severe growth defects on either cellobiose or Avicel (Fig 3-6). While the wild-type strain has no difficulty growing on either cellobiose or Avicel, cellulase gene expression and enzymes are only produced when growing on Avicel. Because the Δ3βG strain lacks the major genes encoding enzymes to degrade cellobiose to glucose, this strain has a severe growth phenotype on both cellobiose and Avicel (100). This strain is able to produce some biomass, indicating that there must be an additional mechanisms to utilize cellobiose. Because the culture supernatant from the Δ3βG strain is almost completely impaired in its ability to produce glucose (producing

only 0.5 milligram glucose per gram protein from Avicel after 36 hours (100)), these observations suggest that the compensatory mechanism is intracellular. If the compensatory mechanism for growth on cellobiose and Avicel is intracellular, a strain lacking both the genes encoding the β-glucosidases and cellodextrin transporters would be predicted to show a growth phenotype that is more severe than the Δ3βG strain alone.

When I examined the above hypothesis in the quadruple, quintuple and sextuple mutant strains, I found that the strain lacking all six genes (Δ3βGΔ3T) was unable to grow on Avicel or cellobiose (Fig 3-6). This severely impaired growth phenotype was also seen in the *cdt-1/2* quintuple deletion strain (Δ3βGΔ2T), again implying that NCU05853 is not required for either the recognition or growth on either cellulose or cellobiose. Interestingly, strains containing either *cdt-1* or *cdt-2* in the Δ3βG background and in the absence of the other transporters, also had growth phenotypes that were more severe than the Δ3βG strain alone. In particular, the strain lacking Δ3βG and *cdt-1* (containing only *cdt-2* transporter) was able to produce more biomass (Fig 3-6), implying that the presence of CDT-2 is more important for growth on cellobiose in the Δ3βG background.

Since these strains lack cellodextrin transporters, Ihypothesized that these strains would also show an additional deficiency in their ability to produce cellulases, as they would be unable to sense the availability of cellobiose. To examine cellulase production, Iused the supernatants from the cellobiose grown cultures pictured in Fig 3-6 in a MuLac assay to quantify the activity of CBH-1 (Fig 3-7). While the wild-type supernatant does not produce any CBH-1 activity when grown on cellobiose for 36 hours, in this same amount of time the Δ3βG strain produces CBH-1 activity equivalent to wild-type after 5-7 days growth on Avicel (100). In support of our hypothesis, Fig 3-7 shows that both the Δ3βGΔ3T and Δ3βGΔ2T produced no CBH-1 activity (despite the highly sensitive nature of the MuLac assay) (102). This result shows that the Δ3βGΔ3T strain does not sense the availability of cellobiose as a signal for the production of cellulases. In contrast, although the strains containing only *cdt-1* or *cdt-2* have a growth phenotype on cellobiose and Avicel that is more severe than the Δ3βG strain, these strains are still able to produce a significant amount of CBH-1 activity (Fig 3-7). However, a strain carrying deletions of both *cdt-1* and *cdt-2* had no detectable CBH-1 activity, indicating that these are the two transporters most important for the sensing of cellobiose. Finally, strains carrying deletions of either *cdt-1* or *cdt-2* showed a similar amount of CBH-1 activity leading us to conclude that even with minimal growth, if cellobiose is recognized and/or transported by one or both transporters, the strain is able to produce active cellulases.

While the above data indicates that both CDT-1 and CDT-2 are involved in the recognition of cellobiose as a signal for cellulose deconstruction, Itested this directly using the transcriptional response assay. Iexpected that both the Δ3βGΔ3T and Δ3βGΔ2T strains would respond to cellobiose in the same way that the Δ3T and the Δ2T responded to Avicel: showing de-repression, but no induction of cellulase gene expression (Fig 3-8). However, while both the Δ3βGΔ3T and Δ3βGΔ2T responded to Avicel as expected for a starvation response and showed only an induction of approximately 10- and 4-fold for *cbh-1* and *gh5-1*, respectively (Fig 3-9 and 3-10), the response to 0.2% (5.8 mM) cellobiose resulted in an approximately 400- and 50-fold induction for *cbh-1* and *gh5-1*, respectively. Although these induction values are still two orders of magnitude lower than in the Δ3βG strain, which shows an approximately 10,000- and 3,000-fold induction

for *cbh-1* and *gh5-1*, respectively, Ihypothesized that this discrepancy between cellobiose and Avicel induction was due to the concentration of cellobiose used in this assay. Because *N. crassa* has many sugar transporters, Ihypothesized that the induction seen by 0.2 cellobiose is due to non-specific transport of cellobiose into the cell through other transporters that results in enzyme induction. Therefore Ipredicted that if the amount of cellobiose used in the induction assay was decreased to a concentration more closely matching what is seen in nature upon degradation of cellulose, Iwould abolish the non-specific transport of cellobiose and prevent the non-specific induction of cellulases.

In order to determine the proper range of cellobiose required for specific induction of cellulases, Imeasured the concentration of glucose and cellobiose produced when wild-type *N. crassa* grows on Avicel by using Dionex-HPLC methodology (Fig 3-11). The highest concentration of cellobiose, approximately 1.5 μM, was found in the media after autoclaving, but prior to inoculating with conidia. While the concentration of glucose rose to approximately 17 μM after 2 days of growth of *N. crassa* on Avicel, the concentration of cellobiose fell from 1.5 μM to 0.75 μM after 2 days growth and then leveled off until 5 days growth (Fig 3-11) when its concentration was below the detection limit. This result led us to conclude that less than 1 μM cellobiose should be used for the transcriptional induction assay. In addition to these measurements, Iexamined the sensitivity of the Δ3βG and Δ3βGΔ3T strains in the transcriptional induction assay by performing this assay in decreasing concentrations of cellobiose (Fig. 3-12). Although the Δ3βG strain showed induction of *cbh-1* with cellobiose concentrations as low as 100 nM (approximately 1,000-fold induction versus the 100-fold induction expected for transcriptional de-repression and 20,000-fold induction expected for full induction) maximal induction of *cbh-1* occurred in 100 μM cellobiose. In contrast, the Δ3βGΔ3T strain required concentrations above 10 μM cellobiose to show any signs of induction above the glucose de-repression level. These results confirm the hypothesis that only minimal amounts of cellobiose are required for full induction of *cbh-1* in the Δ3βG strain. Furthermore, at such a low concentration, there is no transcriptional induction in the Δ3βGΔ3T strain (only transcriptional de-repression equivalent to carbon starvation).

Since 100 μM cellobiose allowed for full induction of *cbh-1* in the Δ3βG strain, but resulted in only a minimal induction in the Δ3βGΔ3T strain, Idecided to examine the response of the other transporter deletion strains in response to Avicel, 100 μM cellobiose, and no carbon (starvation). While Iexpected to see some non-specific induction in the transporter deletion strains at this concentration of cellobiose, the resulting levels of induction should be significantly less than that seen for specific induction of *cbh-1*. Thus it should be relatively straightforward to determine the role of the transporters in cellulase induction.

Similar to the results described in Chapter 2, the wild-type strain exhibited a strong transcriptional response for both *cbh-1* and *gh5-1* in the presence of Avicel, but not in the no carbon or 100 μM cellobiose cultures (Fig 3-9, 3-10) (16-, 22-, and 12,000-fold for *cbh-1* in no carbon, 100 μM cellobiose and Avicel conditions, respectively). The Δ3βG strain showed induction of both *cbh-1* and *gh5-1* in response to either Avicel or 100 μM cellobiose, but only minimal induction under conditions of starvation (30-, 2,800-, and 16,000-fold for *cbh-1* in no carbon, 100 μM cellobiose and Avicel conditions, respectively). As predicted, the Δ3βGΔ3T and Δ3βGΔ2T strains showed no significant induction above glucose de-repression in the no carbon, 100 μM cellobiose and Avicel

culture conditions (Δ3βGΔ3T: 4-, 18-, and 10-fold for *cbh-1* in no carbon, 100 μM cellobiose and Avicel, respectively; Δ3βGΔ2T: 4-, 54-, and 18-fold for *cbh-1* in no carbon, 100 μM cellobiose and Avicel conditions, respectively). These results confirm the hypothesis that cellulase induction by cellobiose is concentration-dependent and that, when examined under conditions closer to those found in nature, the presence of CDT-1 or CDT-2 is required for cellobiose to act as an inducer of cellulase gene expression in the β-glucosidase deletion strain.

To examine if either CDT-1 or CDT-2 was sufficient for cellulose recognition, Iutilized the same transcriptional response assay on strains where either one or two of the transporters was still present. The strains with only one transporter deleted, (Δ3βG Δ*cdt-1*, Δ3βG Δ*cdt-2*, or Δ3βG Δ*ncu05853*) and strains with both *cdt-1* and NCU05853 (Δ3βG *Δcdt-1;* Δ*ncu05853*) or *cdt-2* and NCU05853 (Δ3βG Δ*cdt*-2; Δ*ncu05853*) deleted showed full induction of both *cbh-1* and *gh5-1* in response to 100 μM cellobiose or 1% Avicel (Fig 3-9 and 3-10). On the other hand, the strain with both *cdt-1* and *cdt-2* deleted (Δ3βGΔ2T) was unable to respond to either 100 μM cellobiose or 1% Avicel. The expression of *cbh-1* and *gh5-1* more closely matched the response to starvation, indicating that either CDT-1 or CDT-2 is necessary and sufficient for low-concentrations of cellobiose to induce cellulase expression in the triple β-glucosidase deletion background.

Taken altogether, the results from the triple β-glucosidase deletion strain combined with the single, double, and triple transporter deletion strains allowed us to conclude that NCU05853 is not required for either the transport or recognition of cellobiose as a signal for crystalline cellulose. In addition, while the presence of CDT-1 or CDT-2 is required for the recognition of cellobiose as a signal for crystalline cellulose, the growth assays indicated that the presence of CDT-2 allows for more growth on cellobiose in the absence of β-glucosidase activity. Whether this is simply due to the abundance of transporters present on the cell or its innate ability to transport cellobiose more efficiently than CDT-1 needs to be determined.

3.4 Transport of [^{3}H]-cellobiose in the Δ3βG deletion strain

While the above data and previous studies in *S. cerevisiae* (32, 101) imply that cellobiose is transported into the cell via the transporters, Iwanted to show this directly using [^{3}H]-cellobiose. This method measures the accumulation of [^{3}H]-cellobiose in or on cells. Since the transcription assays were performed using 100 μM cellobiose, Idecided to use the same concentration for the transport assays resulting in a rate of 0.0181±0.0044 picomoles of cellobiose per second per milligram of biomass in the Δ3βG strain (Fig 3-13). In contrast, when Imeasured the rate of cellobiose uptake in the Δ3βGΔ3T strain, only 0.00047±0.00024 picomoles of cellobiose per second per milligram of biomass accumulated in the cells (Fig 3-14). Because Isee almost no [^{3}H]-cellobiose transport in the Δ3βGΔ3T strain, these results confirm that the vast majority of the cellobiose transport occurs via the CDT-1 and CDT-2 transporters analyzed above.

3.5 Discussion

In this study, Iexamined the role of predicted cellodextrin transporters in the induction of plant cell wall degrading enzymes and their involvement in growth on crystalline cellulose in *N. crassa*. Our results indicate that two transporters (CDT-1 and CDT-2) are

equally involved in sensing crystalline cellulose, but CDT-2 is most important for growth on crystalline cellulose. In addition, while a third predicted cellodextrin transporter, NCU05853, is transcriptionally induced when exposed to crystalline cellulose, it does not appear to be required for either cellulose sensing or growth on crystalline cellulose.

While several studies have examined the induction of cellulases using various inducing molecules, only one study has been published which examines cellodextrin uptake in *T. reesei* (31). In contrast to the prior work, Iwas able to show that not only does *N. crassa* possess a mechanism for the uptake of cellobiose (32, 101), but that this uptake mechanism is required for the induction of lignocellulose degrading enzymes. Iidentified two specific *N. crassa* cellodextrin transporters (CDT-1 and CDT-2) which when deleted result in a strain of *N. crassa* that grows similar to wild-type on sucrose, but is unable to grow on crystalline cellulose. Using this strain I was able to show that mycelia lacking both *cdt-1* and *cdt-2* are unable to induce cellulase expression in response to crystalline cellulose, but the presence of either *cdt-1* or *cdt-2* is sufficient for cellulase induction. Previously, Iidentified that in the absence of β-glucosidase activity cellobiose is sufficient to induce the full repertoire of cellulases. By combining the β-glucosidase deletions with the transporter deletions, Ishowed that deletion of both *cdt-1* and *cdt-2* result in a strain of *N. crassa* that grows similarly to wild-type on sucrose, but is unable to grow on cellobiose and is unable to induce cellulases in response to cellobiose. This result leads us to conclude that CDT-1 and/or CDT-2 are required for *N. crassa* to identify cellobiose as a signal for cellulose and, without identification of this signal, *N. crassa* will not strongly induce cellulase gene expression. While this study was unable to show if the transport of cellobiose is required for cellulase induction, Iexpect that non-transporting point mutants in the transporters could clarify whether cellobiose uptake is required for cellulose sensing.

Mechanistic studies of CDT-1 and CDT-2 in *S. cerevisiae* indicate that both act as high affinity (3-4 μM) transporters (32), while studies of fungal β-glucosidases indicate affinities in the low millimolar range, with GH3-3 (NCU08755) having a K_m of 4 mM (71). The results from our study show that concentrations of cellobiose as low as 100 nM provide for the induction of cellulases, allowing us to hypothesize that low concentrations of cellobiose in the environment are used by *N. crassa* to sense and adjust enzyme production. In addition, because CDT-1 uses the plasma membrane proton gradient to act as a symporter while CDT-2 functions as a permease, Ialso hypothesize that in very low concentrations of cellobiose, CDT-1 is able to effectively concentrate cellobiose inside the cell, while CDT-2 is most sensitive to rapidly changing extracellular concentrations of cellobiose allowing for a greater sensitivity to changing environmental conditions. In an environment where resources are scarce and competition is plentiful, one can easily imagine the evolutionary advantage provided by the ability to rapidly adapt to a changing environment of scare carbohydrate availability.

3.6 Methods

3.6.1 Strains
All strains were obtained from the Fungal Genetics Stock Center (FGSC) (90, 91). Multiple deletion strains were made by performing sequential crosses as described on the FGSC website (92). The mating type was determined using the mating type tester strains fl(OR) A (FGSC 4317) and fl(OR) a (FGSC 4347) (92).

3.6.2 Mating
Conidia from the parent strain of one mating type were plated on a Westergaard's plate and the conidia from the other parent of the opposite mating type were inoculated onto a minimal media slant. Both the plate and the slant were incubated in the dark at 30°C for 2-3 days to allow for sufficient hyphal growth. They were then placed at room temperature in the light for an additional 5-7 days to allow for the development of protoperithecia (on the plate) and conidia (on the slant). After visual confirmation of protoperithecial production, the conidia were resuspended in 2 mL of sterile water and diluted 1:100. Approximately 100 µL of this dilution was added to the protoperithecial plate of the opposite mating type and gently spread using a pipette tip. The plates were then allowed to undergo sexual reproduction for approximately 2 weeks, with the result being the production of ascospores, which are ejected from the perithecium and adhere to the lid of the petri plate. The ascospores were collected by pipetting 1 mL of water onto the lid and then collecting in a 1.5-ml microfuge tube. The ascospores were stored at 4°C

3.6.3 germination and selection of ascospores
The ascospores were counted using a hemocytometer and diluted to approximately 500 ascospores per 100 µL water. This dilution underwent a 60°C heat shock for 30 minutes and the entire volume was plated on a minimal media plate supplemented with 200 µg/mL hygromycin as a selection for the deletion genotype. The ascospores were allowed to germinate for 16 hours, right side up at room temperature. Using a dissecting microscope the germinated ascospores were carefully cut out of the plate and transferred to a minimal media slant. This slant was grown for 2 days in the dark at 30°C and then transferred to room temperature for an additional 3 days. Each slant was sub-cultured, and genomic DNA was extracted for genotyping via PCR.

3.6.4 Genomic DNA extraction
Conidia were isolated by adding 2 mL water to each slant and vortexing for 5-10 seconds. The resulting slurry was transferred to a 2-mL screw cap tube and conidia were pelleted at 4000 rpm for 4 minutes. The supernatant and floating mycelia were removed and ~0.3 g of 0.5-mm silica beads and 400 µL of lysis solution (0.05 M NaOH, 1 mM EDTA, 1% Triton-X 100) was added to the pelleted conidia. The sample was shaken in a bead beater for 2 minutes and placed in a 65°C water bath for 30 minutes, vortexing 2-3 times during the incubation to mix. After the addition of 80 µL of 1M Tris pH 7.5, samples were centrifuged at max speed in a bench top centrifuge (5 minutes) and the supernatant was removed. An equal volume of phenol-chloroform was added; samples were again vortexed briefly to mix and then centrifuged again for 10 minutes at max speed. The aqueous phase was transferred to a new tube with 600 µL ice-cold ethanol and placed at -

20°C for at least one hour, but typically overnight to precipitate the genomic DNA. After precipitation, the sample was centrifuged for 15 minutes at 4°C and the pellet was washed with 75% ethanol. The resulting pellet was dried in a speedvac for 10 minutes at 30°C and resuspended in 100 µL water. The concentration was examined using a Nanodrop and volume adjusted to produce 300 ng/µL final concentration.

3.6.5 Genotyping multiple deletion strains

The genotype of each deletion strain was confirmed by performing two different PCR reactions. The first used a gene-specific primer and a common primer for the hygromycin (hph) cassette to confirm the presence of the cassette. The primer for hph was 5'-CGA CAG ACG TCG CGG TGA GTT CAG-3'. Reverse primers were:
NCU00130: 5'-TAG TGT ACA AAC CCC AAG C-3'
NCU004952: 5'-AAC ACA CAC ACA CAC ACT GG-3'
NCU08755: 5'-ACA GTG GAG GTG AGA AAG G-3'
NCU08807: 5'-GTA CTT ACG CAG TAG CGT GG-3'
NCU00801: 5'-TTA GGG TTG TAG ACA CCT GC-3'
NCU08114: 5'-GAC GAC CAG AAC TAG GTA GG-3'
NCU05853: 5'-GAG CAA GGT TAT AGG ACT GC-3'

The second reaction used both a gene specific forward primer and a gene specific reverse primer. The presence of a product in this reaction indicates a wild-type copy of the specific gene. The forward primers were:
NCU00130: 5'-ACA TCA AGC ACA AGA AGG GCG TC-3'
NCU04952: 5'-CCT CAA AAT ATG CAG CCT ACA CGA-3'
NCU08755: 5'-ACG ACA TCA TGT ACA CTG TTA CGG-3'
NCU08807 5'-CAC TCA AAG GAA ACT TCC TGT GCC-3'
NCU00801: 5'-GGC CGC TTA CTT CCT CTT CAA CG-3'
NCU08114: 5'-GCT CAA TAC TTA TGC GAA CCC TGT-3'
NCU05853: 5'-ATA ACA TGG GTT ATA ACG CCC TGA-3'
and the reverse primers were the same as above. In each reaction the presence of a 1500 bp product indicated proper amplification for the reaction.

3.6.6 Phenotyping multiple deletion strains

Conidia from strains were inoculated at a concentration equal to $2x10^6$ conidia per milliliter 100 mL Vogel's salts (93) with 2% w/v sucrose, cellobiose or Avicel in a 250-ml Erlenmeyer flask and grown under constant light at 200 rpm for 2 days (sucrose), 5 days (cellobiose) and 7 days (Avicel). Photos were taken daily.

3.6.6 4-Methylumbelliferyl β-D-cellobioside (MuLac) assay

Cellobiohydrolase I activity was measured using 4-Methylumbelliferyl β-D-cellobioside (MuLac) (Sigma). Each assay was run in triplicate by mixing 20 µL filtered culture supernatant combined with 80 µL MuLac reagent (1.0 mM MuLac and 50 mM NaAc pH5) in a black 96 well, clear bottom plate and read in a plate reader using an assay to measure the MuLac kinetics. Time points were read every 15 seconds for 10 minutes using 360 nm excitation and 465 nm emission. The slope of the resulting line represents the relative amount of cellobiohydrolase I activity as a function of time.

3.6.8 Transcriptional studies

Conidia from strains were inoculated at a concentration equal to $2x10^6$ conidia per milliliter 50 mL Vogel's salts (93) with 2% w/v sucrose in a 250-mL Erlenmeyer flask and grown under constant light at 200 rpm for 16 hours. Biomass was then spun at 4000 rpm for 10 minutes and washed in Vogel's salts (without carbon) twice to remove any excess sucrose. The biomass was then added to a new flask containing 50 mL Vogel's salts supplemented with 1% w/v sucrose, 0.2% w/v cellobiose (Sigma) or 1% w/v Avicel PH 101 (Sigma). Cultures were induced for 4 hours under constant light at 200 rpm. The culture biomass was then harvested by filtration over a Whatman glass microfiber filter (GF/F) on a Buchner funnel and washed with 50 mL Vogel's salts. The biomass was flash frozen in liquid nitrogen and stored at -80°C. Three independent biological duplicates (flasks) were evaluated for each time point.

3.6.9 RNA isolation

RNA was prepared as previously described (10). Total RNA from frozen samples was isolated using Zirconia/Silica beads (0.5-mm diameter; Biospec) and a Mini-Beadbeater-96 (Biospec) with 1 mL TRIzol reagent (Invitrogen) according to the manufacturer's instructions. The total RNA was further purified by digestion with TURBO DNA-free (Ambion) and an RNeasy kit (Qiagen). RNA concentration and integrity was checked by Nanodrop and agarose gel electrophoresis.

3.6.10 Quantitative RT-PCR

Quantitative RT-PCR was performed using the EXPRESS One-Step SYBR GreenER Kit (Invitrogen) and the StepOnePlus Real-Time PCR System (Applied Biosystems). Reactions were performed in triplicate with a total reaction volume of 10 uL including 300 nM each forward and reverse primers and 75 ng template RNA. Data analysis was performed by the StepOne Software (Applied Biosystems) using the Relative Quantitation/Comparative CT ($\Delta\Delta$CT) setting. Data was normalized to the endogenous control actin with expression on sucrose as the reference sample.

3.6.11 RT-PCR primers

The primers for actin (NCU4173) were: forward 5'-TGA TCT TAC CGA CTA CCT-3' and reverse 5'-CAG AGC TTC TCC TTG ATG-3'. The primers for *cbh-1* (NCU07340) were: forward 5'-ATC TGG GAA GCG AAC AAA G-3' and reverse 5'-TAG CGG TCG TCG GAA TAG-3'. The primers for *gh6-2* (NCU09680) were: forward 5'-CCC ATC ACC ACT ACT ACC-3' and reverse 5'-CCA GCC CTG AAC ACC AAG-3'. The primers for *gh5-1* (NCU00762) were: forward 5'- GAG TTC ACA TTC CCT GAC A-3' and reverse 5'-CGA AGC CAA CAC GGA AGA-3'. RT-PCR primers were previously identified and optimized in Tian, *et al*. (10) and Dementhon, *et al*. (96).

3.6.12 [^{3}H]-cellobiose transport assay

Conidia from strains were inoculated at a concentration equal to $2x10^6$ conidia per milliliter into 100 mL Vogel's salts with 2% w/v sucrose in a 250-mL Erlenmeyer flask and grown under constant light at 200 rpm for 16 hours. Biomass was then gently filtered by vacuum filtration and washed twice in Vogel's salts (without carbon) to remove any

excess sucrose. Biomass was then resuspended in 50 mL Vogel's salts (without carbon) and 5 mL were aliquoted to five separate 50 mL-flasks and 5 mL of 200 μM cellobiose containing 20 μCi/μmol [^{3}H]-cellobiose was added. The flasks were allowed to shake at 200 rpm for 2, 4, 6, 8, and 10 minutes at which point 10 mL of ice cold Vogel's salts was added directly to the flask and then immediately filtered by vacuum filtration onto a cellulose nitrate membrane filter (Whatman 7184-002) and washed with an additional two volumes of ice cold Vogel's salts. The filter was then dried at 100°C for 20 minutes and the weighted for biomass determination. The filter was then added to 5 mL of Ultima Gold scintillation fluid, and CPM determined in a Tri-Carb 2900TR scintillation counter. [^{3}H]-cellobiose was purchased from Moravek Biochemicals, Inc. and had a specific activity of 4 Ci/mmol and a purity of >99%. The rates were calculated as picomoles cellobiose transported per milligram biomass. Transport assays were performed in triplicate and the resulting rates were averaged.

References

1. IEA (2011) *Co2 emissions from fuel combustion: 2011 highlights*.

2. IPCC (2007) *Climate change 2007: Synthesis report. Contribution of working groups i, ii and iii to the fourth assessment report of the intergovernmental panel on climate change* (Geneva, Switzerland).

3. Martinez DM & Ebenhack BW (2008) Understanding the role of energy consumption in human development through the use of saturation phenomena. *Energy Policy* 36(4):1430-1435.

4. Pauly M & Keegstra K (2010) Plant cell wall polymers as precursors for biofuels. *Current opinion in plant biology* 13(3):305-312.

5. Jordan DB, Bowman MJ, Braker JD, Dien BS, Hector RE, Lee CC, Mertens JA, & Wagschal K (2012) Plant cell walls to ethanol. *The Biochemical journal* 442(2):241-252.

6. Menon V & Rao M (2012) Trends in bioconversion of lignocellulose: Biofuels, platform chemicals &¬†biorefinery concept. *Progress in Energy and Combustion Science* (0).

7. Balat M (2011) Production of bioethanol from lignocellulosic materials via the biochemical pathway: A review. *Energy Conversion and Management* 52(2):858-875.

8. Himmel ME, Ding SY, Johnson DK, Adney WS, Nimlos MR, Brady JW, & Foust TD (2007) Biomass recalcitrance: Engineering plants and enzymes for biofuels production. *Science* 315(5813):804-807.

9. Le Crom S, Schackwitz W, Pennacchio L, Magnuson JK, Culley DE, Collett JR, Martin J, Druzhinina IS, Mathis H, Monot F, Seiboth B, Cherry B, Rey M, Berka R, Kubicek CP, Baker SE, & Margeot A (2009) Tracking the roots of cellulase hyperproduction by the fungus trichoderma reesei using massively parallel DNA sequencing. *Proceedings of the National Academy of Sciences of the United States of America* 106(38):16151-16156.

10. Tian C, Beeson WT, Iavarone AT, Sun J, Marletta MA, Cate JH, & Glass NL (2009) Systems analysis of plant cell wall degradation by the model filamentous fungus neurospora crassa. *Proc Natl Acad Sci U S A* 106(52):22157-22162.

11. Beadle GW & Tatum EL (1941) Genetic control of biochemical reactions in neurospora. *Proceedings of the National Academy of Sciences of the United States of America* 27(11):499-506.

12. Kubicek CP, Messner R, Gruber F, Mach RL, & Kubicek-Pranz EM (1993) The trichoderma cellulase regulatory puzzle: From the interior life of a secretory fungus. *Enzyme Microb Technol* 15(2):90-99.

13. el-Gogary S, Leite A, Crivellaro O, Eveleigh DE, & el-Dorry H (1989) Mechanism by which cellulose triggers cellobiohydrolase i gene expression in trichoderma reesei. *Proceedings of the National Academy of Sciences of the United States of America* 86(16):6138-6141.

14. Carle-Urioste JC, Escobar-Vera J, El-Gogary S, Henrique-Silva F, Torigoi E, Crivellaro O, Herrera-Estrella A, & El-Dorry H (1997) Cellulase induction in trichoderma reesei by cellulose requires its own basal expression. *The Journal of biological chemistry* 272(15):10169-10174.

15. Schmoll M, Zeilinger S, Mach RL, & Kubicek CP (2004) Cloning of genes expressed early during cellulase induction in hypocrea jecorina by a rapid subtraction hybridization approach. *Fungal Genet Biol* 41(9):877-887.

16. Sipos B, Benko Z, Dienes D, Reczey K, Viikari L, & Siika-aho M (2010) Characterisation of specific activities and hydrolytic properties of cell-wall-degrading enzymes produced by trichoderma reesei rut c30 on different carbon sources. *Appl Biochem Biotechnol* 161(1-8):347-364.

17. Vaheri M, Leisola M, & Kauppinen V (1979) Transglycosylation products of cellulase system of trichoderma-reesei. *Biotechnology Letters* 1(1):41-46.

18. Mandels M, Parrish FW, & Reese ET (1962) Sophorose as an inducer of cellulase in trichoderma viride. *J Bacteriol* 83:400-408.

19. Suto M & Tomita F (2001) Induction and catabolite repression mechanisms of cellulase in fungi. *Journal of Bioscience and Bioengineering* 92(4):305-311.

20. Seiboth B, Hartl L, Pail M, Fekete E, Karaffa L, & Kubicek CP (2004) The galactokinase of hypocrea jecorina is essential for cellulase induction by lactose but dispensable for growth on d-galactose. *Molecular Microbiology* 51(4):1015-1025.

21. Gielkens MM, Dekkers E, Visser J, & de Graaff LH (1999) Two cellobiohydrolase-encoding genes from aspergillus niger require d-xylose and the xylanolytic transcriptional activator xlnr for their expression. *Appl Environ Microbiol* 65(10):4340-4345.

22. Ulmer DC, Leisola MSA, & Fiechter A (1984) Possible induction of the ligninolytic system of phanerochaete chrysosporium. *Journal of Biotechnology* 1(1):13-24.

23. Mandels M & Reese ET (1960) Induction of cellulase in fungi by cellobiose. *J Bacteriol* 79:816-826.

24. Chikamatsu G, Shirai K, Kato M, Kobayashi T, & Tsukagoshi N (1999) Structure and expression properties of the endo-beta-1,4-glucanase a gene from the filamentous fungus aspergillus nidulans. *FEMS Microbiol Lett* 175(2):239-245.

25. Nevalainen KM, Te'o VS, & Bergquist PL (2005) Heterologous protein expression in filamentous fungi. *Trends Biotechnol* 23(9):468-474.

26. Suzuki H, Igarashi K, & Samejima M (2010) Cellotriose and cellotetraose as inducers of the genes encoding cellobiohydrolases in the basidiomycete phanerochaete chrysosporium. *Appl Environ Microbiol* 76(18):6164-6170.

27. Reese ET, Parrish FW, & Ettlinger M (1971) Nojirimycin and d-glucono-1,5-lactone as inhibitors of carbohydrases *Carbohydrate Research* 18(3):381-388.

28. Woodward J & Arnold SL (1981) The inhibition of β-glucosidase activity in trichoderma reesei c30 cellulase by derivatives and isomers of glucose. *Biotechnology and Bioengineering* 23:1553–1562.

29. Freer SN & Greene RV (1990) Transport of glucose and cellobiose by candida wickerhamii and clavispora lusitaniae. *The Journal of biological chemistry* 265(22):12864-12868.

30. Schnetz K, Sutrina SL, Saier MH, Jr., & Rak B (1990) Identification of catalytic residues in the beta-glucoside permease of escherichia coli by site-specific mutagenesis and demonstration of interdomain cross-reactivity between the beta-glucoside and glucose systems. *The Journal of biological chemistry* 265(23):13464-13471.

31. Kubicek CP, Messner R, Gruber F, Mandels M, & Kubicek-Pranz EM (1993) Triggering of cellulase biosynthesis by cellulose in trichoderma reesei. Involvement of a constitutive, sophorose-inducible, glucose-inhibited beta-diglucoside permease. *The Journal of biological chemistry* 268(26):19364-19368.

32. Galazka JM, Tian C, Beeson WT, Martinez B, Glass NL, & Cate JH (2010) Cellodextrin transport in yeast for improved biofuel production. *Science* 330(6000):84-86.

33. Santangelo GM (2006) Glucose signaling in saccharomyces cerevisiae. *Microbiology and Molecular Biology Reviews* 70(1):253-+.

34. Gancedo JM (1998) Yeast carbon catabolite repression. *Microbiology and Molecular Biology Reviews* 62(2):334-+.

35. Mukherjee S, Berger MF, Jona G, Wang XS, Muzzey D, Snyder M, Young RA, & Bulyk ML (2004) Rapid analysis of the DNA-binding specificities of transcription factors with DNA microarrays. *Nature Genetics* 36(12):1331-1339.

36. Lee TI, Rinaldi NJ, Robert F, Odom DT, Bar-Joseph Z, Gerber GK, Hannett NM, Harbison CT, Thompson CM, Simon I, Zeitlinger J, Jennings EG, Murray HL, Gordon DB, Ren B, Wyrick JJ, Tagne JB, Volkert TL, Fraenkel E, Gifford DK, & Young RA (2002) Transcriptional regulatory networks in saccharomyces cerevisiae. *Science* 298(5594):799-804.

37. Lorenz DR, Cantor CR, & Collins JJ (2009) A network biology approach to aging in yeast. *Proceedings of the National Academy of Sciences of the United States of America* 106(4):1145-1150.

38. Treitel MA, Kuchin S, & Carlson M (1998) Snf1 protein kinase regulates phosphorylation of the mig1 repressor in saccharomyces cerevisiae. *Molecular and Cellular Biology* 18(11):6273-6280.

39. Treitel MA & Carlson M (1995) Repression by ssn6-tup1 is directed by mig1, a repressor activator protein. *Proceedings of the National Academy of Sciences of the United States of America* 92(8):3132-3136.

40. Cziferszky A, Mach RL, & Kubicek CP (2002) Phosphorylation positively regulates DNA binding of the carbon catabolite repressor cre1 of hypocrea jecorina (trichoderma reesei). *Journal of Biological Chemistry* 277(17):14688-14694.

41. Cziferszky A, Seiboth B, & Kubicek CP (2003) The snf1 kinase of the filamentous fungus hypocrea jecorina phosphorylates regulation-relevant serine residues in the yeast carbon catabolite repressor mig1 but not in the filamentous fungal counterpart cre1. *Fungal Genetics and Biology* 40(2):166-175.

42. Mach RL, Strauss J, Zeilinger S, Schindler M, & Kubicek CP (1996) Carbon catabolite repression of xylanase i (xyn1) gene expression in trichoderma reesei. *Molecular microbiology* 21(6):1273-1281.

43. Cubero B & Scazzocchio C (1994) Two different, adjacent and divergent zinc finger binding sites are necessary for crea-mediated carbon catabolite repression in the proline gene cluster of aspergillus nidulans. *The EMBO journal* 13(2):407-415.

44. Mach-Aigner AR, Pucher ME, Steiger MG, Bauer GE, Preis SJ, & Mach RL (2008) Transcriptional regulation of xyr1, encoding the main regulator of the xylanolytic and cellulolytic enzyme system in hypocrea jecorina. *Applied and Environmental Microbiology* 74(21):6554-6562.

45. Takashima S, Iikura H, Nakamura A, Masaki H, & Uozumi T (1996) Analysis of cre1 binding sites in the trichoderma reesei cbh1 upstream region. *Fems Microbiology Letters* 145(3):361-366.

46. Portnoy T, Margeot A, Linke R, Atanasova L, Fekete E, Sandor E, Hartl L, Karaffa L, Druzhinina IS, Seiboth B, Le Crom S, & Kubicek CP (2011) The cre1 carbon catabolite repressor of the fungus trichoderma reesei: A master regulator of carbon assimilation. *BMC Genomics* 12(1):269.

47. Sun J & Glass NL (2011) Identification of the cre-1 cellulolytic regulon in neurospora crassa. *PLoS One* 6(9):e25654.

48. Karaffa L, Fekete E, Gamauf C, Szentirmai A, Kubicek CP, & Seiboth B (2006) D-galactose induces cellulase gene expression in hypocrea jecorina at low growth rates. *Microbiology* 152(Pt 5):1507-1514.

49. Calero-Nieto F, Hera C, Di Pietro A, Orejas M, & Roncero MI (2008) Regulatory elements mediating expression of xylanase genes in fusarium oxysporum. *Fungal genetics and biology : FG & B* 45(1):28-34.

50. de Vries RP, van de Vondervoort PJ, Hendriks L, van de Belt M, & Visser J (2002) Regulation of the alpha-glucuronidase-encoding gene (agua) from aspergillus niger. *Molecular genetics and genomics : MGG* 268(1):96-102.

51. Marui J, Tanaka A, Mimura S, de Graaff LH, Visser J, Kitamoto N, Kato M, Kobayashi T, & Tsukagoshi N (2002) A transcriptional activator, aoxlnr, controls the expression of genes encoding xylanolytic enzymes in aspergillus oryzae. *Fungal genetics and biology : FG & B* 35(2):157-169.

52. Noguchi Y, Sano M, Kanamaru K, Ko T, Takeuchi M, Kato M, & Kobayashi T (2009) Genes regulated by aoxlnr, the xylanolytic and cellulolytic transcriptional regulator, in aspergillus oryzae. *Applied microbiology and biotechnology* 85(1):141-154.

53. van Peij NN, Visser J, & de Graaff LH (1998) Isolation and analysis of xlnr, encoding a transcriptional activator co-ordinating xylanolytic expression in aspergillus niger. *Molecular Microbiology* 27(1):131-142.

54. van Peij NN, Gielkens MM, de Vries RP, Visser J, & de Graaff LH (1998) The transcriptional activator xlnr regulates both xylanolytic and endoglucanase gene expression in aspergillus niger. *Applied and Environmental Microbiology* 64(10):3615-3619.

55. Hasper AA, Visser J, & de Graaff LH (2000) The aspergillus niger transcriptional activator xlnr, which is involved in the degradation of the polysaccharides xylan

and cellulose, also regulates d-xylose reductase gene expression. *Molecular Microbiology* 36(1):193-200.

56. Royer JC & Nakas JP (1990) Interrelationship of xylanase induction and cellulase induction of trichoderma longibrachiatum. *Applied and Environmental Microbiology* 56(8):2535-2539.

57. Omony J, de Graaff LH, van Straten G, & van Boxtel AJ (2011) Modeling and analysis of the dynamic behavior of the xlnr regulon in aspergillus niger. *BMC systems biology* 5 Suppl 1:S14.

58. Stricker AR, Mach RL, & de Graaff LH (2008) Regulation of transcription of cellulases- and hemicellulases-encoding genes in aspergillus niger and hypocrea jecorina (trichoderma reesei). *Applied microbiology and biotechnology* 78(2):211-220.

59. Brunner K, Lichtenauer AM, Kratochwill K, Delic M, & Mach RL (2007) Xyr1 regulates xylanase but not cellulase formation in the head blight fungus fusarium graminearum. *Current genetics* 52(5-6):213-220.

60. Calero-Nieto F, Di Pietro A, Roncero MI, & Hera C (2007) Role of the transcriptional activator xlnr of fusarium oxysporum in regulation of xylanase genes and virulence. *Molecular plant-microbe interactions : MPMI* 20(8):977-985.

61. Aro N, Pakula T, & Penttila M (2005) Transcriptional regulation of plant cell wall degradation by filamentous fungi. *FEMS Microbiol Rev* 29(4):719-739.

62. Aro N, Saloheimo A, Ilmen M, & Penttila M (2001) Aceii, a novel transcriptional activator involved in regulation of cellulase and xylanase genes of trichoderma reesei. *The Journal of biological chemistry* 276(26):24309-24314.

63. Coradetti ST, Craig JP, Xiong Y, Shock T, Tian C, & Glass NL (2012) Conserved and essential transcription factors for cellulase gene expression in ascomycete fungi. *Proceedings of the National Academy of Sciences of the United States of America*.

64. Wyman CE (1999) Biomass ethanol: Technical progress, opportunities, and commercial challenges. *Annual Review of Energy and the Environment* 24(1):189-226.

65. Rubin EM (2008) Genomics of cellulosic biofuels. *Nature* 454(7206):841-845.

66. Cherry JR & Fidantsef AL (2003) Directed evolution of industrial enzymes: An update. *Curr Opin Biotechnol* 14(4):438-443.

67. Schmoll M & Kubicek CP (2005) Ooc1, a unique gene expressed only during growth of hypocrea jecorina (anamorph: Trichoderma reesei) on cellulose. *Curr Genet* 48(2):126-133.

68. Sternberg D & Mandels GR (1980) Regulation of the cellulolytic system in trichoderma reesei by sophorose: Induction of cellulase and repression of beta-glucosidase. *J Bacteriol* 144(3):1197-1199.

69. Davis RH (2000) *Neurospora : Contributions of a model organism* (Oxford University Press, New York) pp xii, 333 p.

70. Maddi A, Bowman SM, & Free SJ (2009) Trifluoromethanesulfonic acid-based proteomic analysis of cell wall and secreted proteins of the ascomycetous fungi neurospora crassa and candida albicans. *Fungal Genet Biol* 46(10):768-781.

71. Bohlin C, Olsen SN, Morant MD, Patkar S, Borch K, & Westh P (2010) A comparative study of activity and apparent inhibition of fungal beta-glucosidases. *Biotechnol Bioeng* 107(6):943-952.

72. Koivula A, Ruohonen L, Wohlfahrt G, Reinikainen T, Teeri TT, Piens K, Claeyssens M, Weber M, Vasella A, Becker D, Sinnott ML, Zou JY, Kleywegt GJ, Szardenings M, Stahlberg J, & Jones TA (2002) The active site of cellobiohydrolase cel6a from trichoderma reesei: The roles of aspartic acids d221 and d175. *J Am Chem Soc* 124(34):10015-10024.

73. Vrsanska M & Biely P (1992) The cellobiohydrolase-i from trichoderma-reesei qm-9414 - action on cello-oligosaccharides. *Carbohydrate Research* 227:19-27.

74. Levine SE, Fox JM, Clark DS, & Blanch HW (2011) A mechanistic model for rational design of optimal cellulase mixtures. *Biotechnol Bioeng*.

75. Sternberg D & Mandels GR (1979) Induction of cellulolytic enzymes in trichoderma reesei by sophorose. *J Bacteriol* 139(3):761-769.

76. Messner R, Gruber F, & Kubicek CP (1988) Differential regulation of synthesis of multiple forms of specific endoglucanases by trichoderma reesei qm9414. *J Bacteriol* 170(8):3689-3693.

77. Seiboth B, Hofmann G, & Kubicek CP (2002) Lactose metabolism and cellulase production in hypocrea jecorina: The gal7 gene, encoding galactose-1-phosphate uridylyltransferase, is essential for growth on galactose but not for cellulase induction. *Mol Genet Genomics* 267(1):124-132.

78. Fekete E, Seiboth B, Kubicek CP, Szentirmai A, & Karaffa L (2008) Lack of aldose 1-epimerase in hypocrea jecorina (anamorph trichoderma reesei): A key to

cellulase gene expression on lactose. *Proc Natl Acad Sci U S A* 105(20):7141-7146.

79. Morozova O, Hirst M, & Marra MA (2009) Applications of new sequencing technologies for transcriptome analysis. *Annu Rev Genomics Hum Genet* 10:135-151.

80. Langmead B, Trapnell C, Pop M, & Salzberg SL (2009) Ultrafast and memory-efficient alignment of short DNA sequences to the human genome. *Genome Biol* 10(3):R25.

81. Roberts A, Trapnell C, Donaghey J, Rinn JL, & Pachter L (2011) Improving rna-seq expression estimates by correcting for fragment bias. *Genome Biol* 12(3):R22.

82. Cantarel BL, Coutinho PM, Rancurel C, Bernard T, Lombard V, & Henrissat B (2009) The carbohydrate-active enzymes database (cazy): An expert resource for glycogenomics. *Nucleic Acids Res* 37(Database issue):D233-238.

83. Nielsen H, Emanuelsson O, Brunak S, & von Heijne G (2007) Locating proteins in the cell using targetp, signalp and related tools. *Nature Protocols* 2(4):953-971.

84. Ruepp A, Zollner A, Maier D, Albermann K, Hani J, Mokrejs M, Tetko I, Guldener U, Mannhaupt G, Munsterkotter M, & Mewes HW (2004) The funcat, a functional annotation scheme for systematic classification of proteins from whole genomes. *Nucleic Acids Res* 32(18):5539-5545.

85. Phillips CM, Iavarone AT, & Marletta MA (2011) A quantitative proteomic approach for cellulose degradation by neurospora crassa. *J Proteome Res* 10(9):4177-4185.

86. Tamayo EN, Villanueva A, Hasper AA, de Graaff LH, Ramon D, & Orejas M (2008) Crea mediates repression of the regulatory gene xlnr which controls the production of xylanolytic enzymes in aspergillus nidulans. *Fungal Genet Biol* 45(6):984-993.

87. Nakari-Setala T, Paloheimo M, Kallio J, Vehmaanpera J, Penttila M, & Saloheimo M (2009) Genetic modification of carbon catabolite repression in trichoderma reesei for improved protein production. *Appl Environ Microbiol* 75(14):4853-4860.

88. Ilmen M, Saloheimo A, Onnela ML, & Penttila ME (1997) Regulation of cellulase gene expression in the filamentous fungus trichoderma reesei. *Appl Environ Microbiol* 63(4):1298-1306.

89. Gibbs PA, Seviour RJ, & Schmid F (2000) Growth of filamentous fungi in submerged culture: Problems and possible solutions. *Crit Rev Biotechnol* 20(1):17-48.

90. Colot HV, Park G, Turner GE, Ringelberg C, Crew CM, Litvinkova L, Weiss RL, Borkovich KA, & Dunlap JC (2006) A high-throughput gene knockout procedure for neurospora reveals functions for multiple transcription factors. *Proceedings of the National Academy of Sciences of the United States of America* 103(27):10352-10357.

91. McCluskey K, Wiest A, & Plamann M (2010) The fungal genetics stock center: A repository for 50 years of fungal genetics research. *Journal of biosciences* 35(1):119-126.

92. FGSC (2011) Neurospora protocol guide. Http://www.Fgsc.Net/neurospora/neurosporaprotocolguide.Htm.

93. Vogel H (1956) A convenient growth medium for neurospora. *Microbial Genetics Bulletin* 13:42-46.

94. Marshall AG & Hendrickson CL (2008) High-resolution mass spectrometers. *Annu Rev Anal Chem (Palo Alto Calif)* 1:579-599.

95. Tamura K, Peterson D, Peterson N, Stecher G, Nei M, & Kumar S (2011) Mega5: Molecular evolutionary genetics analysis using maximum likelihood, evolutionary distance, and maximum parsimony methods. *Mol Biol Evol* 28(10):2731-2739.

96. Dementhon K, Iyer G, & Glass NL (2006) Vib-1 is required for expression of genes necessary for programmed cell death in neurospora crassa. *Eukaryot Cell* 5(12):2161-2173.

97. de Hoon MJL, Imoto S, Nolan J, & Miyano S (2004) Open source clustering software. *Bioinformatics* 20(9):1453-1454.

98. Roepstorff P & Fohlman J (1984) Proposal for a common nomenclature for sequence ions in mass spectra of peptides. *Biomed Mass Spectrom* 11(11):601.

99. Reese ET, Levinson HS, Downing MH, & White WL (1950) Quartermaster culture collection. *Farlowia* 4(1):45-86.

100. Znameroski EA, Coradetti ST, Roche CM, Tsai JC, Iavarone AT, Cate JH, & Glass NL (2012) Induction of lignocellulose-degrading enzymes in neurospora crassa by cellodextrins. *Proceedings of the National Academy of Sciences of the United States of America*.

101. Galazka JM (2011) Cellodextrin transporters of neurospora crassa and their utility in *saccharomyces cerevisiae* during a biofuel production process. Ph.D. (University of California, Berkeley).

102. Chernoglazov VM, Jafarova AN, & Klyosov AA (1989) Continuous photometric determination of endo-1,4-beta-d-glucanase (cellulase) activity using 4-methylumbelliferyl-beta-d-cellobioside as a substrate. *Analytical biochemistry* 179(1):186-189.

Figures

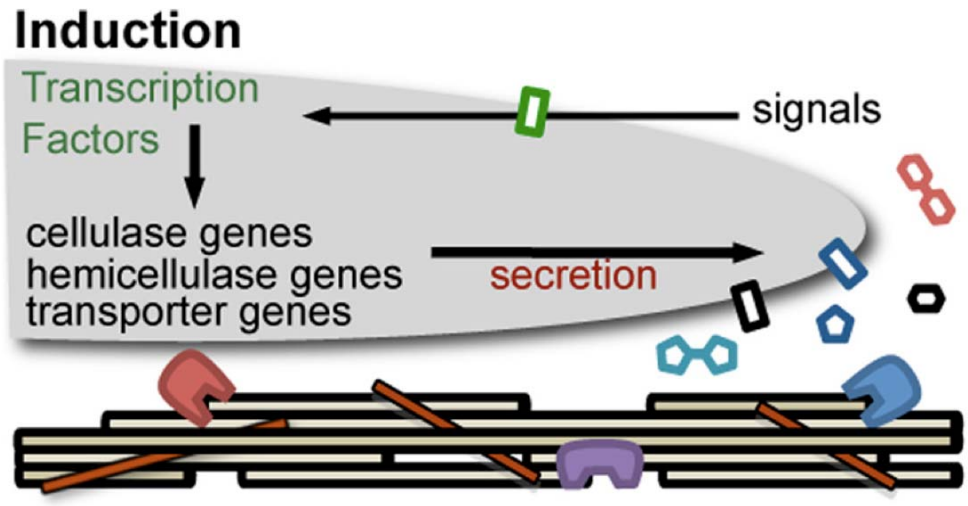

Tian et al. (2009) PNAS 106:22157-22162.

Figure 1-1 Model of plant cell wall induction in *N. crassa*.
Extracellular enzymes expressed at low levels generate metabolites that signal *N. crassa* to dramatically increase the expression level of genes encoding plant cell wall degrading enzymes.

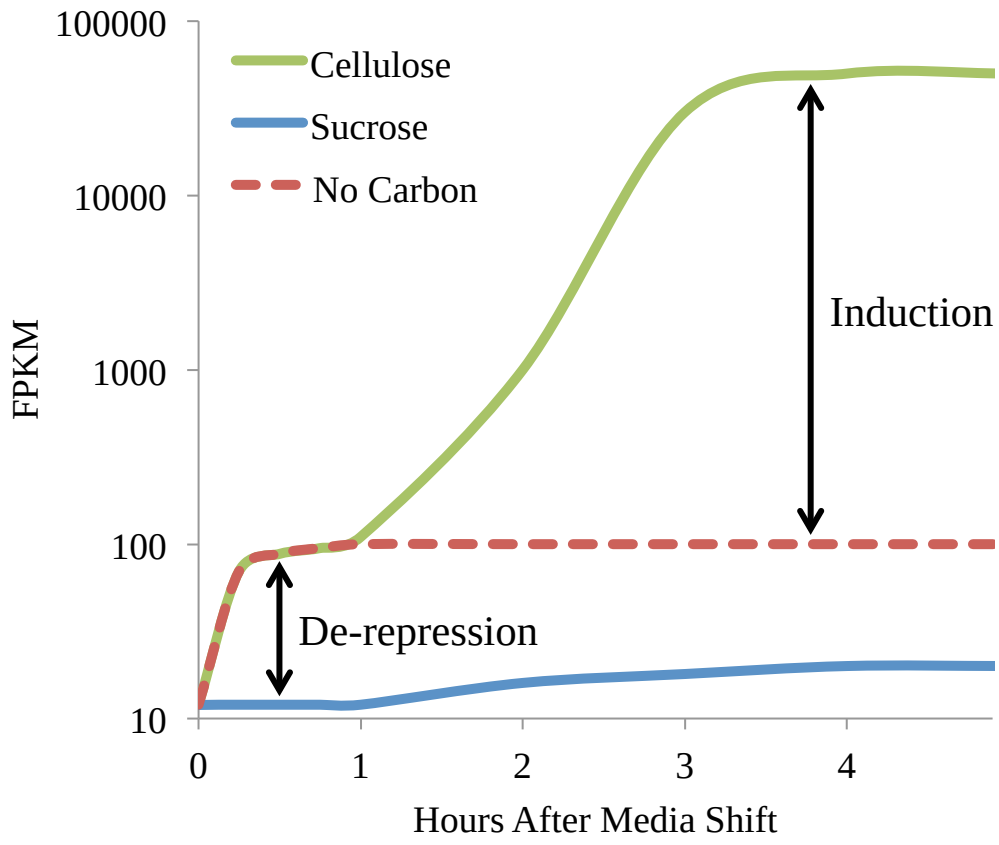

Figure 1-2 De-repression and induction of genes encoding lignocellulose degrading enzymes.
Cellulase and hemicellulase gene expression requires both low glucose (de-repression) and the presence of a specific inducer (induction).

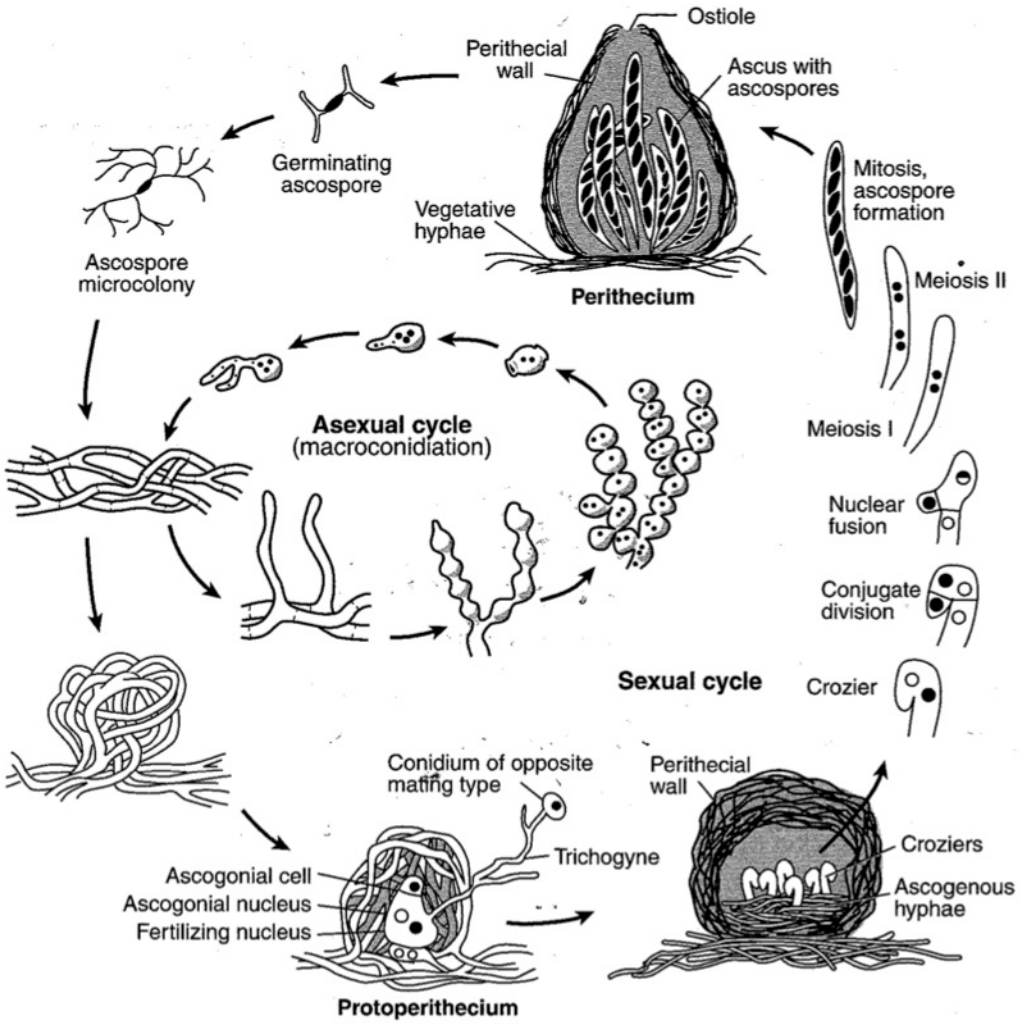

Figure 2-1 The life cycle of *Neurospora*.
Neurospora undergoes both an asexual (inner) and sexual (outer) reproduction (69).

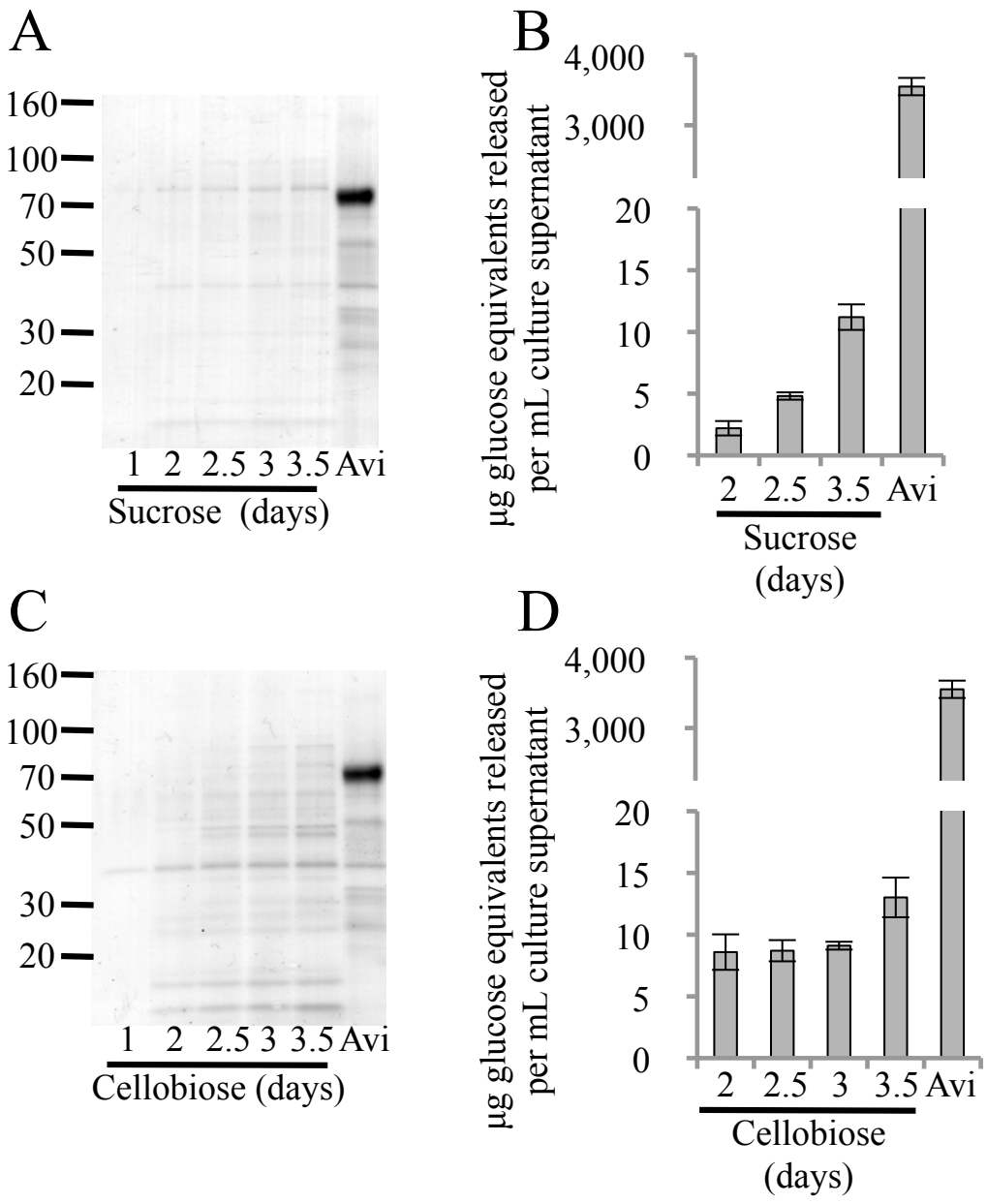

Figure 2-2 Protein production and enzyme activity are not induced by starvation. (A) SDS-PAGE of secreted proteins in culture filtrates from WT grown on sucrose for 3.5 days and (B) supernatant activity (from A) towards Avicel. (C) SDS-PAGE of secreted proteins in culture filtrates from WT grown on cellobiose for 3.5 days and (D) supernatant activity (from C) towards Avicel. Error bars are 1 standard deviation.

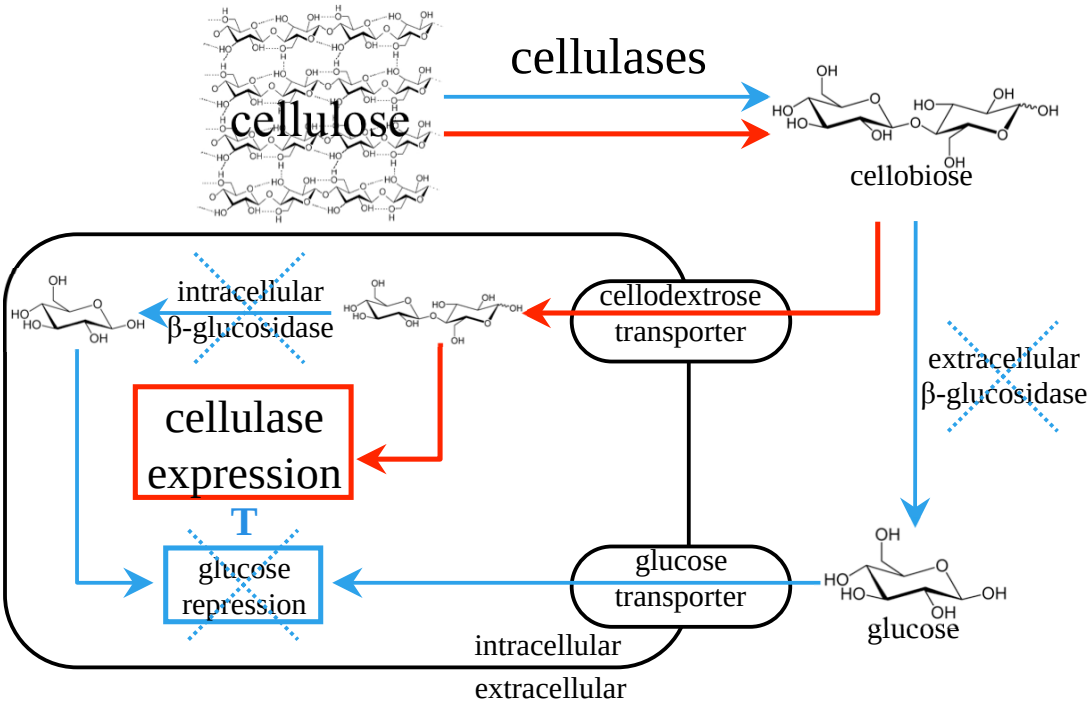

Figure 2-3 Model for transcriptional regulation of cellulases in β-glucosidase deletion strains of *N. crassa*.
Both transcriptional derepression and specific induction are required to achieve maximal transcriptional activation of cellulase expression. Arrows indicate possible pathways for cellulose metabolites. Blue lines and red lines indicate pathways hypothesized to be minimized and to be most active, respectively, in the Δ3βG and Δ3βGΔcre deletion strains.

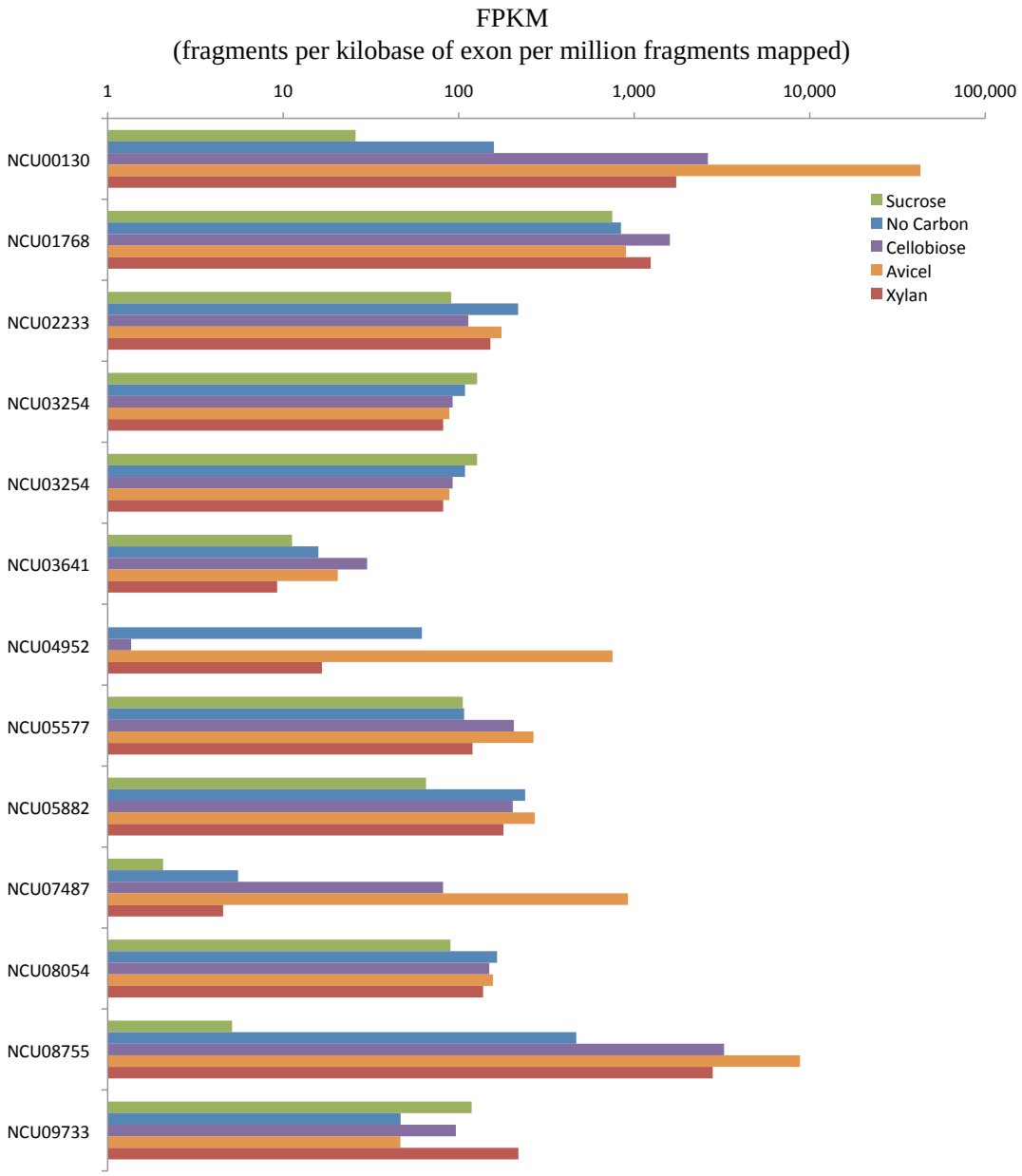

Figure 2-4 Expression of predicted β-glucosidase genes.
The expression of predicted β-Glucosidase genes in wild type N. crassa when exposed to Sucrose, No Carbon (Starvation), Cellobiose, Avicel, and Xylan.

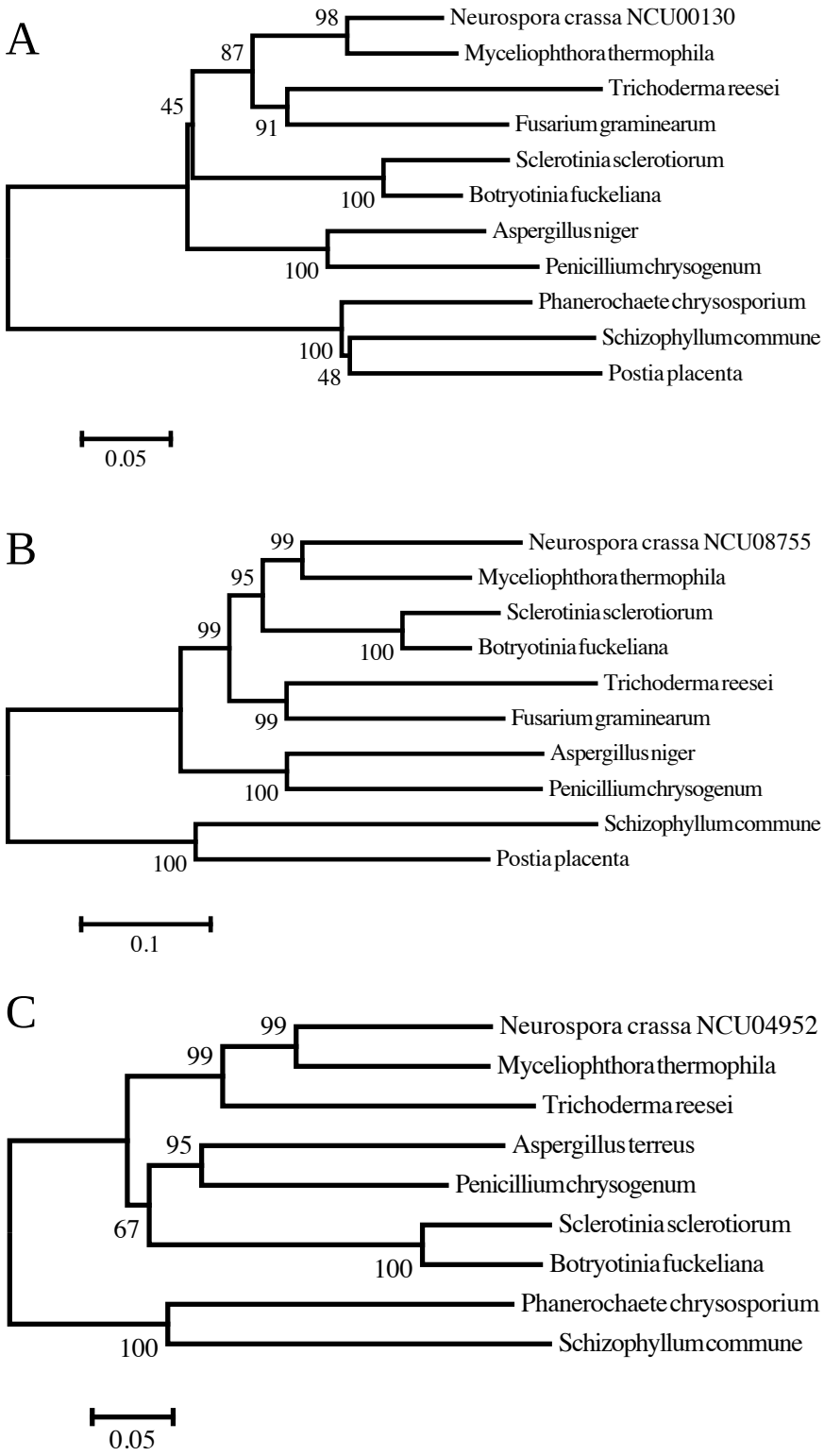

Figure 2-5 Maximum likelihood phylogenetic analysis of the deleted β-glucosidases in various filamentous fungi.

(A) NCU08755, (B) NCU04952 and (C) NCU00130. Accession numbers for each gene are listed in the Methods 2.6.5.

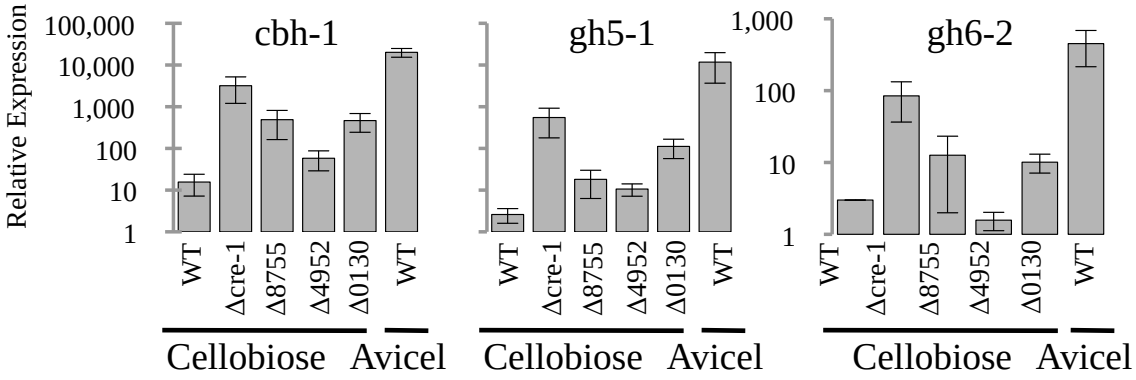

Figure 2-6 Cellulase induction in WT and single β-glucosidase deletion strains after induction with cellobiose or Avicel.

(A) Gene expression of select cellulases after 4 hour induction with 0.2% cellobiose or 1% Avicel in WT, Δcre-1, ΔNCU08755, Δ NCU04952, and Δ NCU00130. Gene expression levels of *cbh*-1, *gh6-2* and *gh5-1* were normalized to 1 when switched to 1% sucrose. Actin was used as an endogenous control in all samples. Each strain was grown in triplicate and error bars indicate 1 standard deviation.

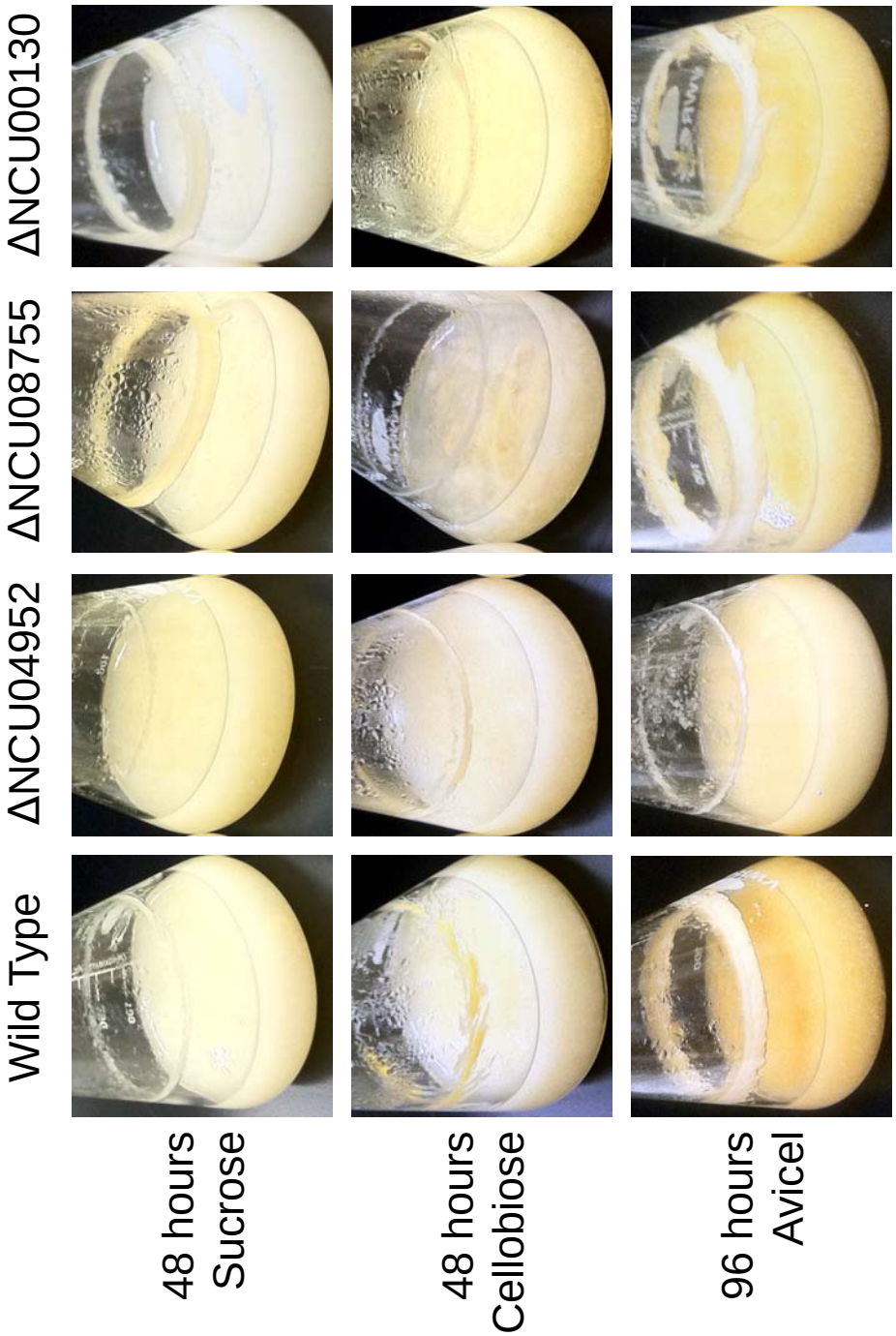

Figure 2-7 Phenotypes for the β-glucosidase deletion strains.
The growth phenotypes for the single β-glucosidase deletion strains after growth on either sucrose, cellobiose or Avicel. Conidia from strains were inoculated at a concentration equal to $2x10^6$ conidia per milliliter 100ml Vogel's salts (93) with 2% w/v sucrose, cellobiose or Avicel in a 250ml Erlenmeyer flask and grown under constant light at 200 rpm for 2 days (sucrose), 2 days (cellobiose) and 4 days (Avicel). Photos were taken daily.

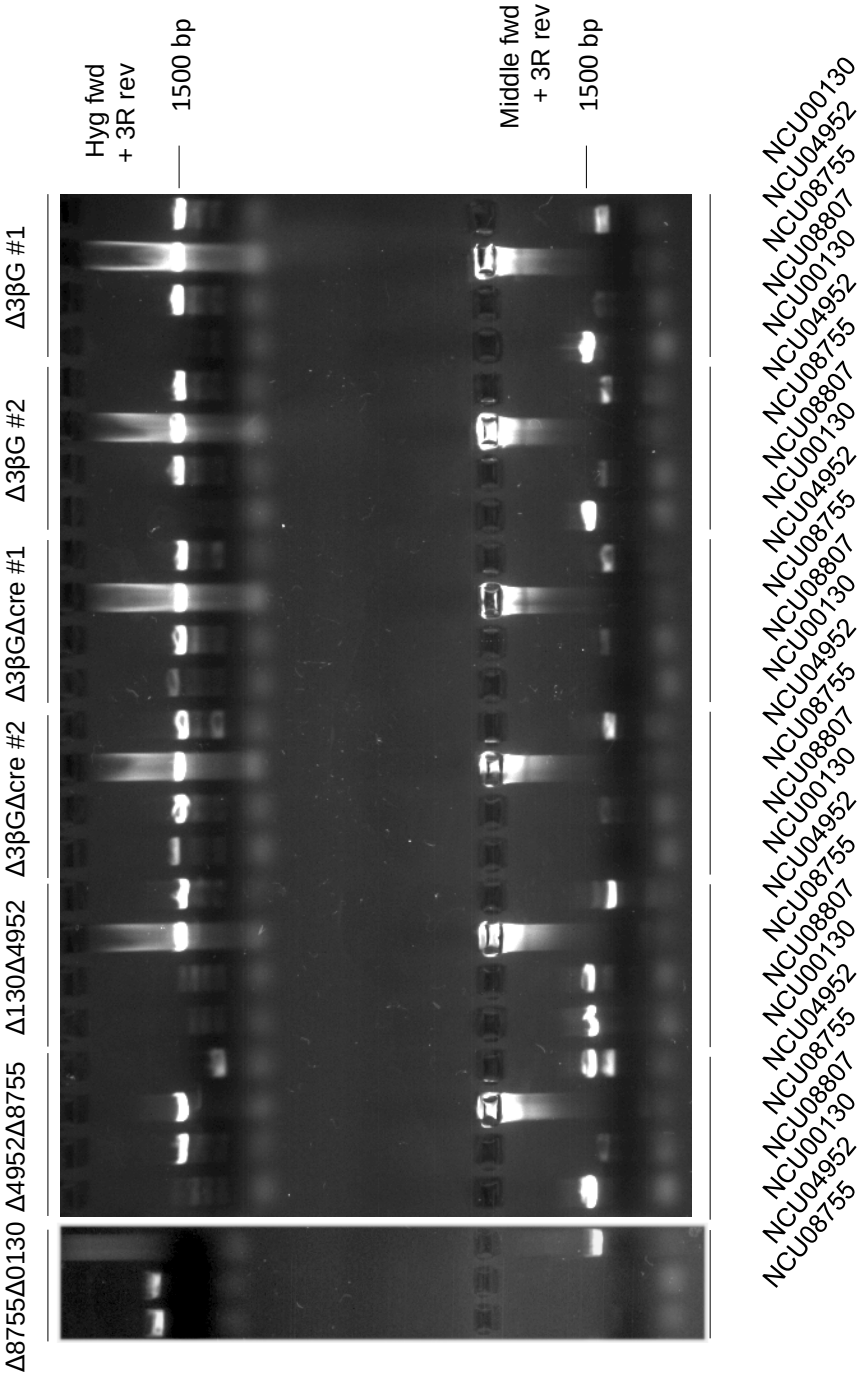

Figure 2-8 PCR genotyping for the multiple β-glucosidase deletion strains.
Each cross was genotyped using two different sets of PCR Primers: (Top) The hygromycin specific forward and gene specific reverse primer (outside of the deletion cassette) only produces a product in the presence of the knockout cassette, and (Bottom) a forward primer specifically designed to be within the gene and gene specific reverse primer (outside of the deletion cassette) only produces a product in an intact gene.

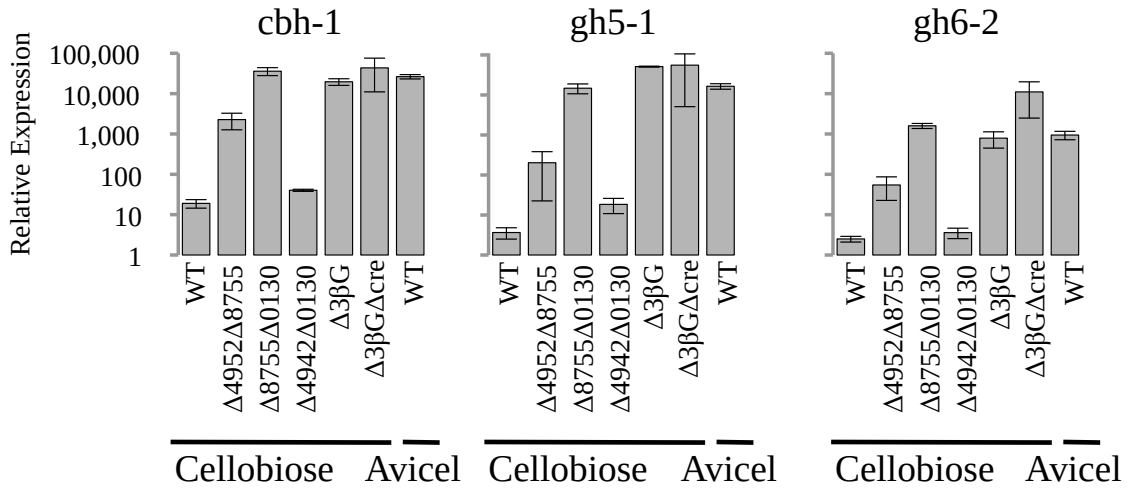

Figure 2-9 Cellulase induction in WT and double β-glucosidase deletion strains after induction with cellobiose or Avicel.
Gene expression of select cellulases after 4 hour induction with 0.2% cellobiose or 1% Avicel in WT, Δ3βG and Δ3βGΔcre. Gene expression levels of *cbh-1*, *gh6-2*, and *gh5-1* were normalized to 1 when induced with 1% sucrose. Actin was used as an endogenous control in all samples. Each strain was grown in triplicate and error bars indicate 1 standard deviation.

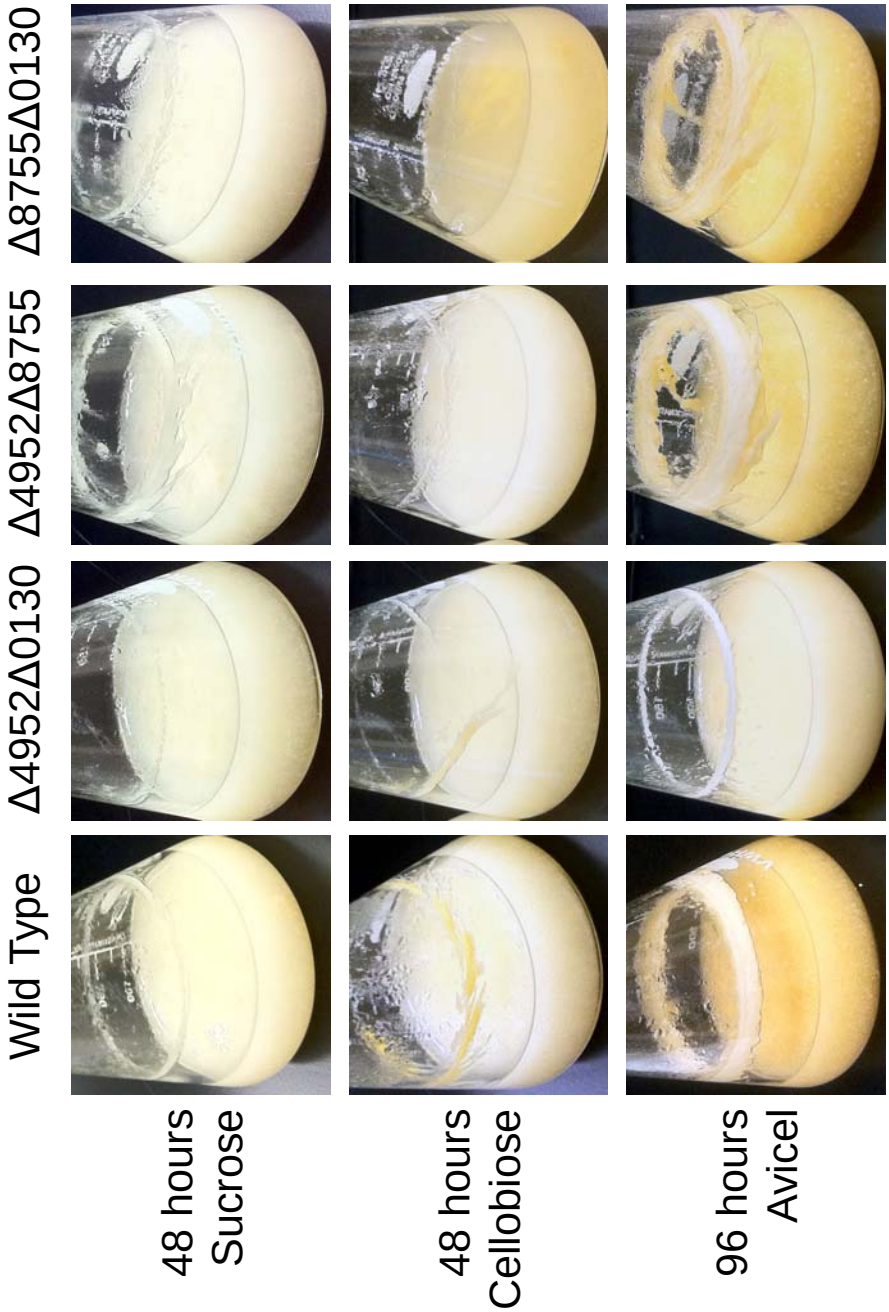

Figure 2-10 Phenotypes for the multiple β-glucosidase deletion strains.
The growth phenotypes for the multiple β-glucosidase deletion strains after growth on either sucrose, cellobiose or Avicel. Conidia from strains were inoculated at a concentration equal to $2x10^6$ conidia per milliliter 100ml Vogel's salts (93) with 2% w/v sucrose, cellobiose or Avicel in a 250ml Erlenmeyer flask and grown under constant light at 200 rpm for 2 days (sucrose), 2 days (cellobiose) and 4 days (Avicel). Photos were taken daily.

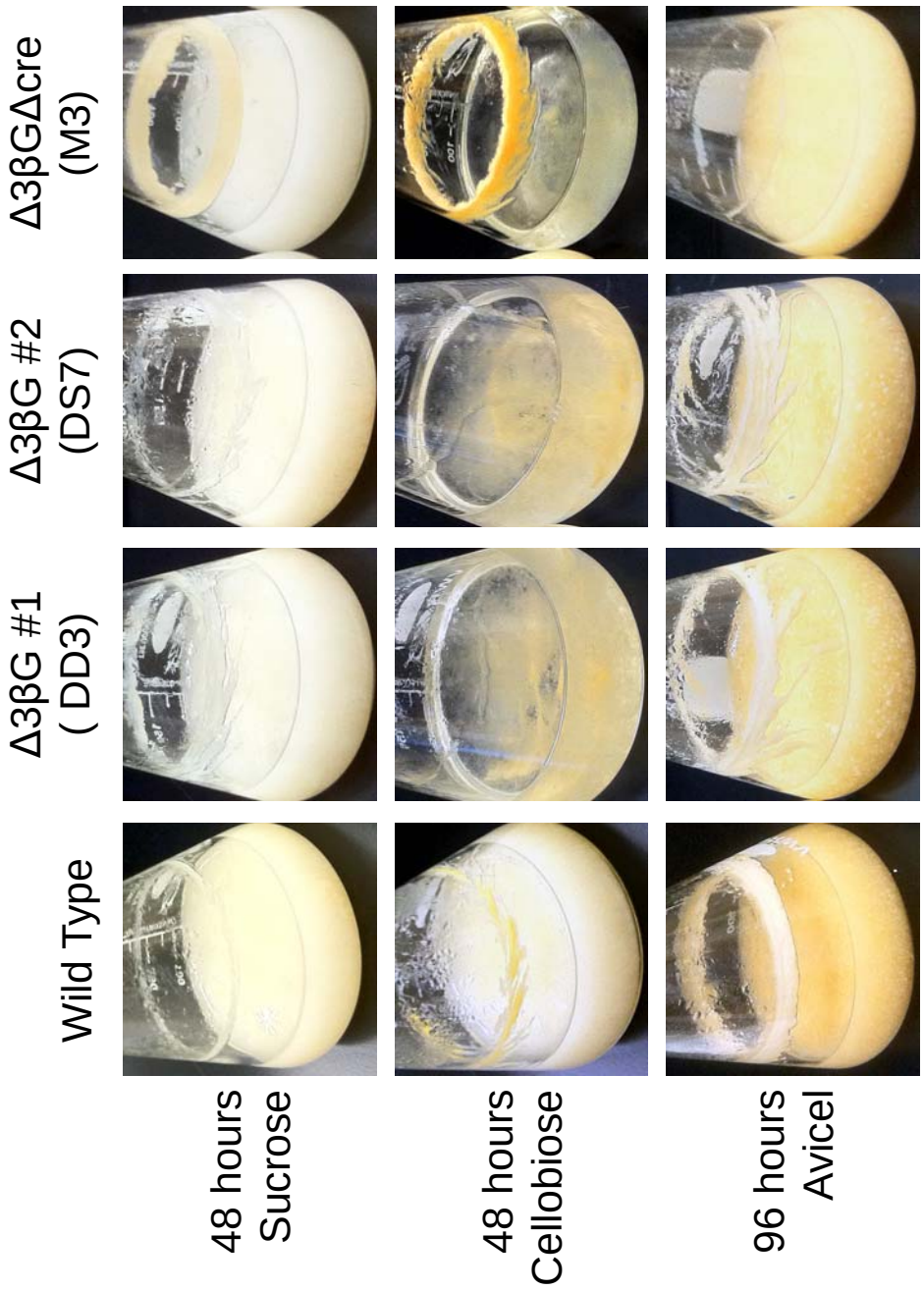

Figure 2-11 Phenotype for the triple β-glucosidase deletion strains.
The growth phenotypes for the triple β-glucosidase deletion strains after growth on either sucrose, cellobiose or Avicel. Two individual ascospores were followed throughout the study to confirm all results. Conidia from strains were inoculated at a concentration equal to $2x10^6$ conidia per milliliter 100ml Vogel's salts (93) with 2% w/v sucrose, cellobiose or Avicel in a 250ml Erlenmeyer flask and grown under constant light at 200 rpm for 2 days (sucrose), 2 days (cellobiose) and 4 days (Avicel). Photos were taken daily.

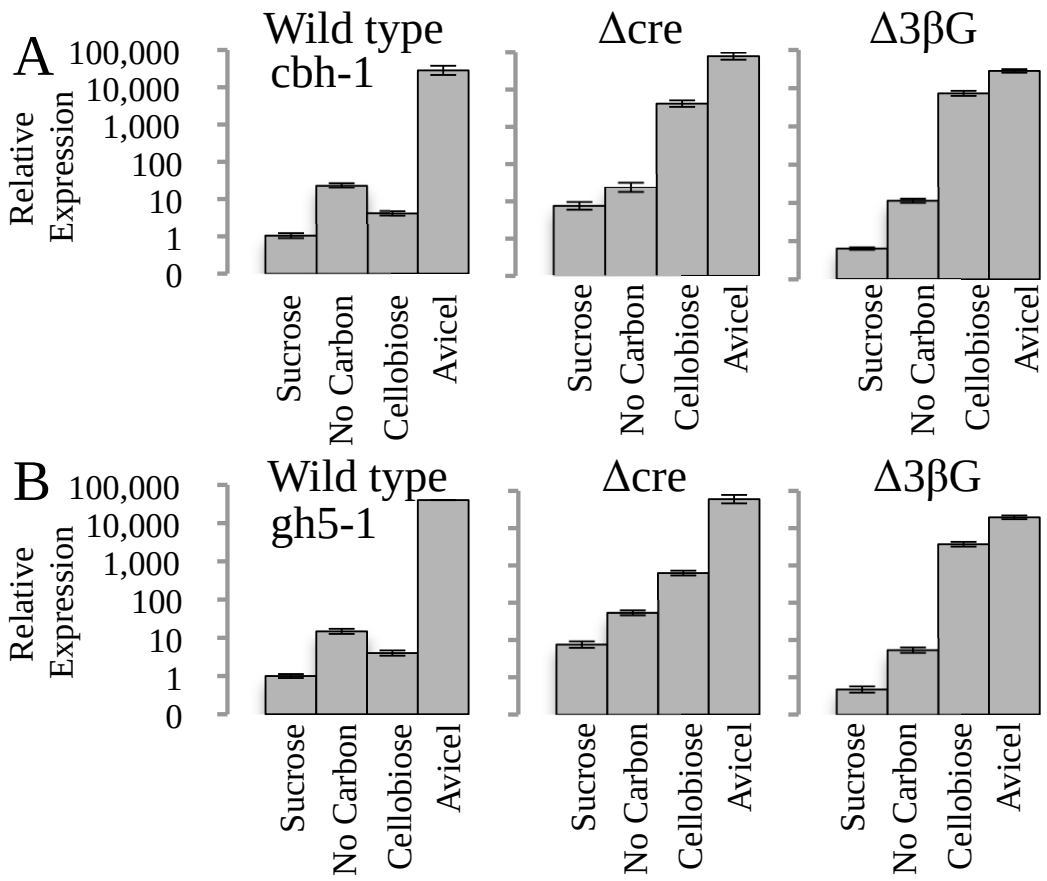

Figure 2-12 Cellulase induction in WT, Δ*cre-1*, and Δ3βG after 4 hours response to sucrose, no carbon (starvation), cellobiose and Avicel.
(A) *cbh*-1 and (B) expression in WT, Δcre, and Δ3βG after a 4 hour induction with 1% sucrose, no carbon (Vogel's salt solution only), 0.2% cellobiose, or 1% Avicel. Expression levels for all genes were normalized to 1 when induced with 1% sucrose. Actin (NCU04173) gene expression levels were used as an endogenous control in all samples. Each reaction was done in triplicate and error bars indicate 1 standard deviation.

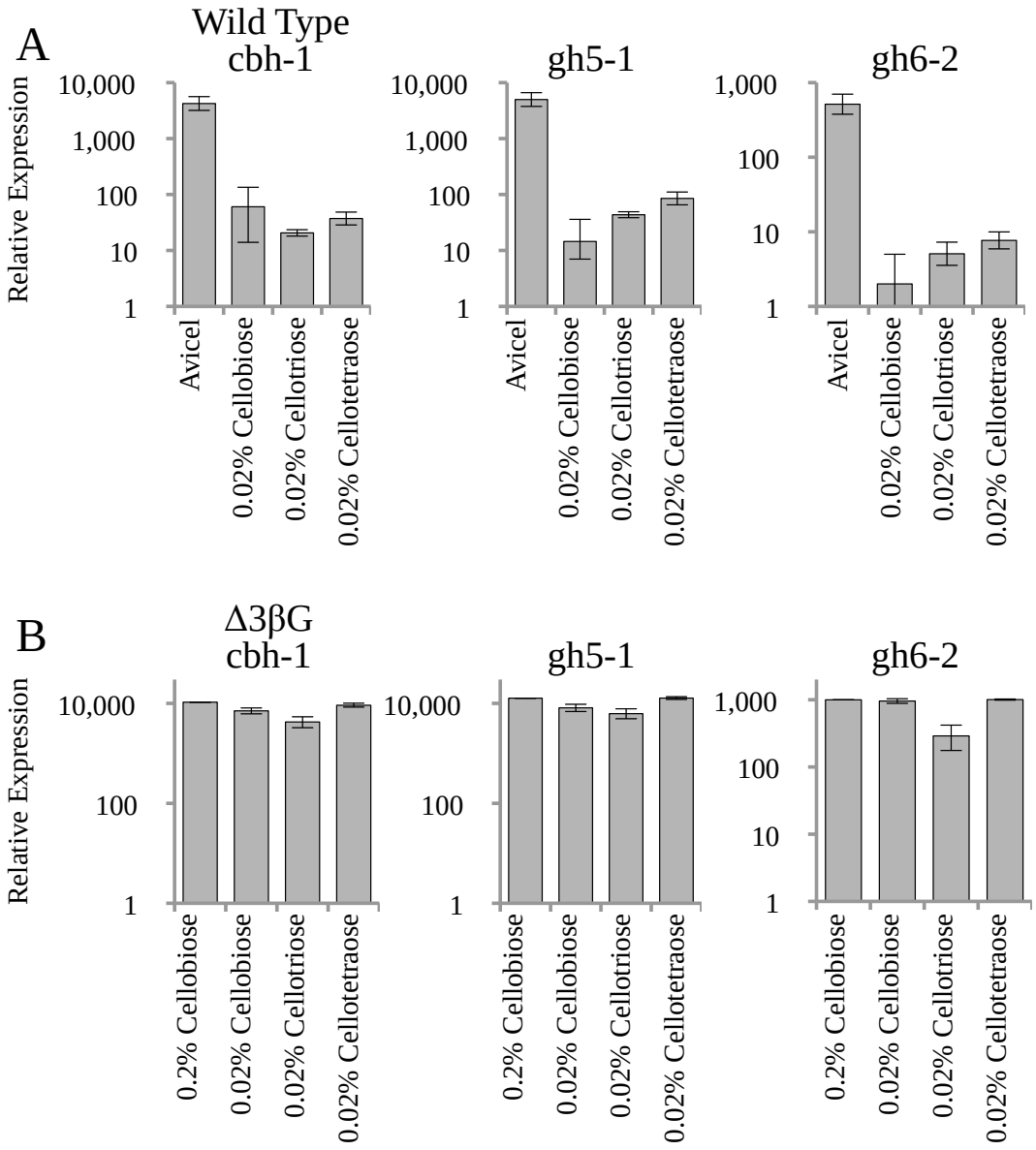

Figure 2-13 Cellulase induction by cellobiose, cellotriose and cellotetraose.
Gene expression of select cellulases after 4 hour induction with 0.2% cellobiose, 0.02% cellobiose, 0.02% cellotriose, or 0.02% cellotetraose, in (A) WT and (B) Δ3βG. Gene expression levels of *cbh*-1, *gh6-2* and *gh5-1* were normalized to 1 when switched to 1% sucrose. Actin was used as an endogenous control in all samples. Each strain was grown in triplicate and error bars indicate 1 standard deviation.

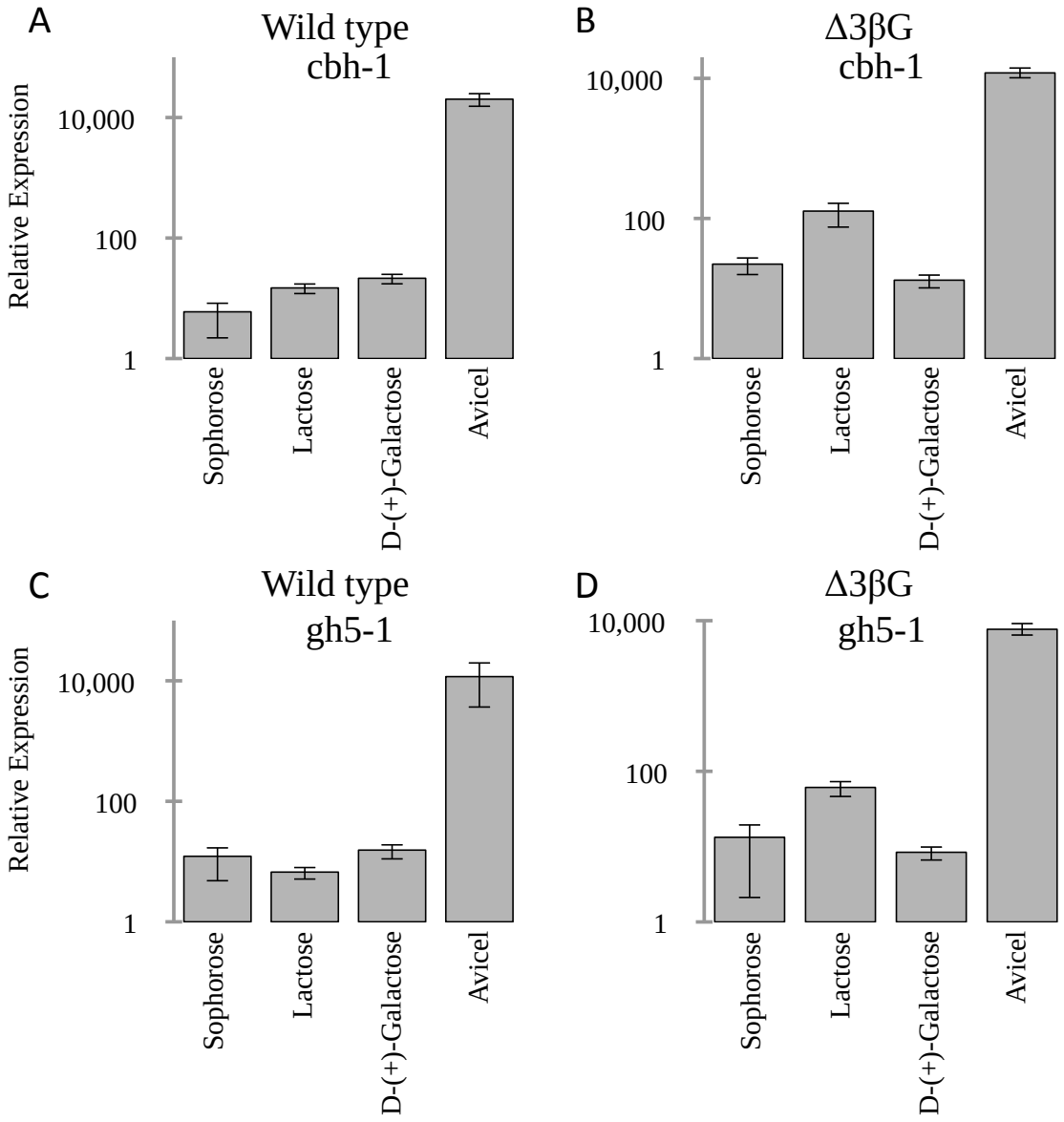

Figure 2-14 Cellulase induction in WT and Δ3βG after induction with common *T. reesei* inducers.

cbh-1 expression in (A) WT and (B) Δ3βG and *gh6-2* expression in (C) WT and (D) Δ3βG after a 4 hour induction with 1mM sophorose, 1mM lactose or 1mM D-(+)-galactose. Gene expression levels of *cbh*-1 and *gh6-2* were normalized to 1 when induced with 1% sucrose. Actin (NCU04173) gene expression levels were used as an endogenous control in all samples. Error bars indicate 1 standard deviation.

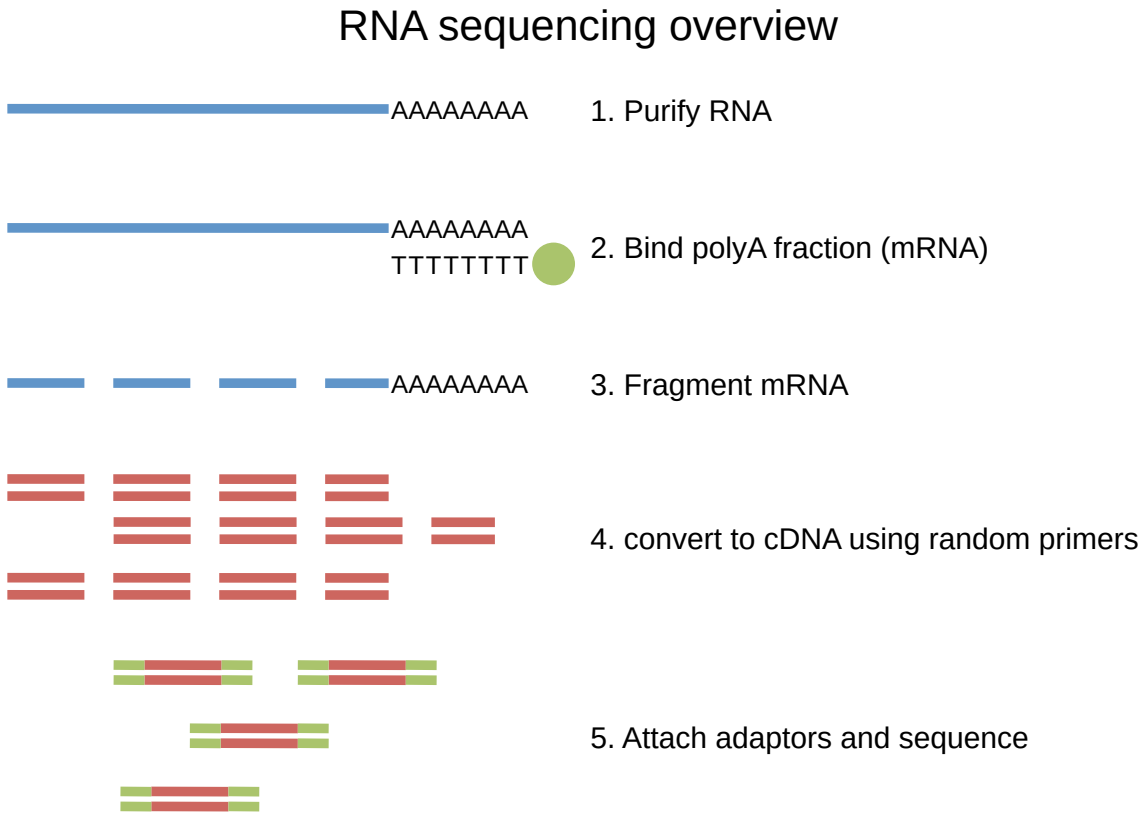

Figure 2-15 RNA sequencing overview.

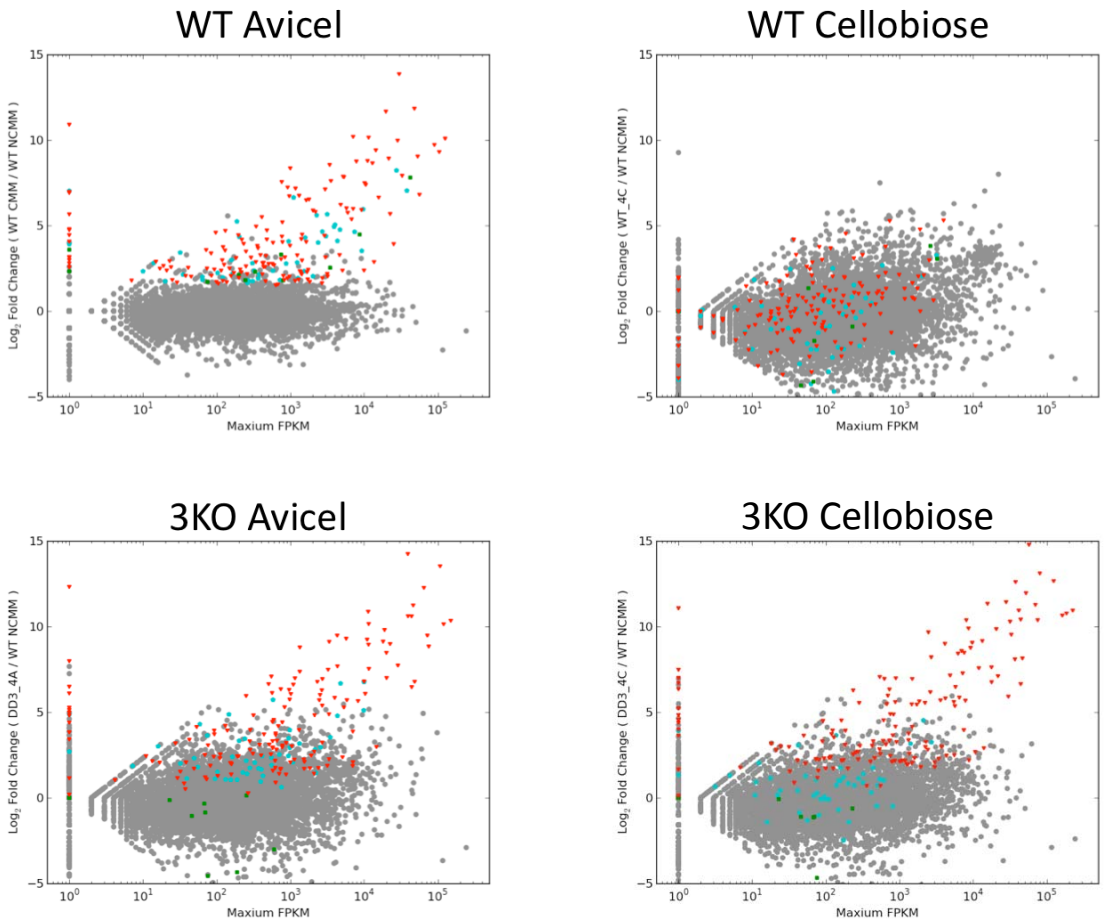

Figure 2-16 RNA sequencing of the WT and Δ3βG strains.
Scatter plots comparing the full genomic pattern of gene expression change in (A) WT induced with Avicel, (B) WT induced with cellobiose, (C) Δ3βG induced with Avicel, and (D) Δ3βG induced with Cellobiose as compared to WT under conditions of starvation. All strains were grown for 16 hours on 2% sucrose, followed by a transfer to no carbon source (Vogels salt solution only), 0.2% cellobiose or 1% Avicel for 4 hours. Colored dots represent the cellulose regulon. Red dots indicate genes induced by cellobiose in the Δ3βG strain, blue dots indicate genes not induced by cellobiose in the Δ3βG strain and green dots indicate genes not induced by either cellobiose or Avicel in the Δ3βG deletion strain.

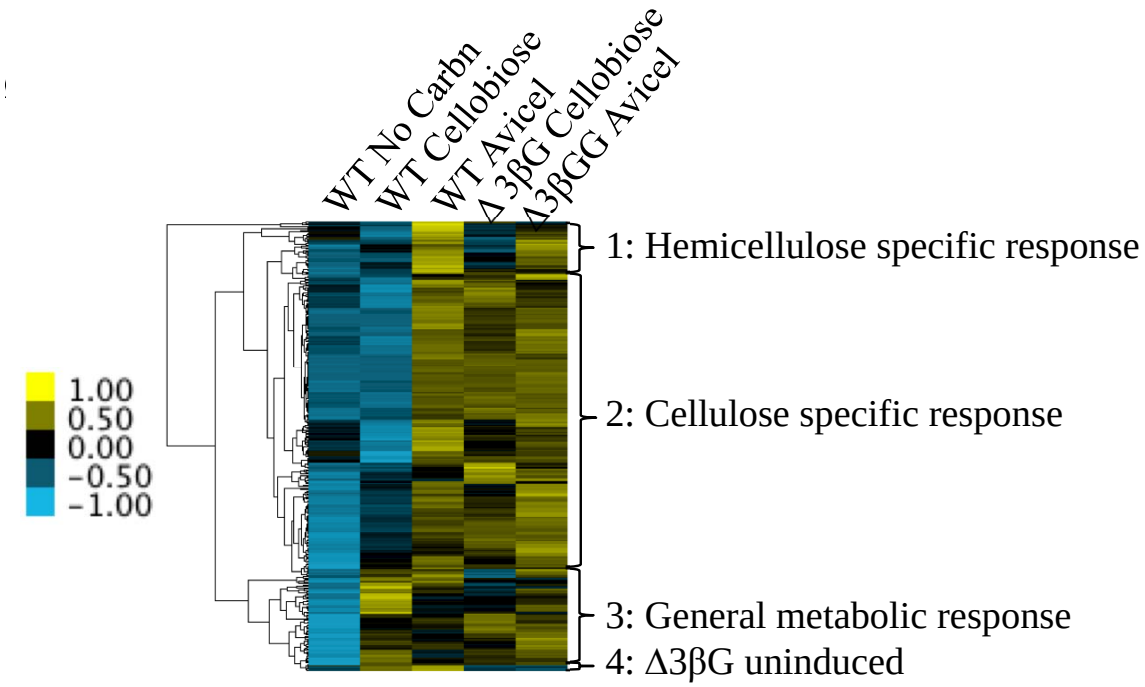

Figure 2-17 RNA sequencing of the WT and Δ3βG strains.
(A) Hierarchical clustering analysis of 318 genes differentially induced in WT *N. crassa* by Avicel, compared to induction by cellobiose. Yellow indicates higher relative expression and blue indicates lower relative expression.

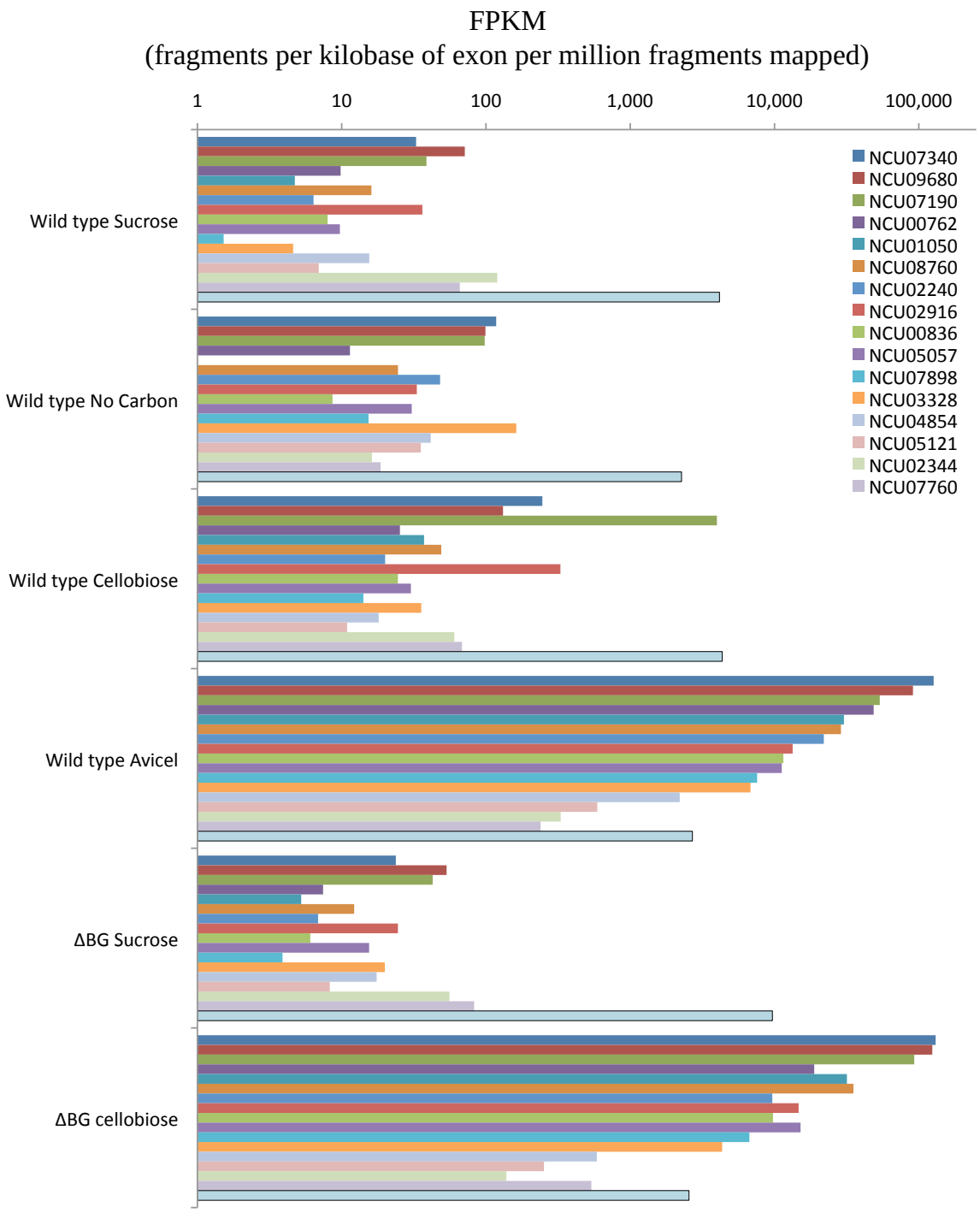

Figure 2-18 Cellulase expression in FPKMs.
FPKMs (fragments per kilobase of exon per million fragments mapped) for the WT exposed to sucrose, no carbon, cellobiose or Avicel compared to Δ3βG exposed to sucrose or cellobiose. All strains were grown for 16 hours on 2% sucrose, followed by a transfer to no carbon source (Vogels salt solution only), 0.2% cellobiose or 1% Avicel for 4 hours.

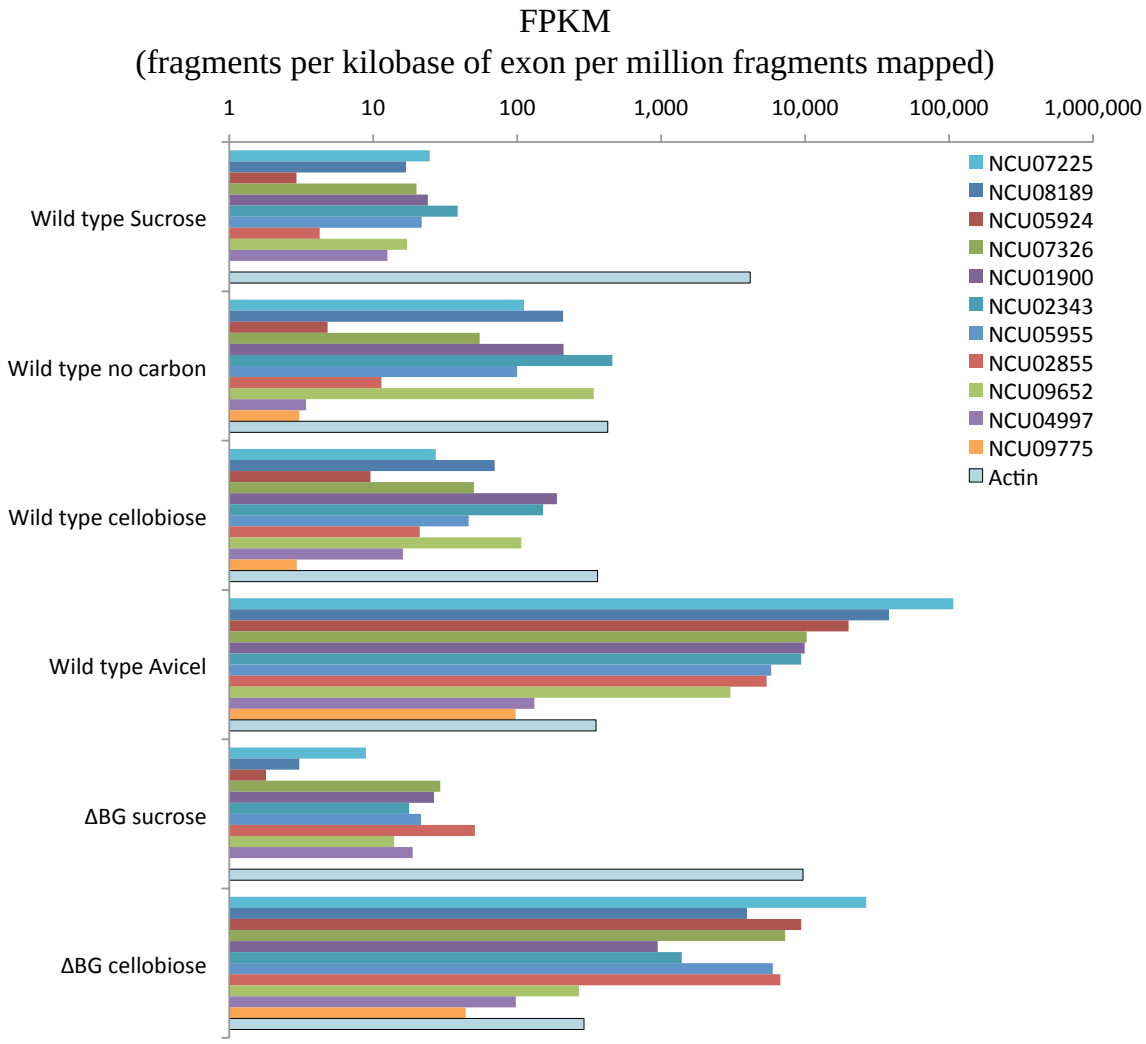

Figure 2-19 Hemicellulase expression in FPKMs.
FPKMs (fragments per kilobase of exon per million fragments mapped) for the WT exposed to sucrose, no carbon, cellobiose or Avicel compared to Δ3βG exposed to sucrose or cellobiose. All strains were grown for 16 hours on 2% sucrose, followed by a transfer to no carbon source (Vogels salt solution only), 0.2% cellobiose or 1% Avicel for 4 hours.

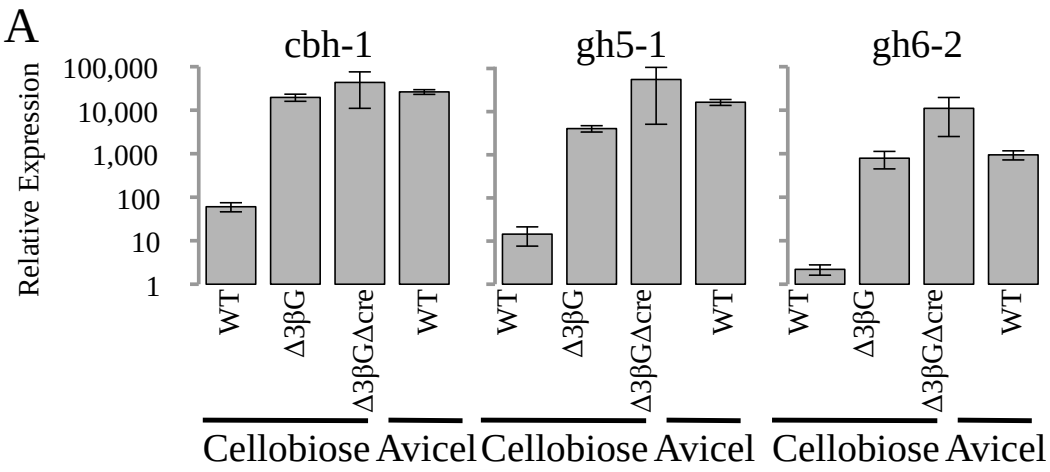

Figure 2-20 Cellulase induction in WT, Δ3βG, and Δ3βGΔ*cre-1* in response to cellobiose or Avicel.

cbh-1, *gh5-1*, and *gh6-2* expression in WT, Δ3βG, and Δ3βGΔ*cre* after a 4 hour induction with 1% sucrose, 0.2% cellobiose, or 1% Avicel. Expression levels for all genes were normalized to 1 when induced with 1% sucrose. Actin (NCU04173) gene expression levels were used as an endogenous control in all samples. Each reaction was done in triplicate and error bars indicate 1 standard deviation.

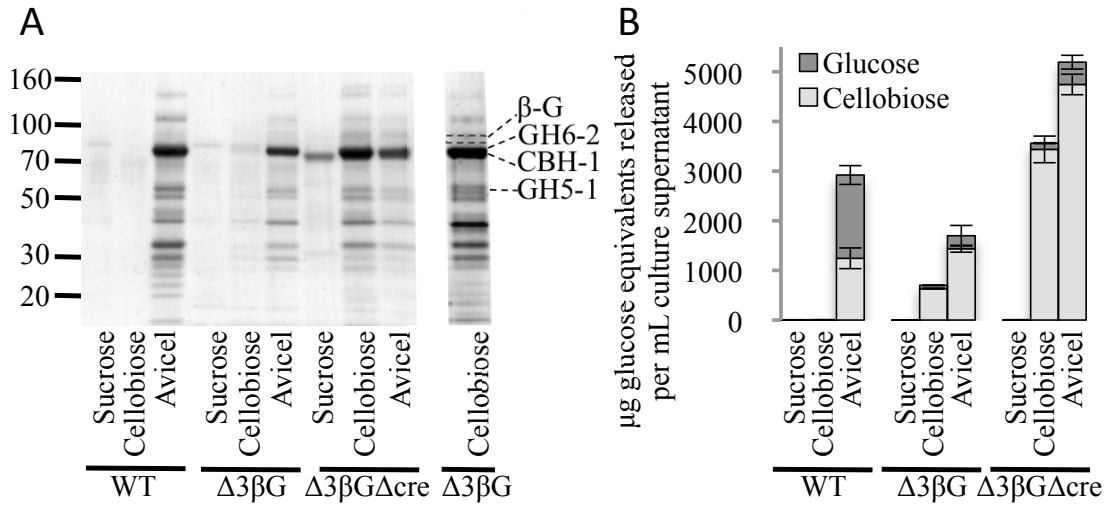

Figure 2-21 Cellulase expression in WT and β-glucosidase deletion strains after exposure to sucrose, cellobiose or Avicel.

(A) SDS-PAGE of secreted proteins in culture filtrates from WT, Δ3βG and Δ3βGΔcre. Growth and induction conditions are described in the Methods 2.6.14-2.6.15. Protein bands representing CBH-1, GH6-2, and GH5-1 are marked. In addition, the absence of the extracellular β-glucosidase (NCU04952) is marked in the triple knockout. The presence of glucoamylase I (NCU01517) correlates with the deletion of the cre gene. (B) Activity of supernatant from (A) towards Avicel. Glucose (dark grey) and cellobiose (light grey) were measured after 24 hours of incubation with 1% Avicel at 50 °C. Error bars are 1 standard deviation.

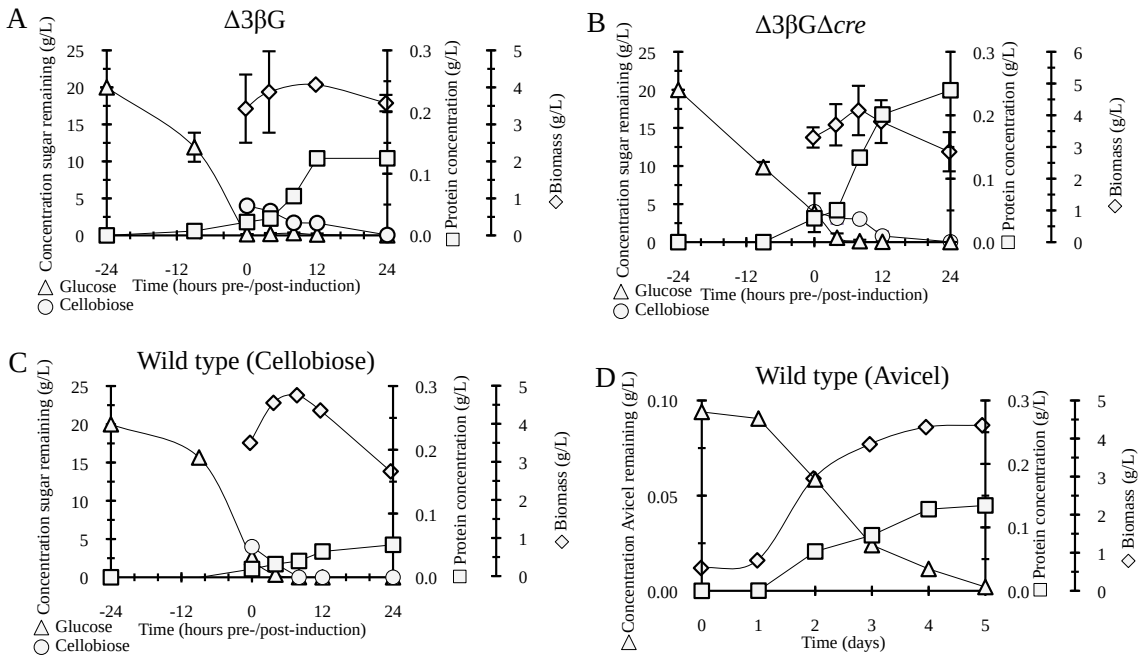

Figure 2-22 Production of cellulases in a bioreactor.
(A) Δ3βG induced with cellobiose, (B) Δ3βGΔcre induced with cellobiose, (C) WT induced with cellobiose and (D) WT grown 5 days on Avicel. Cellobiose-induced strains were pre-grown in minimal media with 1% sucrose for 24 hours before induction with 0.2% cellobiose for 36 hours. The concentration of sucrose, glucose, fructose (in glucose equivalents; triangle) cellobiose (circle), protein production (square), and biomass accumulation (diamond) were measured.

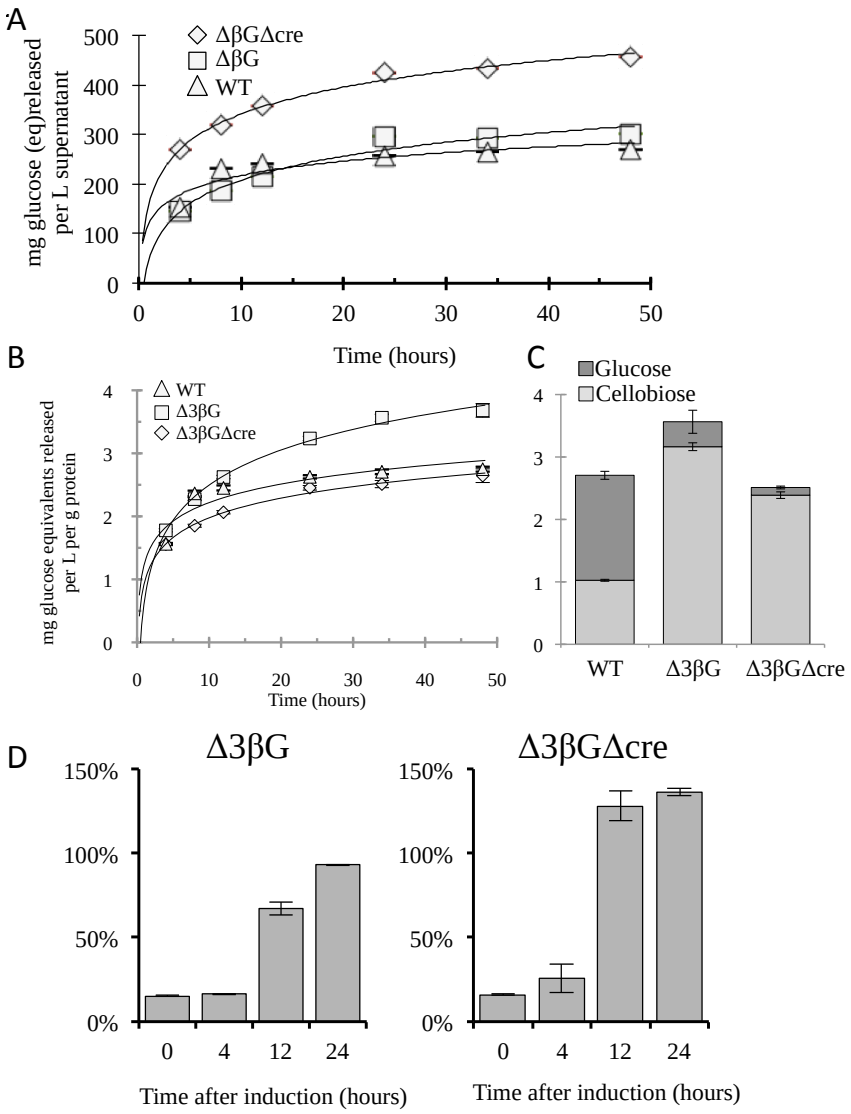

Figure 2-23 Enzyme activity from bioreactor produced culture supernatant.
(A) 24-hour induced supernatant activity from Figure 17 A, B, and D towards Avicel expressed as mg glucose (equivalents) released per L supernatant and (B) 24-hour induced supernatant activity from Figure 17 A, B, and D towards Avicel expressed as mg glucose (equivalents) released per grams protein. Cellulase activity of culture supernatant from Δ3βG (squares) and Δ3βGΔcre (triangle) induced with cellobiose for 24 hours compared to culture supernatants from WT grown on Avicel for 5 days (diamond). Error bars are 1 standard deviation. (C) Breakdown of cellobiose (light grey) and glucose (dark grey) produced in the Avicel hydrolysis assay (from A) after 36 hours. Error bars are 1 standard deviation. (D) Azo-CMC (endoglucanase) activity time course from bioreactor culture supernatants in Figure 17 A and B. Azo-CMC activity is expressed as a percentage of activity from WT culture supernatant grown on 2% Avicel for 5 days.

NCU #	Annotation	WT No Carbon	WT Cellobiose	WT Avicel	Δ3Gβ Cellobiose	Δ3Gβ Avicel	Cluster	CAZy	Signal P	Signal P Confidence	Annotation (Tians, et al.)
NCU05832	hypothetical protein	544	791	2539	1656	1423	1: Hemicellulose specific		Mitochondrion	5	
NCU08384	xylose reductase	72	590	27876	1200	10154	1: Hemicellulose specific		Other	2	
NCU01900	xylosidase/arabinosidase	210	189	9922	946	4492	1: Hemicellulose specific	GH43	Other	2	Hemicellulase
NCU00891	xylitol dehydrogenase	330	299	7632	902	3586	1: Hemicellulose specific		Other	2	
NCU10497	oligosaccharyl transferase STT3 subunit	602	795	1362	737	1112	1: Hemicellulose specific		Other	3	
NCU08687	galactokinase	283	380	1449	718	632	1: Hemicellulose specific		Other	2	
NCU03305	calcium-transporting ATPase	367	669	859	545	1081	1: Hemicellulose specific		Other	3	
NCU07705	C6 finger domain-containing protein	173	156	807	346	580	1: Hemicellulose specific		Other	4	
NCU07453	hypothetical protein	204	151	538	341	186	1: Hemicellulose specific		Other	2	
NCU09652	beta-xylosidase	340	107	3024	268	634	1: Hemicellulose specific	GH43	Other	2	Hemicellulase
NCU04932	hypothetical protein	136	414	1111	222	1468	1: Hemicellulose specific		Secretory Pathway	2	
NCU06364	GDSL lipase/acylhydrolase	108	224	877	193	405	1: Hemicellulose specific		Secretory Pathway	2	
NCU07737	salicylate hydroxylase	113	124	809	123	258	1: Hemicellulose specific		Other	3	
NCU00809	MFS monosaccharide transporter	85	89	233	89	210	1: Hemicellulose specific		Other	1	
NCU10014	hypothetical protein	93	251	1147	89	873	1: Hemicellulose specific		Secretory Pathway	2	
NCU02485	hypothetical protein	30	42	252	83	83	1: Hemicellulose specific		Other	2	
NCU07546	multidrug resistance protein MDR	70	111	259	82	417	1: Hemicellulose specific		Other	1	
NCU05591	ABC transporter CDR4	94	80	380	81	957	1: Hemicellulose specific		Other	4	
NCU04475	lipase B	231	38	4771	76	429	1: Hemicellulose specific		Secretory Pathway	1	
NCU08117	hypothetical protein	35	40	166	71	104	1: Hemicellulose specific		Other	4	
NCU04298	pentafunctional AROM polypeptide	105	35	226	63	145	1: Hemicellulose specific		Other	2	
NCU09823	hypothetical protein	101	29	295	54	131	1: Hemicellulose specific		Secretory Pathway	1	
NCU00710	acetyl xylan esterase	11	14	1119	53	588	1: Hemicellulose specific	CBM1, CE1	Secretory Pathway	2	
NCU09856	hypothetical protein	26	18	98	48	22	1: Hemicellulose specific		Other	2	
NCU04933	nucleoside-diphosphate-sugar epimerase	27	71	168	48	221	1: Hemicellulose specific		Secretory Pathway	5	
NCU05350	hypothetical protein	37	5	308	32	95	1: Hemicellulose specific		Secretory Pathway	1	
NCU04170	hypothetical protein	35	21	248	31	39	1: Hemicellulose specific		Secretory Pathway	2	
NCU07336	hypothetical protein	15	22	87	25	37	1: Hemicellulose specific		Other	4	
NCU08113	hypothetical protein	4	6	190	22	150	1: Hemicellulose specific		Other	2	
NCU05011	polyketide synthase 2	17	24	44	20	37	1: Hemicellulose specific		Other	3	
NCU10697	hypothetical protein	20	15	161	15	206	1: Hemicellulose specific		Mitochondrion	2	
NCU04167	hypothetical protein	19	9	68	14	23	1: Hemicellulose specific		Other	2	
NCU04168	hypothetical protein	18	3	151	13	36	1: Hemicellulose specific	GH16	Other	2	
NCU01003	hypothetical protein	9	13	37	7	38	1: Hemicellulose specific		Other	3	
NCU04557	hypothetical protein	2	3	24	6	17	1: Hemicellulose specific		Mitochondrion	2	
NCU08383	hypothetical protein	1		15		7	1: Hemicellulose specific		Mitochondrion	5	
NCU04169	hypothetical protein	20		3498		75	1: Hemicellulose specific		Secretory Pathway	1	
NCU07340	exoglucanase 1	118	246	126816	130865	151613	2: Cellulose specific	CBM1, GH7	Secretory Pathway	2	Cellulase
NCU09680	exoglucanase 2	99	131	91158	124112	123749	2: Cellulose specific	CBM1, GH6	Secretory Pathway	1	Cellulase
NCU07190	exoglucanase 3	98	3989	53665	93034	73075	2: Cellulose specific	GH6	Secretory Pathway	3	Cellulase
NCU04522	hypothetical protein	16	753	1810	74727	48249	2: Cellulose specific		Other	3	
NCU08756	hypothetical protein	10	55	122	63514	108054	2: Cellulose specific		Secretory Pathway	2	
NCU08114	hexose transporter	508	2126	56814	44948	44589	2: Cellulose specific		Other	2	
NCU00801	MFS lactose permease	262	1804	22730	36108	48887	2: Cellulose specific		Other	1	
NCU08760	endoglucanase II	25	49	28883	35258	44786	2: Cellulose specific	CBM1, GH61	Secretory Pathway	1	Cellulase
NCU01050	endoglucanase II		37	30298	31766	40084	2: Cellulose specific	GH61	Secretory Pathway	2	Cellulase
NCU07225	endo-1,4-beta-xylanase 2	111	27	106895	26528	78012	2: Cellulose specific	CBM1, GH11	Secretory Pathway	2	Hemicellulase
NCU05159	acetylxylan esterase	91	39	32482	21636	28978	2: Cellulose specific	CBM1, CE5	Secretory Pathway	1	
NCU00762	endoglucanase 3	11	25	48678	18848	65402	2: Cellulose specific	CBM1, GH5	Secretory Pathway	2	Cellulase
NCU08785	fungal cellulose binding domain-containing	26	9	5271	16506	2762	2: Cellulose specific	CE1	Secretory Pathway	1	Cellulase
NCU05057	endoglucanase EG-1	31	30	11230	15157	39741	2: Cellulose specific	GH7	Secretory Pathway	2	Cellulase
NCU02916	endoglucanase II	33	328	13361	14692	18839	2: Cellulose specific	CBM1, GH61	Secretory Pathway	3	Cellulase
NCU05864	hypothetical protein	64	94	10540	14084	11756	2: Cellulose specific		Secretory Pathway	2	
NCU05853	MFS sugar transporter	1550	406	25378	11528	7102	2: Cellulose specific		Other	2	
NCU07143	6-phosphogluconolactonase	86	204	15820	11191	20252	2: Cellulose specific		Secretory Pathway	1	
NCU00206	cellobiose dehydrogenase	24	23	14607	11099	19311	2: Cellulose specific	CBM1	Secretory Pathway	3	
NCU00836	hypothetical protein	9	25	11514	9766	11793	2: Cellulose specific	CBM1, GH61	Secretory Pathway	4	Cellulase
NCU02240	endoglucanase II	48	20	21969	9652	22893	2: Cellulose specific	CBM1, GH61	Secretory Pathway	2	Cellulase
NCU05924	endo-1,4-beta-xylanase	5	10	20023	9388	11455	2: Cellulose specific	GH10	Secretory Pathway	2	Hemicellulase
NCU09175	GPI-anchored cell wall beta-1,3-endoglucanase	5190	8178	12194	8652	12993	2: Cellulose specific	GH17	Secretory Pathway	3	
NCU07326	hypothetical protein	55	50	10245	7262	20145	2: Cellulose specific	GH43	Secretory Pathway	1	Hemicellulase
NCU02855	endo-1,4-beta-xylanase A	11	21	5398	6727	11729	2: Cellulose specific	GH11	Secretory Pathway	3	Hemicellulase
NCU07898	endoglucanase IV	15	14	7579	6699	11087	2: Cellulose specific	GH61	Secretory Pathway	1	Cellulase
NCU05846	hypothetical protein	120	655	2944	6644	5444	2: Cellulose specific		Mitochondrion	5	
NCU09223	protein disulfide-isomerase	1972	1949	10102	6583	7211	2: Cellulose specific		Secretory Pathway	2	
NCU11068	endo-beta-1,4-mannanase	71	145	9329	6402	10616	2: Cellulose specific		Other	3	
NCU03982	glucose-regulated protein	1679	2892	13596	6345	14820	2: Cellulose specific		Secretory Pathway	1	
NCU04910	hypothetical protein	3082	2132	6991	6079	3648	2: Cellulose specific		Other	3	
NCU05955	Cel74a	100	46	5805	5957	10105	2: Cellulose specific	CBM1, GH74	Secretory Pathway	2	Hemicellulase
NCU02009	FreB	443	1504	4704	5583	7137	2: Cellulose specific		Other	3	

Table 2-1 Data from RNA sequencing.

Table 2-1 Data from RNA sequencing.
Page 2 of 5

NCU #	Annotation	WT No Carbon	WT Cellobiose	WT Avicel	Δ3Gβ Cellobiose	Δ3Gβ Avicel	Cluster	CAZy	Signal P	Signal P Confidence	Annotation (Tians, et al.)
NCU09689	hypothetical protein	105	308	6053	5127	5889	2: Cellulose specific		Other	1	
NCU04870	acetyl xylan esterase	6	2	7234	4850	3457	2: Cellulose specific	CE1	Secretory Pathway	1	
NCU09764	hypothetical protein	9	118	3408	4616	5837	2: Cellulose specific	CBM1	Secretory Pathway	1	
NCU09524	hypothetical protein	14	13	3041	4546	4520	2: Cellulose specific		Secretory Pathway	5	
NCU03013	anchored cell wall protein 10	1461	845	4084	4461	2739	2: Cellulose specific		Secretory Pathway	3	
NCU03328	endoglucanase II	162	36	6820	4334	8313	2: Cellulose specific	GH61	Secretory Pathway	1	Cellulase
NCU08398	aldose 1-epimerase	52	6	4848	4321	2728	2: Cellulose specific		Secretory Pathway	4	
NCU00870	hypothetical protein	103	165	7180	4078	3385	2: Cellulose specific		Other	4	
NCU03813	formate dehydrogenase	589	100	2060	3965	2079	2: Cellulose specific		Other	2	
NCU08189	endo-1,4-beta-xylanase	208	70	38246	3944	9970	2: Cellulose specific	GH10	Secretory Pathway	1	Hemicellulase
NCU02455	FKBP-type peptidyl-prolyl cis-trans isomerase	1985	2132	5505	3921	4665	2: Cellulose specific		Secretory Pathway	1	
NCU08397	hypothetical protein	224	438	1745	3799	1192	2: Cellulose specific		Other	1	
NCU04904	hypothetical protein	572	895	1598	3607	2217	2: Cellulose specific		Other	3	
NCU09265	calreticulin	952	1598	5142	3580	5152	2: Cellulose specific		Secretory Pathway	4	
NCU05574	hypothetical protein, variant	59	60	459	3272	2188	2: Cellulose specific		Other	3	
NCU07487	periplasmic beta-glucosidase	6	81	922	3250	4383	2: Cellulose specific	GH3	Other	2	
NCU09582	chitin deacetylase	17	16	3551	3030	3283	2: Cellulose specific	CE4	Secretory Pathway	1	
NCU09425	NdvB protein	740	329	3245	2470	2120	2: Cellulose specific	GH94	Other	5	
NCU08897	protein transporter SEC61 subunit alpha	727	1755	3200	2211	3385	2: Cellulose specific		Secretory Pathway	4	
NCU04127	hypothetical protein	968	1490	2702	2186	3199	2: Cellulose specific		Other	1	
NCU08750	isoamyl alcohol oxidase	213	585	1374	2101	2729	2: Cellulose specific		Secretory Pathway	1	
NCU03319	COPII-coated vesicle protein SurF4/Erv29	1076	1071	2801	2083	2421	2: Cellulose specific		Other	5	
NCU08044	oxidoreductase	420	524	1433	1957	1351	2: Cellulose specific		Mitochondrion	2	
NCU00449	hypothetical protein	7	3	1181	1941	1359	2: Cellulose specific		Secretory Pathway	1	
NCU08379	hypothetical protein	786	1179	2741	1930	2426	2: Cellulose specific		Mitochondrion	4	
NCU05170	hypothetical protein	205	240	603	1904	1164	2: Cellulose specific		Other	2	
NCU01648	dolichyl-phosphate-mannose-protein	418	1140	1674	1550	2374	2: Cellulose specific	GT39	Other	2	
NCU10045	pectinesterase	71	46	1651	1549	788	2: Cellulose specific	CE8	Secretory Pathway	1	
NCU06607	hypothetical protein	21	67	773	1464	2347	2: Cellulose specific		Secretory Pathway	2	
NCU03651	NADP-dependent malic enzyme	51	589	1087	1397	3602	2: Cellulose specific		Mitochondrion	3	
NCU01146	signal sequence receptor alpha chain	761	1416	2003	1391	1857	2: Cellulose specific		Secretory Pathway	1	
NCU02343	alpha-L-arabinofuranosidase 2	458	151	9367	1391	2241	2: Cellulose specific	GH51	Secretory Pathway	1	Hemicellulase
NCU00813	disulfide isomerase	590	502	1839	1373	1858	2: Cellulose specific		Secretory Pathway	2	
NCU05751	cellulose-binding protein	10	5	969	1354	1164	2: Cellulose specific	CE3	Secretory Pathway	1	
NCU07997	hypothetical protein	299	411	813	1324	2072	2: Cellulose specific		Other	2	
NCU04905	hypothetical protein	354	580	1339	1287	1811	2: Cellulose specific		Other	1	
NCU06704	hypothetical protein	347	582	1691	1237	1927	2: Cellulose specific		Other	5	
NCU08746	starch binding domain-containing protein	44	181	346	1211	643	2: Cellulose specific	CBM20	Secretory Pathway	3	
NCU06971	transcriptional activator xlnR	336	193	1169	1193	882	2: Cellulose specific		Mitochondrion	5	
NCU03329	hypothetical protein	170	230	972	1191	1003	2: Cellulose specific		Other	2	
NCU02681	translocation protein	372	460	1058	1107	1426	2: Cellulose specific		Secretory Pathway	1	
NCU00304	hypothetical protein	480	377	1043	1104	1069	2: Cellulose specific		Mitochondrion	3	
NCU03181	acetylxylan esterase	32	11	2012	994	2694	2: Cellulose specific		Secretory Pathway	3	
NCU03322	GDSL family lipase	73	18	1417	958	580	2: Cellulose specific		Other	1	
NCU08042	fungal specific transcription factor	9	10	1316	936	970	2: Cellulose specific		Other	3	
NCU06333	translocation protein SEC62	307	407	1409	922	1532	2: Cellulose specific		Other	2	
NCU01944	hypothetical protein	20	113	468	920	639	2: Cellulose specific		Other	4	
NCU05863	hypothetical protein	21	12	478	892	572	2: Cellulose specific		Secretory Pathway	5	
NCU02915	hypothetical protein	77	62	854	882	902	2: Cellulose specific		Other	3	
NCU08784	hypothetical protein	61	79	251	837	243	2: Cellulose specific		Other	3	
NCU01068	BAR domain-containing protein	371	398	1218	808	1627	2: Cellulose specific		Other	2	
NCU03725	VIB-1	184	659	1345	790	708	2: Cellulose specific		Other	2	
NCU09491	feruloyl esterase B	19	3	471	763	286	2: Cellulose specific	CE1	Secretory Pathway	2	
NCU11198	arabinogalactan endo-1,4-beta-galactosidase	40	97	771	751	689	2: Cellulose specific		Secretory Pathway	1	
NCU05755	hypothetical protein	123	170	537	729	3130	2: Cellulose specific		Other	2	
NCU00169	translocation complex componenet	315	478	1304	688	1573	2: Cellulose specific		Other	3	
NCU00669	oligosaccharyl transferase subunit	336	638	795	685	682	2: Cellulose specific		Secretory Pathway	1	
NCU09485	chaperone dnaK	248	497	920	676	1141	2: Cellulose specific		Secretory Pathway	1	
NCU08607	endoplasmic reticulum-Golgi intermediate	312	396	702	668	866	2: Cellulose specific		Other	4	
NCU09705	GAL10	266	193	4400	615	1083	2: Cellulose specific		Secretory Pathway	3	
NCU04130	acylase ACY 1	155	156	357	610	389	2: Cellulose specific		Other	5	
NCU01076	hypothetical protein	3		782	610	566	2: Cellulose specific		Secretory Pathway	1	
NCU00965	hypothetical protein	321	319	916	609	863	2: Cellulose specific		Other	2	
NCU05855	O-methyltransferase	20	33	294	602	448	2: Cellulose specific		Other	5	
NCU03083	hypothetical protein	273	525	836	591	745	2: Cellulose specific		Secretory Pathway	2	
NCU04854	endoglucanase EG-1	41	18	2203	587	2556	2: Cellulose specific	GH7	Secretory Pathway	2	Cellulase
NCU09416	cellulose-binding GDSL lipase/acylhydrolase		4	1947	559	5227	2: Cellulose specific	CBM1, CE16	Secretory Pathway	1	
NCU07746	F-box domain-containing protein	249	287	728	555	650	2: Cellulose specific		Other	1	
NCU04494	acetyl xylan esterase	74	127	570	553	1318	2: Cellulose specific	CE1	Secretory Pathway	1	
NCU11118	hypothetical protein	125	283	466	541	630	2: Cellulose specific		Mitochondrion	3	

Table 2-1 Data from RNA sequencing.
Page 3 of 5

NCU #	Annotation	WT No Carbon	WT Cellobiose	WT Avicel	Δ3Gβ Cellobiose	Δ3Gβ Avicel	Cluster	CAZy	Signal P	Signal P Confidence	Annotation (Tians, et al.)
NCU00289	hypothetical protein	105	215	372	538	712	2: Cellulose specific		Other	2	
NCU07760	endoglucanase IV	19	68	239	538	1055	2: Cellulose specific	CBM1, GH61	Secretory Pathway	2	Cellulase
NCU08176	pectate lyase A	18	18	1655	526	990	2: Cellulose specific	PL3	Secretory Pathway	2	
NCU05501	hypothetical protein	55	44	432	520	403	2: Cellulose specific		Other	2	
NCU09664	acetylxylan esterase		2	997	516	1346	2: Cellulose specific	CE5	Secretory Pathway	1	
NCU01013	delta-aminolevulinic acid dehydratase	183	240	439	500	551	2: Cellulose specific		Mitochondrion	4	
NCU02059	endothiapepsin	83	521	1254	491	1055	2: Cellulose specific		Secretory Pathway	2	
NCU08164	retinol dehydrogenase 13	193	155	612	486	327	2: Cellulose specific		Other	2	
NCU05906	hypothetical protein	207	72	518	482	284	2: Cellulose specific		Other	2	
NCU06387	hypothetical protein	42	178	353	464	483	2: Cellulose specific		Other	4	
NCU08761	vacuolar sorting receptor	117	212	279	463	410	2: Cellulose specific		Secretory Pathway	2	
NCU06143	hypothetical protein	147	19	4081	461	712	2: Cellulose specific	GH115	Secretory Pathway	2	
NCU00890	beta-mannosidase	63	65	1451	446	660	2: Cellulose specific	GH2	Other	3	
NCU09176	hypothetical protein	63	99	424	428	528	2: Cellulose specific		Other	3	
NCU05852	glucuronan lyase A	67	17	198	418	132	2: Cellulose specific	PL20	Secretory Pathway	1	
NCU08752	acetylcholinesterase	146	34	3093	415	1345	2: Cellulose specific		Secretory Pathway	1	
NCU10039	hypothetical protein	56	53	755	412	658	2: Cellulose specific		Secretory Pathway	3	
NCU01386	hypothetical protein	69	204	305	401	910	2: Cellulose specific		Other	1	
NCU06055	extracellular alkaline protease	151	242	399	393	481	2: Cellulose specific		Secretory Pathway	2	
NCU03152	DUF1348 domain-containing protein	89	243	269	379	528	2: Cellulose specific		Other	2	
NCU06386	dolichyl-phosphate beta-glucosyltransferase	127	183	337	379	393	2: Cellulose specific	GT2	Secretory Pathway	2	
NCU10721	solute carrier family 35 member B1 protein	116	178	423	358	560	2: Cellulose specific		Other	4	
NCU01430	hypothetical protein	92	64	587	353	381	2: Cellulose specific		Other	2	
NCU08371	hypothetical protein	176	61	642	337	271	2: Cellulose specific	GH125	Secretory Pathway	2	
NCU11268	hypothetical protein	140	42	427	314	649	2: Cellulose specific		Secretory Pathway	4	
NCU07432	tetraspanin	180	278	565	312	627	2: Cellulose specific		Secretory Pathway	1	
NCU09098	tetracycline transporter	72	137	258	310	575	2: Cellulose specific		Secretory Pathway	1	
NCU05854	hypothetical protein	49	31	203	305	300	2: Cellulose specific		Other	4	
NCU04401	fructose-bisphosphate aldolase	66	14	3213	302	990	2: Cellulose specific		Other	4	
NCU09523	hypothetical protein	27	63	201	268	313	2: Cellulose specific		Other	4	
NCU05121	endoglucanase V	35	11	591	252	800	2: Cellulose specific	CBM1, GH45	Secretory Pathway	2	Cellulase
NCU01059	glycosyl hydrolase family 47 protein	42	79	252	238	161	2: Cellulose specific	GH47	Secretory Pathway	3	
NCU08790	hypothetical protein	10	2	414	234	769	2: Cellulose specific		Secretory Pathway	1	
NCU08624	hypothetical protein	26	18	350	233	596	2: Cellulose specific		Other	3	
NCU08115	DNA mismatch repair protein Msh3	48	69	396	229	287	2: Cellulose specific		Mitochondrion	5	
NCU08748	hypothetical protein	71	135	208	219	137	2: Cellulose specific		Other	1	
NCU10107	ribose 5-phosphate isomerase	165		2400	216	559	2: Cellulose specific		Other	2	
NCU07668	MFS multidrug transporter	38	54	172	211	198	2: Cellulose specific		Other	5	
NCU06138	quinate permease	167	5	3949	204	992	2: Cellulose specific		Other	5	
NCU05908	hypothetical protein	20	25	50	200	46	2: Cellulose specific		Secretory Pathway	2	
NCU10521	hypothetical protein	103	78	503	187	581	2: Cellulose specific		Other	5	
NCU05068	hypothetical protein	39	88	2288	184	4841	2: Cellulose specific		Other	3	
NCU03819	COPII coat assembly protein sec-16	109	186	259	177	302	2: Cellulose specific		Other	2	
NCU06032	long-chain fatty acid transporter	137	93	323	173	323	2: Cellulose specific		Secretory Pathway	2	
NCU04467	hypothetical protein	56	49	310	170	194	2: Cellulose specific		Secretory Pathway	1	
NCU09522	hypothetical protein	46	83	214	168	355	2: Cellulose specific		Other	5	
NCU07979	hypothetical protein	31	39	122	168	193	2: Cellulose specific		Other	4	
NCU04623	beta-galactosidase	40	20	137	163	104	2: Cellulose specific	GH35	Secretory Pathway	4	
NCU11278	hypothetical protein	65	10	438	160	160	2: Cellulose specific		Other	3	
NCU03903	lipase/esterase	97	50	375	159	267	2: Cellulose specific		Secretory Pathway	2	
NCU04618	hypothetical protein	35	37	157	154	156	2: Cellulose specific		Other	2	
NCU04948	hypothetical protein	2	9	19	154	55	2: Cellulose specific		Secretory Pathway	1	
NCU02600	DUF1479 domain-containing protein	8	30	25	148	133	2: Cellulose specific		Mitochondrion	4	
NCU02344	fungal cellulose binding domain-containing	16	60	330	138	1105	2: Cellulose specific	GH61	Secretory Pathway	4	Cellulase
NCU07339	hypothetical protein	10		200	134	141	2: Cellulose specific		Other	4	
NCU08038	CAS1	85	32	272	133	332	2: Cellulose specific		Secretory Pathway	1	
NCU02625	hypothetical protein	45	45	158	132	199	2: Cellulose specific		Mitochondrion	5	
NCU11690	hypothetical protein	60	23	126	130	142	2: Cellulose specific		Other	3	
NCU09518	glucooligosaccharide oxidase	32	14	111	128	332	2: Cellulose specific		Secretory Pathway	1	
NCU10110	3-hydroxyisobutyrate dehydrogenase	56	15	955	115	254	2: Cellulose specific		Secretory Pathway	5	
NCU09426	hypothetical protein	29	8	88	111	68	2: Cellulose specific		Other	4	
NCU11542	hypothetical protein	76	16	262	109	157	2: Cellulose specific		Secretory Pathway	1	
NCU05351	hypothetical protein	14	36	52	100	141	2: Cellulose specific		Mitochondrion	4	
NCU00292	cholinesterase	64	9	2789	98	566	2: Cellulose specific		Secretory Pathway	2	
NCU04997	xylanase	3	16	131	98	507	2: Cellulose specific	CBM1, GH10	Secretory Pathway	2	Hemicellulase
NCU11932	hypothetical protein	47	3	325	97	133	2: Cellulose specific		Mitochondrion	1	
NCU09424	hypothetical protein	13	8	50	89	39	2: Cellulose specific		Secretory Pathway	1	
NCU01148	methyltransferase	27	27	104	86	70	2: Cellulose specific		Other	2	
NCU07055	monooxygenase	16	2	151	82	39	2: Cellulose specific		Secretory Pathway	3	
NCU05056	hypothetical protein			27	82	40	2: Cellulose specific		Other	2	

Table 2-1 Data from RNA sequencing.
Page 4 of 5

NCU #	Annotation	WT No Carbon	WT Cellobiose	WT Avicel	Δ3Gβ Cellobiose	Δ3Gβ Avicel	Cluster	CAZy	Signal P	Signal P Confidence	Annotation (Tians, et al.)
NCU08867	hypothetical protein	17	32	127	78	114	2: Cellulose specific		Other	5	
NCU09415	hypothetical protein	10	31	185	77	840	2: Cellulose specific		Other	2	
NCU07736	PEP5	17	96	177	73	164	2: Cellulose specific		Other	2	
NCU01077	hypothetical protein	10	6	45	69	33	2: Cellulose specific		Other	1	
NCU08635	hypothetical protein	29	17	74	62	79	2: Cellulose specific		Secretory Pathway	4	
NCU11342	MFS hexose transporter	19	5	116	61	111	2: Cellulose specific		Other	2	
NCU06373	hypothetical protein	42	17	210	59	158	2: Cellulose specific		Mitochondrion	5	
NCU09848	hypothetical protein	15	45	71	59	65	2: Cellulose specific		Secretory Pathway	2	
NCU00763	hypothetical protein	0		129	58	262	2: Cellulose specific		Other	2	
NCU01058	hypothetical protein	14	11	75	56	30	2: Cellulose specific		Secretory Pathway	4	
NCU07897	hypothetical protein	16	12	94	56	92	2: Cellulose specific		Other	1	
NCU04400	hypothetical protein	78		1596	55	227	2: Cellulose specific		Other	5	
NCU07413	cytosine deaminase, variant	11	34	51	46	56	2: Cellulose specific		Other	1	
NCU09775	alpha-N-arabinofuranosidase	3	3	97	44	255	2: Cellulose specific	GH54	Secretory Pathway	1	Hemicellulase
NCU01049	hypothetical protein			52	41	92	2: Cellulose specific		Other	3	
NCU03433	hypothetical protein	8	24	41	38	94	2: Cellulose specific		Other	3	
NCU09976	rhamnogalacturonan acetylesterase	4	7	74	34	96	2: Cellulose specific	CE12	Secretory Pathway	4	
NCU09445	Cip2			28	34	36	2: Cellulose specific	CE15	Secretory Pathway	1	
NCU00496	hypothetical protein	15	12	43	32	42	2: Cellulose specific		Other	3	
NCU08043	hypothetical protein	13	3	36	31	32	2: Cellulose specific		Other	3	
NCU05875	hypothetical protein	26	11	66	31	35	2: Cellulose specific		Other	2	
NCU07270	hypothetical protein	19	9	64	29	40	2: Cellulose specific		Other	2	
NCU08634	hypothetical protein	28	11	68	28	88	2: Cellulose specific		Mitochondrion	4	
NCU09923	beta-xylosidase	12	1	221	24	70	2: Cellulose specific	GH3	Secretory Pathway	1	
NCU09924	BNR/Asp-box repeat protein	19		120	22	50	2: Cellulose specific	GH93	Secretory Pathway	1	
NCU07224	monooxygenase			125	21	70	2: Cellulose specific		Secretory Pathway	2	
NCU11905		3	2	28	20	68	2: Cellulose specific				
NCU11769		6	5	19	18	44	2: Cellulose specific				
NCU00709	beta-xylosidase	6	2	204	16	51	2: Cellulose specific	GH3	Secretory Pathway	1	
NCU00761	triacylglycerol lipase	3	1	24	12	29	2: Cellulose specific		Secretory Pathway	1	
NCU07510	hypothetical protein			134	11	29	2: Cellulose specific		Other	2	
NCU00871	hypothetical protein	3		17	11	14	2: Cellulose specific		Other	2	
NCU09774	cellulase			17	10	16	2: Cellulose specific	CE1	Secretory Pathway	1	
NCU11801		5	10	20	10	23	2: Cellulose specific				
NCU04871	hypothetical protein	1	1	15	9	11	2: Cellulose specific		Mitochondrion	5	
NCU08116	hypothetical protein	3	2	14	8	7	2: Cellulose specific		Other	5	
NCU09172	hypothetical protein			7	3	2	2: Cellulose specific		Secretory Pathway	5	
NCU10051	flavohemoglobin	301	8597	11553	30405	30181	3: Metabolic response		Other	4	
NCU00575	glucokinase	677	4007	2259	5975	5399	3: Metabolic response		Other	1	
NCU07277	anchored cell wall protein 8	1273	5363	4199	5957	7751	3: Metabolic response		Secretory Pathway	1	
NCU01856	transcriptional activator hac1	504	3062	2325	2334	2895	3: Metabolic response		Other	1	
NCU00326	calcium homeostasis protein Regucalcin	430	1188	1744	2133	1563	3: Metabolic response		Other	1	
NCU11828		76	1911	995	2124	4041	3: Metabolic response				
NCU11722		224	990	675	1426	743	3: Metabolic response				
NCU05841	UMTA	46	617	452	1226	768	3: Metabolic response		Other	2	
NCU05133	udp-glucose 4-epimerase	320	3566	1973	973	2324	3: Metabolic response		Other	2	
NCU03791	hypothetical protein	221	1742	499	965	1646	3: Metabolic response		Mitochondrion	2	
NCU03293	hypothetical protein	118	14374	469	954	1182	3: Metabolic response		Secretory Pathway	1	
NCU04720	nitrite reductase	231	2599	1752	933	2174	3: Metabolic response		Other	3	
NCU04830	hypothetical protein	66	382	436	792	882	3: Metabolic response		Other	2	
NCU05598	rhamnogalacturonase B	26	249	376	695	297	3: Metabolic response	PL4	Secretory Pathway	1	
NCU00633	hypothetical protein	87	733	225	649	785	3: Metabolic response		Other	2	
NCU10283	tryptophan synthetase	121	1159	647	647	1415	3: Metabolic response		Other	5	
NCU11291	hypothetical protein	9	137	60	615	356	3: Metabolic response		Other	4	
NCU02882	hypothetical protein	16	180	218	604	391	3: Metabolic response		Other	3	
NCU00554	aspartate-semialdehyde dehydrogenase	87	1571	366	536	878	3: Metabolic response		Mitochondrion	4	
NCU10687	hypothetical protein	62	779	235	496	733	3: Metabolic response		Secretory Pathway	2	
NCU03748	saccharopine dehydrogenase	95	1825	272	464	257	3: Metabolic response		Other	4	
NCU01353	mixed-linked glucanase	104	1432	537	439	674	3: Metabolic response	GH16	Secretory Pathway	3	
NCU10284		46	448	272	426	654	3: Metabolic response				
NCU02657	s-adenosylmethionine synthetase	70	4039	251	404	703	3: Metabolic response		Other	2	
NCU05548	phospho-2-dehydro-3-deoxyheptonate aldolase	111	662	629	354	847	3: Metabolic response		Other	2	
NCU05230	hypothetical protein	23	153	65	324	374	3: Metabolic response		Secretory Pathway	1	
NCU01744	glutamate synthase	197	985	541	318	342	3: Metabolic response		Other	1	
NCU04698	spermine/spermidine synthase	178	403	500	313	336	3: Metabolic response		Other	2	
NCU05304	nuclear segregation protein	188	1080	413	301	521	3: Metabolic response		Other	2	
NCU03131	FAD dependent oxidoreductase superfamily	68	150	194	285	229	3: Metabolic response		Mitochondrion	1	
NCU03963	5'-methylthioadenosine phosphorylase	15	542	172	275	270	3: Metabolic response		Other	2	
NCU04077	assimilatory sulfite reductase	38	1263	268	255	408	3: Metabolic response		Other	3	
NCU09003	hypothetical protein	69	264	147	247	262	3: Metabolic response		Other	5	

NCU #	Annotation	WT No Carbon	WT Cellobiose	WT Avicel	Δ3Gβ Cellobiose	Δ3Gβ Avicel	Cluster	CAZy	Signal P	Signal P Confidence	Annotation (Tians, et al.)
NCU05134	hypothetical protein	65	3174	1270	237	2586	3: Metabolic response		Secretory Pathway	1	
NCU01983	hypothetical protein	36	358	174	237	230	3: Metabolic response		Mitochondrion	2	
NCU03137	nuclear elongation and deformation protein 1	112	230	256	234	320	3: Metabolic response		Other	2	
NCU11397		48	721	184	221	280	3: Metabolic response				
NCU01720	hypothetical protein	61	1083	215	178	279	3: Metabolic response		Secretory Pathway	2	
NCU02785	phospho-2-dehydro-3-deoxyheptonate aldolase	62	907	157	175	463	3: Metabolic response		Other	2	
NCU10762	UDP-N-acetyl-glucosamine-1-P transferase Alg7	47	183	140	163	406	3: Metabolic response		Secretory Pathway	5	
NCU02904	alpha/beta hydrolase fold protein	40	265	118	137	235	3: Metabolic response		Secretory Pathway	1	
NCU05829	hypothetical protein	22	260	62	136	186	3: Metabolic response		Secretory Pathway	3	
NCU05848	cytochrome P450 monooxygenase		4	22	128	33	3: Metabolic response		Secretory Pathway	2	
NCU06235	hypothetical protein	34	161	104	127	156	3: Metabolic response		Other	2	
NCU00798	hypothetical protein	182	894	1008	126	559	3: Metabolic response		Mitochondrion	5	
NCU09295	hypothetical protein	86	243	265	118	286	3: Metabolic response		Secretory Pathway	1	
NCU02478	alpha-1,3-glucan synthase Ags2	16	159	59	108	137	3: Metabolic response	GT5, GH13	Secretory Pathway	2	
NCU06189	5-aminolevulinate synthase	38	333	93	97	247	3: Metabolic response		Mitochondrion	4	
NCU06983	hypothetical protein	103	350	739	87	401	3: Metabolic response		Secretory Pathway	2	
NCU09498	hypothetical protein	67	182	305	86	242	3: Metabolic response		Secretory Pathway	3	
NCU06181	hypothetical protein	37	103	112	84	160	3: Metabolic response		Mitochondrion	4	
NCU05826	hypothetical protein	25	978	173	82	65	3: Metabolic response		Other	1	
NCU01136	hypothetical protein	36	124	99	76	70	3: Metabolic response		Other	5	
NCU10009	ATP-binding cassette transporter	37	102	96	74	54	3: Metabolic response		Other	2	
NCU04928	hypothetical protein	3	40	21	69	43	3: Metabolic response		Other	2	
NCU05909	hypothetical protein	1	16	28	68	24	3: Metabolic response		Mitochondrion	4	
NCU07222	hypothetical protein	2	90	132	63	321	3: Metabolic response		Secretory Pathway	1	
NCU01998	septin	46	178	120	58	79	3: Metabolic response		Mitochondrion	4	
NCU09506	hypothetical protein	2	229	39	36	52	3: Metabolic response		Secretory Pathway	1	
NCU04998	hypothetical protein	5	33	20	35	75	3: Metabolic response		Secretory Pathway	1	
NCU11095	hypothetical protein	8	46	30	33	35	3: Metabolic response		Other	2	
NCU04537	monosaccharide transporter	15	127	48	30	91	3: Metabolic response		Other	1	
NCU07481	morphogenesis protein	25	81	60	30	52	3: Metabolic response		Other	2	
NCU06991	hypothetical protein	22	126	105	26	246	3: Metabolic response		Secretory Pathway	1	
NCU02795	histone deacetylase phd1	24	59	62	24	65	3: Metabolic response		Other	2	
NCU05319	LysM domain-containing protein	5	35	29	22	52	3: Metabolic response		Other	3	
NCU00931	lysyl-tRNA synthetase	6	52	18	19	38	3: Metabolic response		Other	3	
NCU09906	hypothetical protein	38	112	155	43	36	4: Δ3Gβ uninduced	GTNC	Other	3	
NCU09904	glucan 1,3-beta-glucosidase	16	58	76	18	21	4: Δ3Gβ uninduced	GH16	Other	1	
NCU08087	hypothetical protein	4	23	36	4	2	4: Δ3Gβ uninduced	GH26	Other	2	Hemicellulase
NCU02061	hypothetical protein	17	25	55	2	2	4: Δ3Gβ uninduced		Mitochondrion	2	

Table 2-1 Data from RNA sequencing.
Page 5 of 5

Gene	Annotation	Wild Type	Δ3βG	Δ3βGΔcre	Secretome Percentage*
Cellulases					
NCU07340	CBH-1	+	+	+	39.5%
NCU09680	GH6-2	+	+	+	13.4%
NCU07898	GH61-2	+		+	6.6%
NCU00762	GH5-1	+	+	+	5.9%
NCU08760	GH61-5	+	+	+	4.6%
NCU05057	GH7-1	+	+	+	4.0%
NCU02240	GH61-1	+		+	3.4%
NCU07190	GH6-3	+	+	+	3.2%
Accessory Proteins					
NCU04952	GH3-4	+	N/A	N/A	3.8%
NCU00206	CDH-1	+	+	+	2.4%
NCU09764	N/A	+	+	+	1.6%
NCU05137	NCW-1	+	+	+	1.5%
NCU07143	LAC-2	+	+	+	1.0%

GH, glycoside hydrolase; N/A, gene knockout

*Avicel induced secretome identified by AQUA Mass Spectrometry, *Phillips, et al.* (13 proteins represent 91% of the total secretome with all other proteins representing less than 1% of the secretome.)

Table 2-2 Mass spectrometry of the most abundant secreted proteins in wild type (Avicel), Δ3βG (cellobiose), and Δ3βGΔ*cre-1* (cellobiose) Neurospora crassa.

		Wild type Avicel			Δ3βG cellobiose			Δ3βGΔcre cellobiose		
	GH family	Whole Supernatant*	PASC bound†	PASC unbound‡	Whole Supernatant	PASC bound	PASC unbound	Whole Supernatant	PASC bound	PASC unbound
NCU04952	3	+		+						
NCU00762	5	+	+	+	+	+		+	+	
NCU08412	5	+		+	+		+	+		+
NCU07190	6	+		+	+	+	+	+	+	+
NCU09680	6	+	+					+	+	
NCU05057	7	+		+	+		+	+		+
NCU07340	7	+	+	+	+	+	+	+		+
NCU05924	10	+		+				+		+
NCU08189	10	+		+						
NCU02855	11	+		+						
NCU07225	11	+	+	+				+	+	
NCU04431	16				+		+			
NCU05686	16				+		+			
NCU05974	16	+		+	+		+			
NCU01517	17				+		+	+		+
NCU09175	17	+			+	+	+	+		+
NCU04395	30				+		+			
NCU04265	32				+	+	+	+		+
NCU07326	43	+	+	+				+		+
NCU05121	45	+								
NCU02343	51				+		+			
NCU09775	54				+					
NCU07523	55				+	+	+			
NCU00836	61	+	+							
NCU01050	61	+	+	+				+	+	
NCU02240	61	+	+	+				+	+	
NCU07898	61	+	+	+				+	+	
NCU08760	61	+	+	+	+	+		+	+	
NCU06781	72				+	+	+			
NCU08909	72				+		+			
NCU05955	74	+	+	+		+		+	+	
NCU00206	CBM1	+		+		+		+		
NCU09764	CBM1	+	+					+	+	
NCU05159	CBM1/CE5	+	+						+	
NCU04870	CE1	+		+						
NCU08785	CE1	+		+						
NCU09491	CE1	+		+	+		+	+		+
NCU09664	CE5	+	+					+		+
NCU05852	PL20	+		+						
NCU08936	GH NC				+	+	+		+	
NCU05598	PL4	+		+	+		+			
NCU00449		+		+						
NCU00798					+		+			
NCU01595			+			+				+
NCU02133					+		+			
NCU02136					+		+			
NCU02696		+	+			+				
NCU04202					+	+				
NCU04205		+			+					
NCU04482					+					
NCU04522					+	+	+			
NCU05134					+		+			
NCU05137		+	+	+	+	+	+	+		+
NCU07143		+		+	+		+	+		+
NCU07200					+	+	+			
NCU07281					+					
NCU07787					+	+	+	+		+
NCU08171		+		+	+		+			
NCU08398		+		+						
NCU09024		+		+	+		+			
NCU09046		+		+						
NCU09267					+		+			+
NCU09992					+		+			

GH, glycoside hydrolase; CBM1, carbohydrate binding module; CE, carbohydrate esterase; PL, polysaccharide lyase; NC, Not Classified; N/A, gene knockout.

*Whole Supernatant, peptides detected from a tryptic digest of all extracellular proteins; †PASC bound, peptides detected after enrichment for proteins that bind to phosphoric acid swollen cellulose; ‡PASC unbound, proteins remaining in solution after removal of PASC bound proteins.

Table 2-3 Mass spectrometry of all secreted proteins in wild type (Avicel), Δ3βG (cellobiose), and Δ3βGΔ*cre-1* (cellobiose) Neurospora crassa.

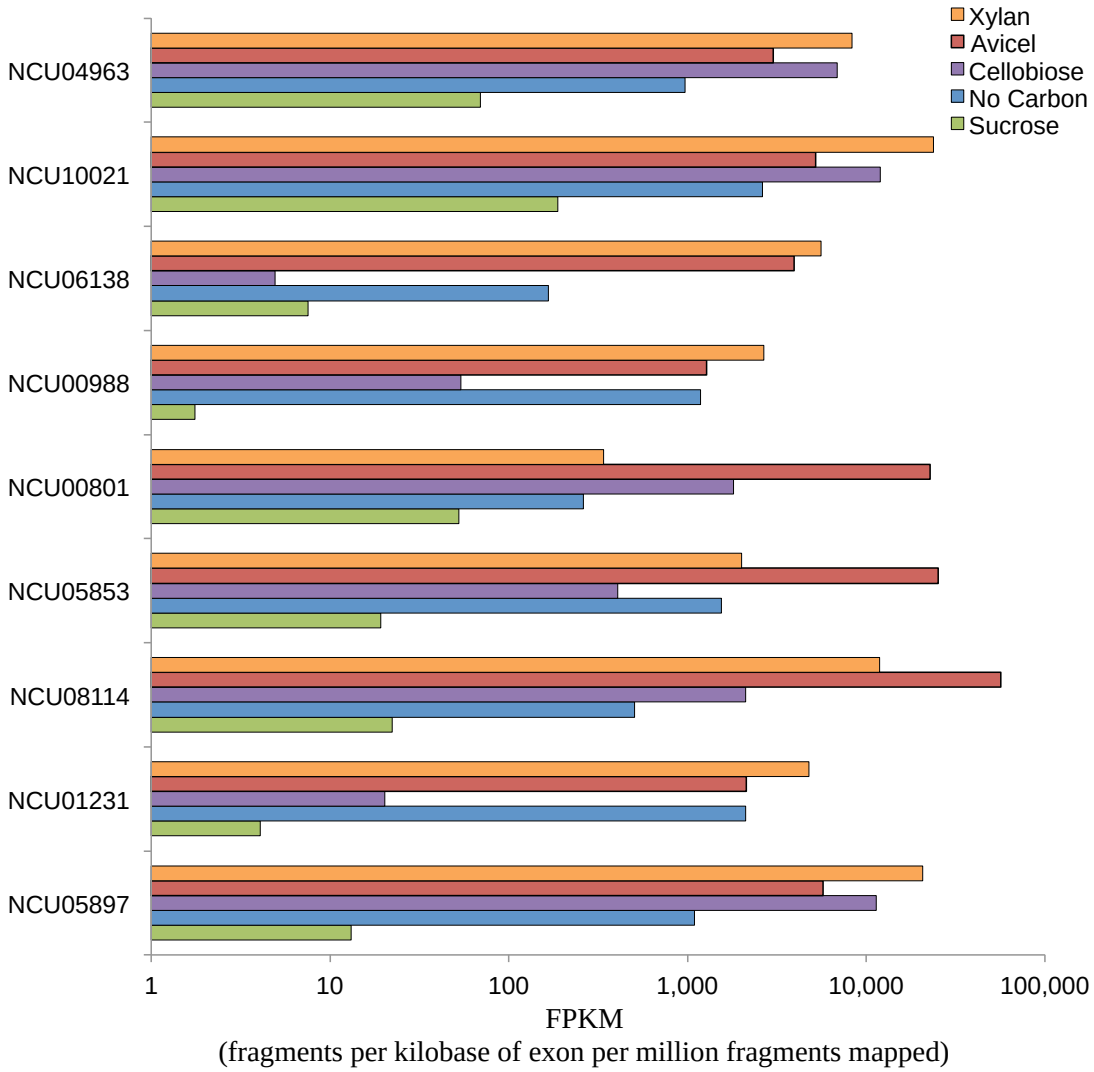

Figure 3-1 Expression of predicted cellodextrin transporter genes.
The expression of predicted cellodextrin transporter genes in wild type N. crassa when exposed to Sucrose, No Carbon (Starvation), Cellobiose, Avicel, and Xylan.

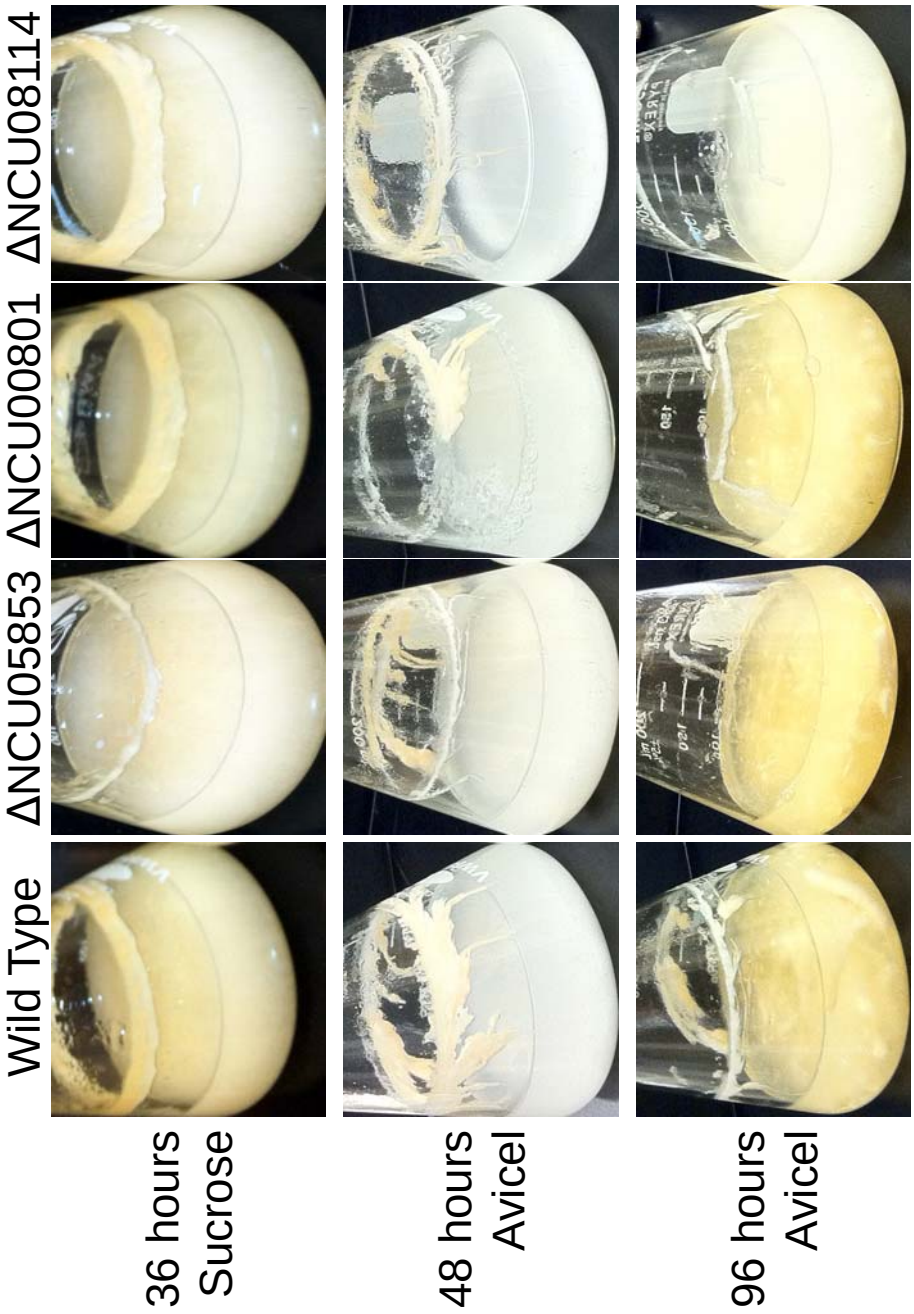

Figure 3-2 Phenotypes for the predicted cellodextrin transporter deletion strains. The growth phenotypes for the single cellodextrin transporter deletion strains after growth on either sucrose or Avicel. Conidia from strains were inoculated at a concentration equal to $2x10^6$ conidia per milliliter into 100ml Vogel's salts (93) with 2% w/v sucrose or Avicel in a 250ml Erlenmeyer flask and grown under constant light at 200 rpm for 36 hours (sucrose), 2 days (Avicel) and 4 days (Avicel).

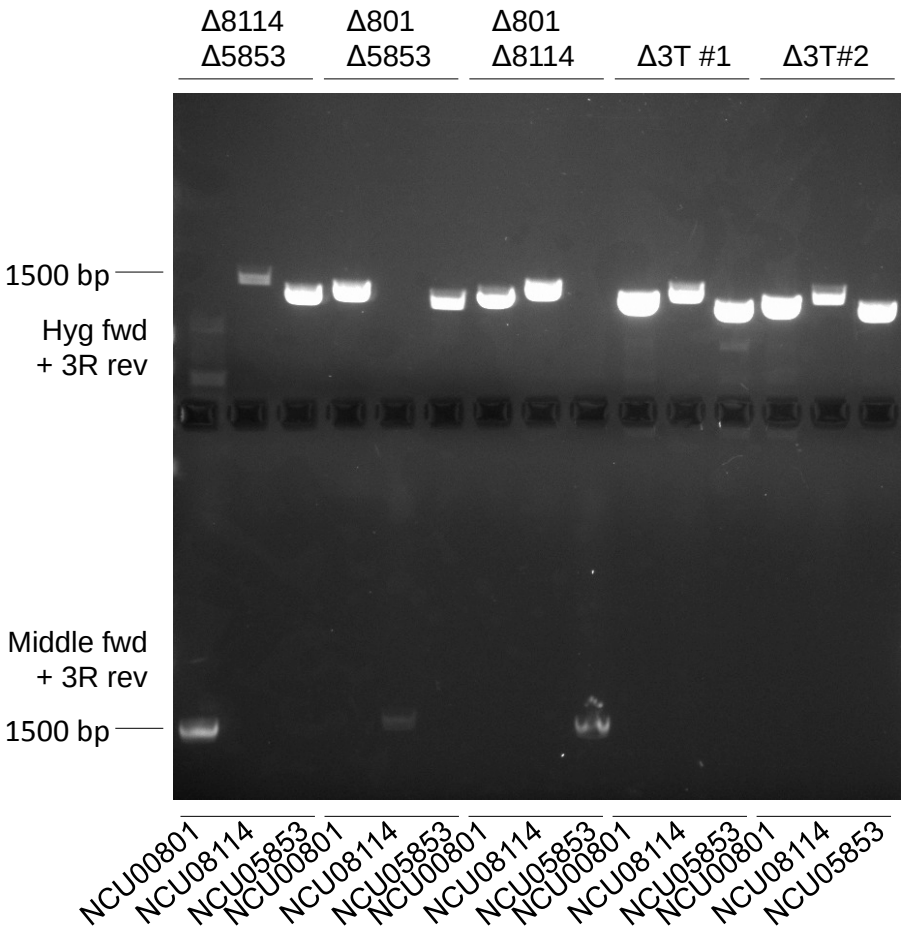

Figure 3-3 PCR genotyping for the multiple transporter deletion strains.
Each cross was genotyped using two different sets of PCR Primers: (Top) The hygromycin specific forward and gene specific reverse primer (outside of the deletion cassette) only produces a product in the presence of the knockout cassette, and (Bottom) a forward primer specifically designed to be within the gene and gene specific reverse primer (outside of the deletion cassette) only produces a product in an intact gene.

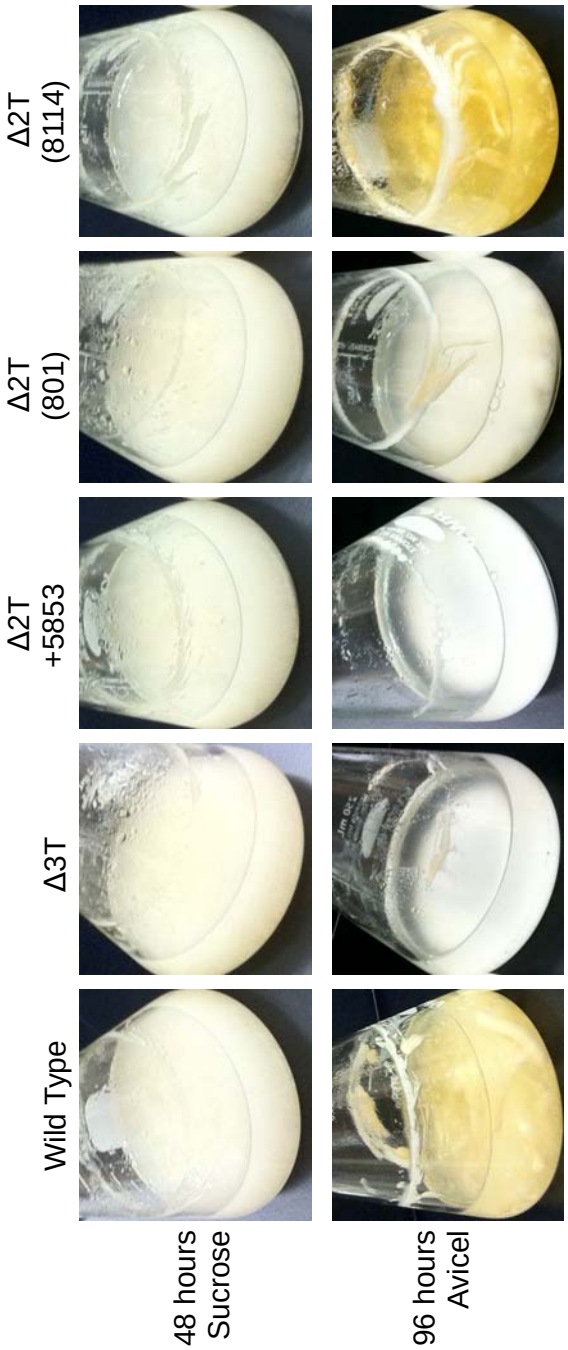

Figure 3-4 Phenotypes for the multiple cellodextrin transporter deletion strains. The growth phenotypes for the multiple cellodextrin transporter deletion strains after growth on either sucrose or Avicel. Conidia from strains were inoculated at a concentration equal to $2x10^6$ conidia per milliliter into 100ml Vogel's salts (93) with 2% w/v sucrose or Avicel in a 250ml Erlenmeyer flask and grown under constant light at 200 rpm for 36 hours (sucrose) and 4 days (Avicel).

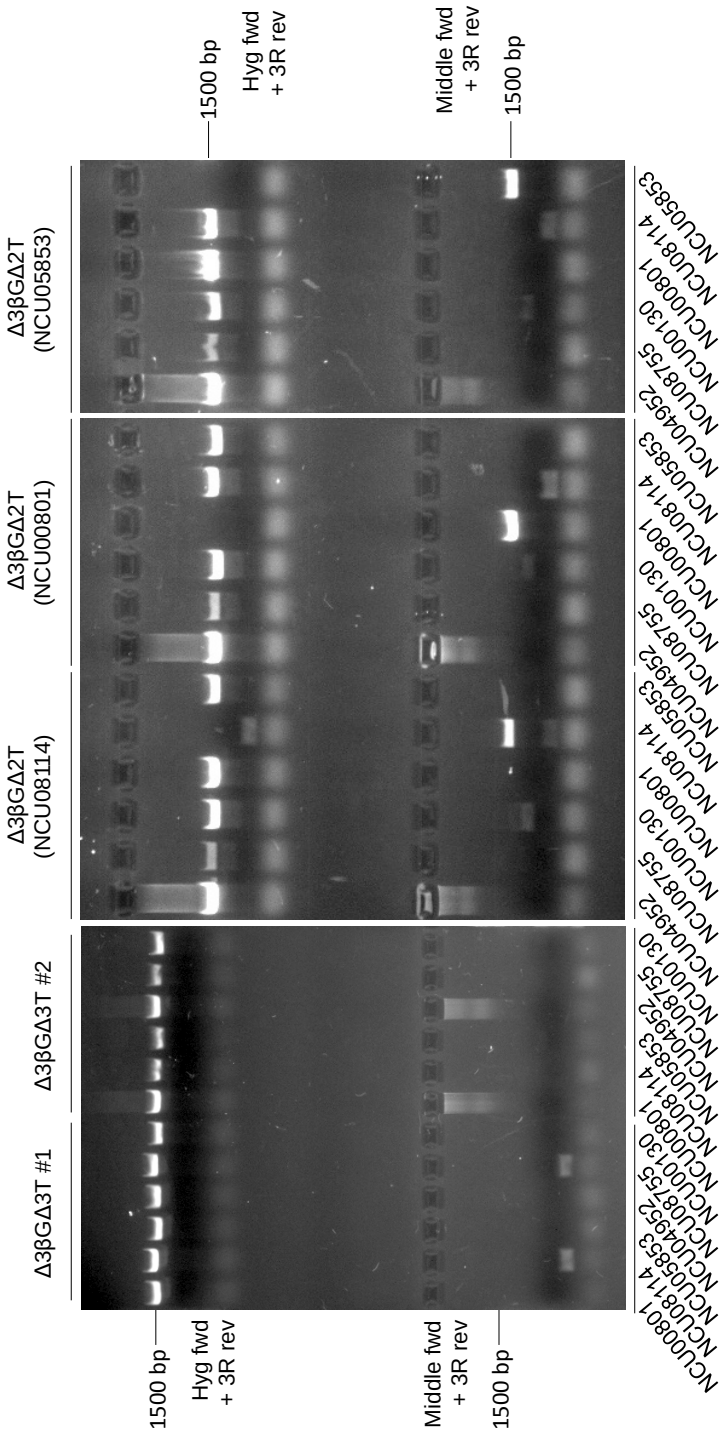

Figure 3-5 PCR genotyping for the Δ3βG multiple transporter deletion strains. Each cross was genotyped using two different sets of PCR Primers: (Top) The hygromycin specific forward and gene specific reverse primer (outside of the deletion cassette) only produces a product in the presence of the knockout cassette, and (Bottom) a forward primer specifically designed to be within the gene and gene specific reverse primer (outside of the deletion cassette) only produces a product in an intact gene.

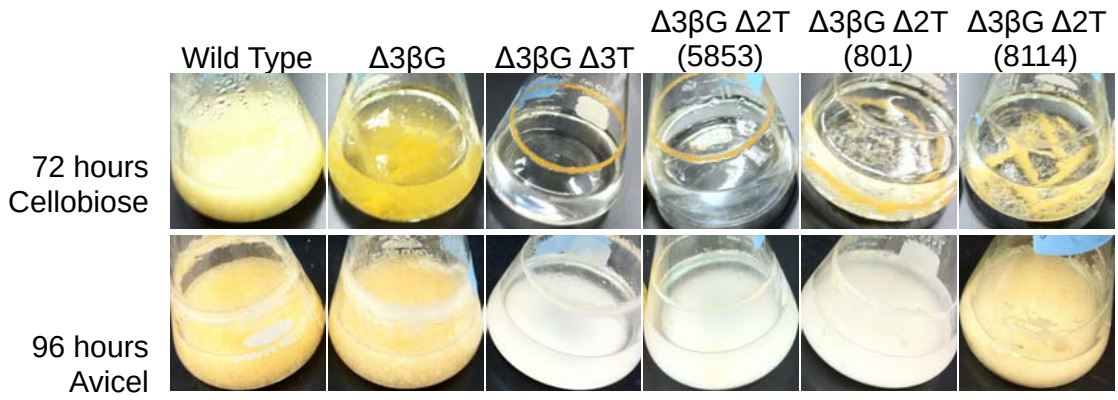

Figure 3-6 Phenotypes for the Δ3βG multiple transporter deletion strains.
The growth phenotypes for the Δ3βG multiple cellodextrin transporter deletion strains after growth on either cellobiose or Avicel. Conidia from strains were inoculated at a concentration equal to $2x10^6$ conidia per milliliter into 100ml Vogel's salts (93) with 2% w/v cellobiose or Avicel in a 250ml Erlenmeyer flask and grown under constant light at 200 rpm for 72 hours (cellobiose) and 4 days (Avicel).

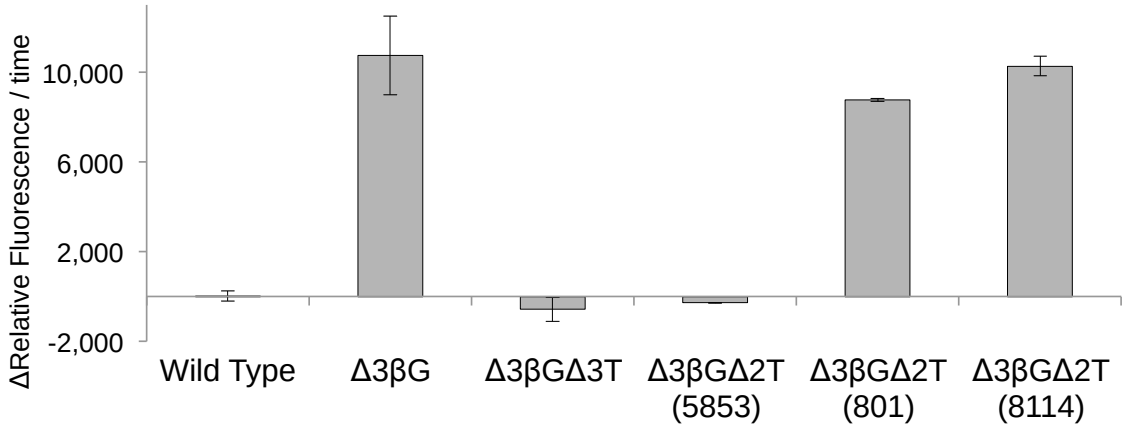

Figure 3-7 Cellulase production in the Δ3βG transporter deletion strains.
The amount of 4-Methylumbelliferyl β-D-cellobioside (MuLac) activity from the cellobiose grown cultures in Figure 3-6 for the WT, Δ3βG, Δ3βGΔ3T, Δ3βGΔ2T(5853), Δ3βGΔ2T(801), and Δ3βGΔ2T(8114)

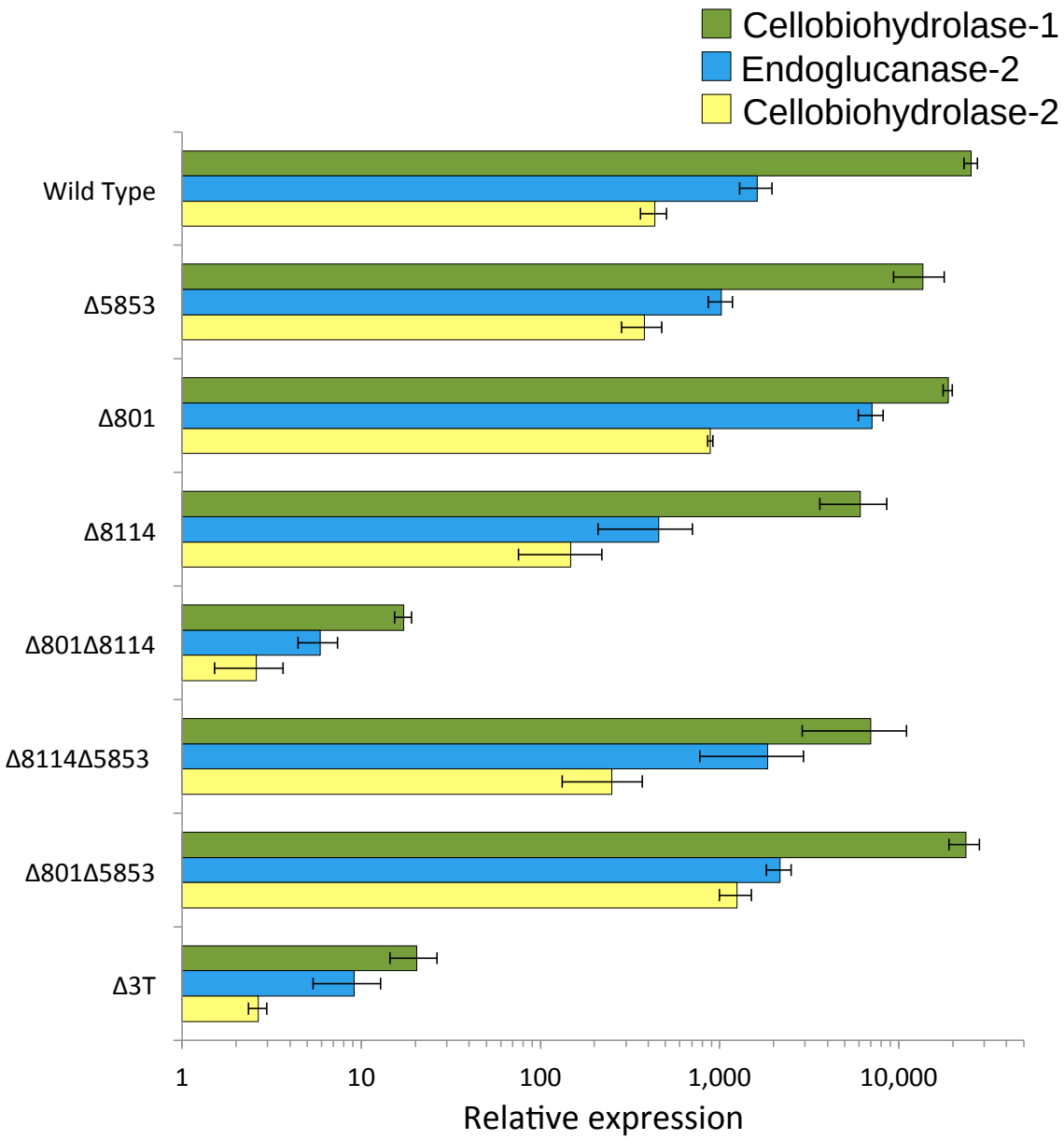

Figure 3-8 Cellulase induction by Avicel in the transporter deletion strains. Gene expression of select cellulases after 4 hour induction with 1% Avicel in WT, ΔNCU05853, ΔNCU00801, ΔNCU08114, ΔNCU00801ΔNCU08114, ΔNCU08114ΔNCU05853, ΔNCU00801ΔNCU05853 and Δ3T (NCU00801ΔNCU08114 ΔNCU05853). Gene expression levels of *cbh-1* (green), *gh6-2* (blue), and *gh5-1* (yellow) were normalized to 1 when induced with 1% sucrose. Actin was used as an endogenous control in all samples. Each strain was grown in triplicate and error bars indicate 1 standard deviation.

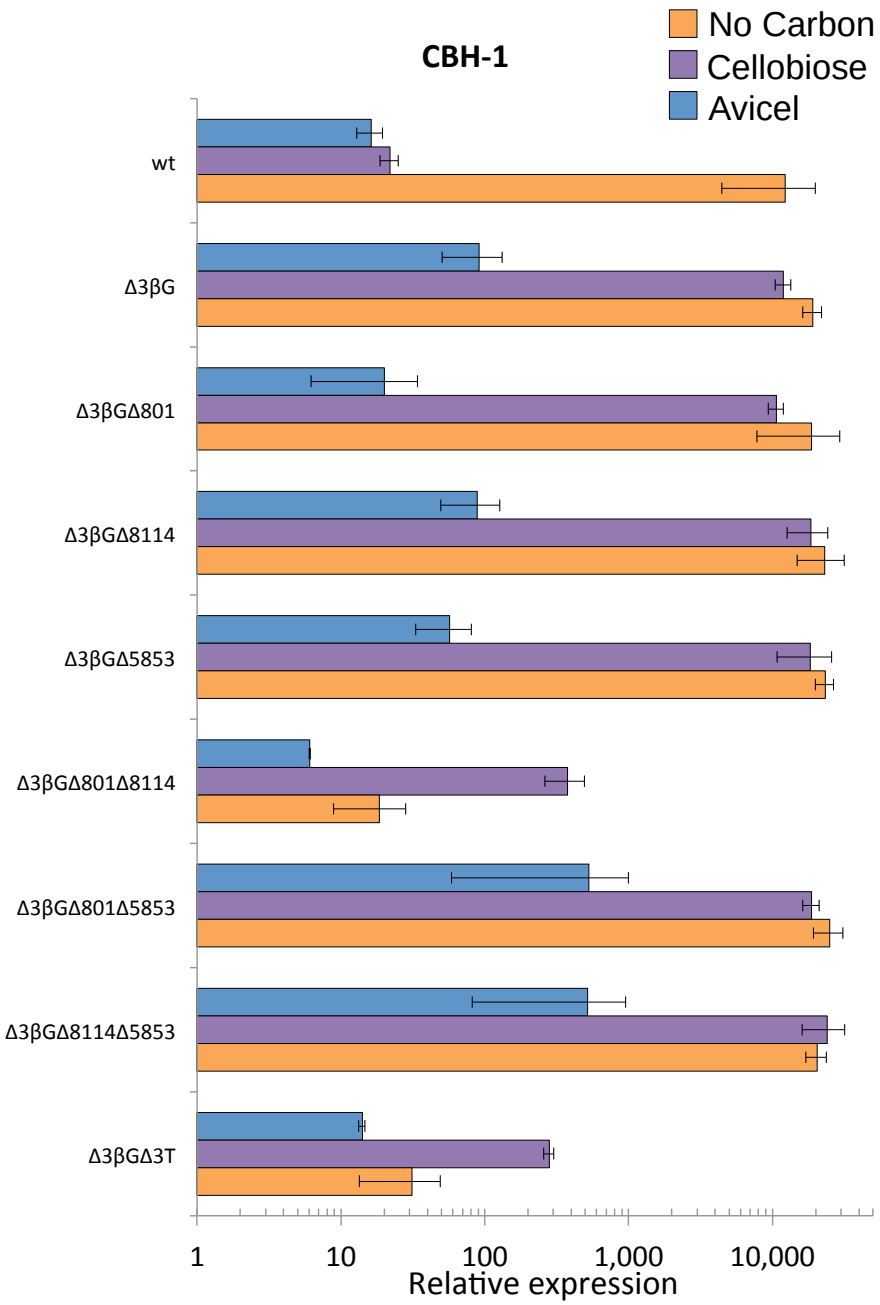

Figure 3-9 Cellulase induction in the Δ3βG transporter deletion strains.
Gene expression of *cbh-1* after 4 hour induction with no carbon (blue), .2% cellobiose (purple) or 1% Avicel (orange) in WT, Δ3βG, , Δ3βGΔNCU00801, Δ3βGΔNCU08114, Δ3βGΔNCU05853,Δ3βGΔNCU00801ΔNCU08114, Δ3βGΔNCU00801ΔNCU05853, Δ3βGΔNCU08114ΔNCU05853, and Δ3βGΔ3T (NCU00801ΔNCU08114 ΔNCU05853). Gene expression levels of, *cbh-1* were normalized to 1 when induced with 1% sucrose. Actin was used as an endogenous control in all samples. Each strain was grown in triplicate and error bars indicate 1 standard deviation.

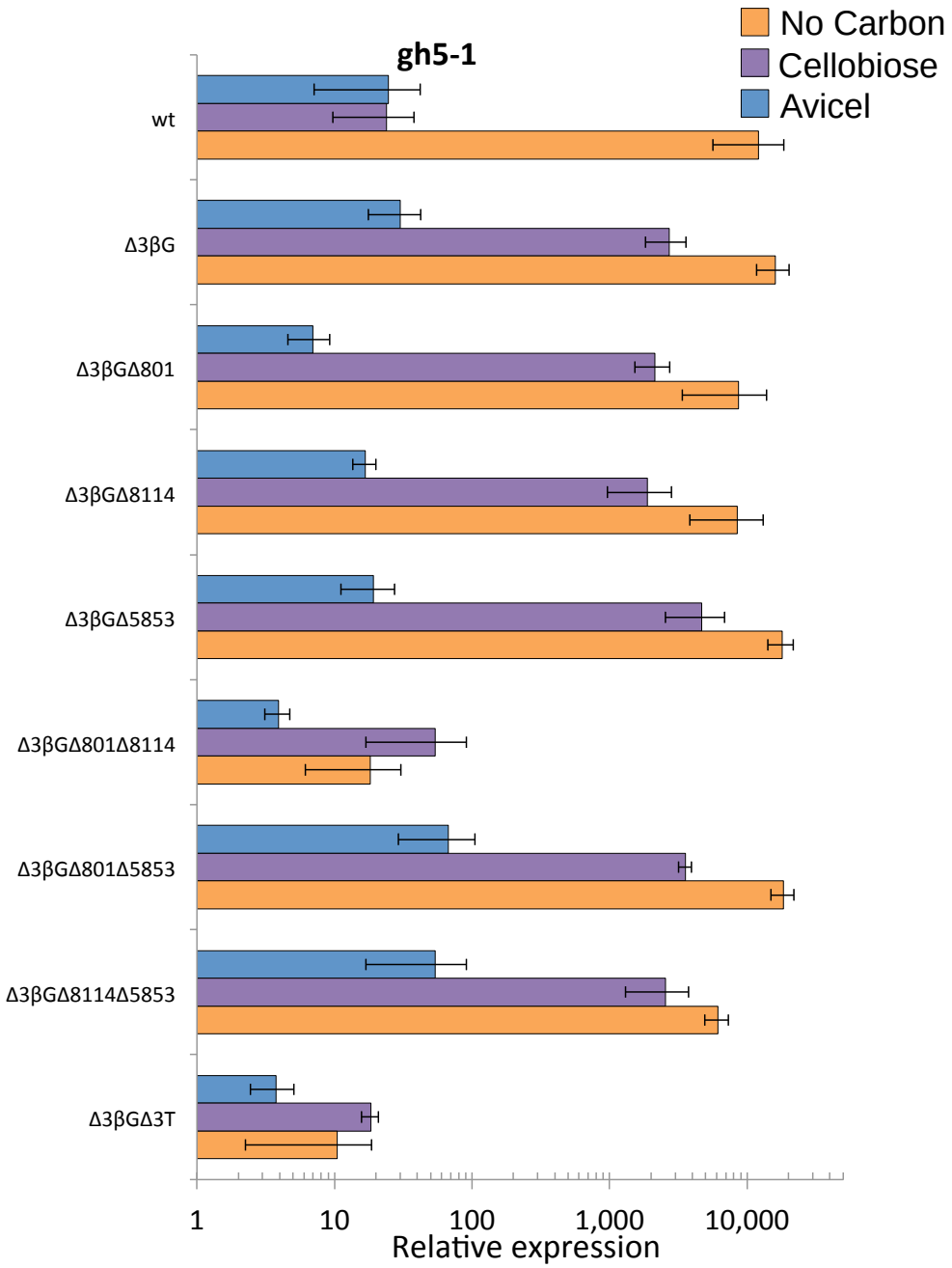

Figure 3-10 Cellulase induction in the Δ3βG transporter deletion strains.
Gene expression of *gh5-1* after 4 hour induction with no carbon (blue), .2% cellobiose (purple) or 1% Avicel (orange) in WT, Δ3βG, Δ3βGΔNCU00801, Δ3βGΔNCU08114, Δ3βGΔNCU05853,Δ3βGΔNCU00801ΔNCU08114, Δ3βGΔNCU00801ΔNCU05853, Δ3βGΔNCU08114ΔNCU05853, and Δ3βGΔ3T (NCU00801ΔNCU08114 ΔNCU05853). Gene expression levels of, *gh5-1* were normalized to 1 when induced with 1% sucrose. Actin was used as an endogenous control in all samples. Each strain was grown in triplicate and error bars indicate 1 standard deviation.

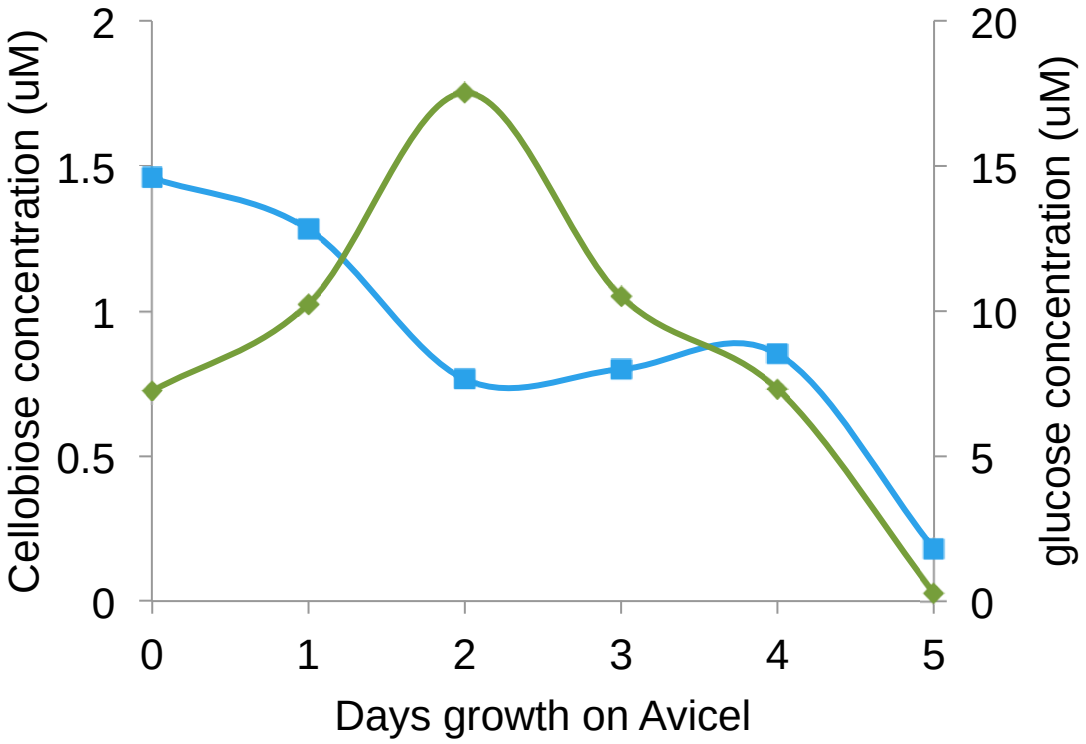

Figure 3-11 Concentration of glucose and cellobiose in Avicel grown cultures. Conidia from WT was inoculated at a concentration equal to $2x10^6$ conidia per milliliter into 100ml Vogel's salts (93) with 2% w/v Avicel in a 250ml Erlenmeyer flask and grown under constant light at 200 rpm for 5 days (Avicel). Each day supernatant samples were removed and at the end of the experiment all samples were analyzed via HPLC for the concentration of glucose and cellobiose.

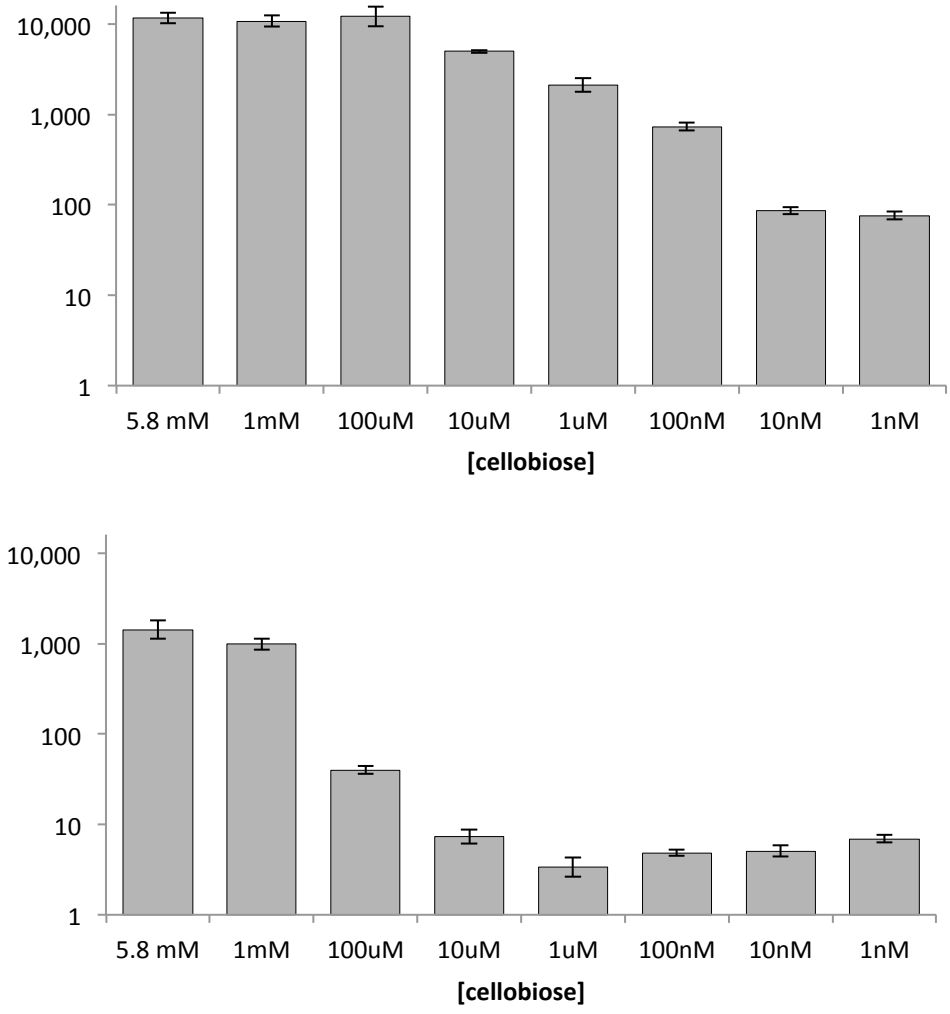

Figure 3-12 Cellulase induction with varied concentrations of cellobiose.
Gene expression of *cbh-1* after 4 hour induction with concentrations of cellobiose ranging from 5nM to 5.8mM in the Δ3βG and Δ3βGΔ3T strains.

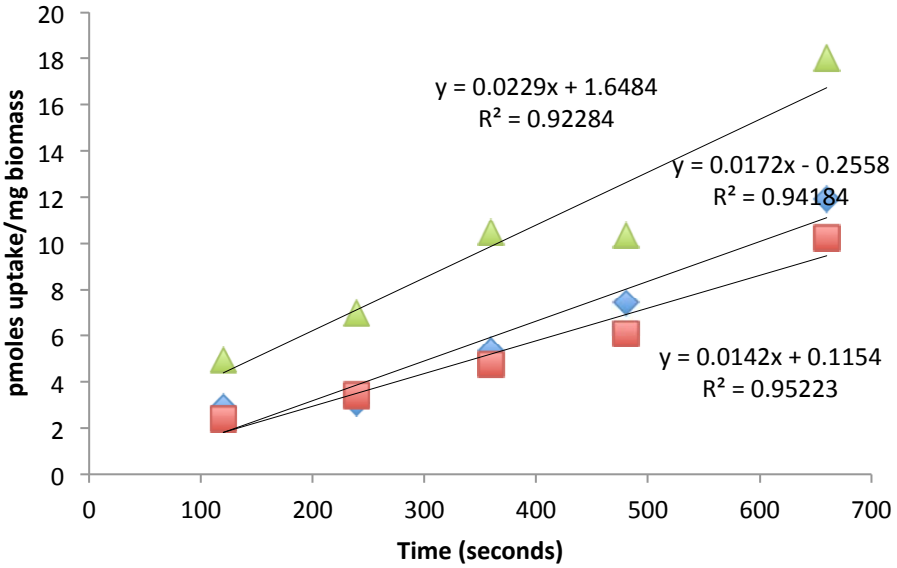

Figure 3-13 Transport of ^{3}H-cellobiose in the Δ3βG strain.

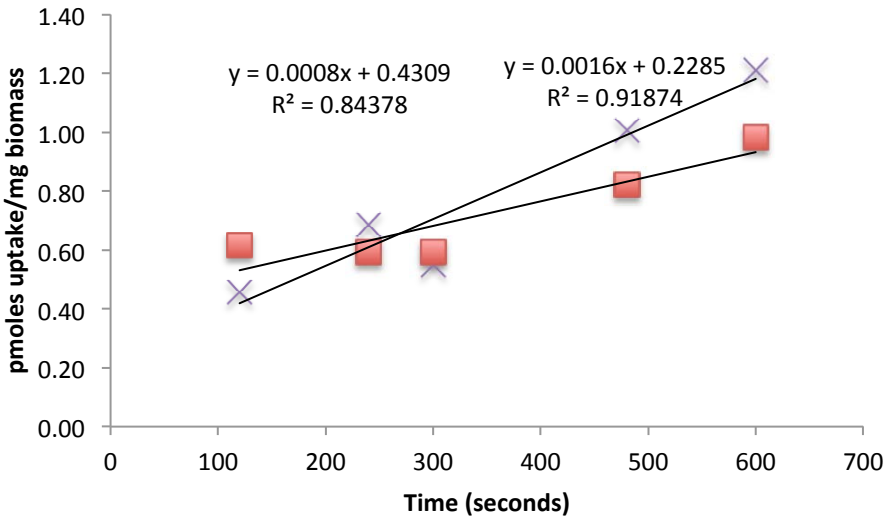

Figure 3-14 Transport of ^{3}H-cellobiose in the Δ3βGΔ3T strain.

	NCU00130	NCU04952	NCU08755	NCU08114	NCU00801	NCU05853
Δ3βGΔ8114	-	-	-	-	+	+
Δ3βGΔ801	-	-	-	+	-	+
Δ3βGΔ5853	-	-	-	+	+	-
Δ3βGΔ801Δ8114	-	-	-	-	-	+
Δ3βGΔ801Δ5853	-	-	-	+	-	-
Δ3βGΔ8114Δ5853	-	-	-	-	+	-
Δ3βGΔ801Δ8114 Δ5853	-	-	-	-	-	-

Table 3-1 Strains used in Chapter 3